Surface Tension Measurement of Polystyrenes in Supercritical Fluids

by

Hyuk Sang Park

A thesis
presented to the University of Waterloo
in fulfillment of the
thesis requirement for the degree of
Doctor of Philosophy
in
Chemical Engineering

Waterloo, Ontario, Canada, 2007

AUTHOR'S DECLARATION

I hereby declare that I am the sole author of this thesis. This is a true copy of the thesis, including any required final revisions, as accepted by my examiners.

I understand that my thesis may be made electronically available to the public.

Abstract

Interfacial tension provides valuable information about polymer processes such as foaming, particle (pigment) suspension, wetting, and blending. Among the methods commonly used to measure surface tension, drop shape methods entail several advantages such as simplicity and versatility. The profile of the drop, which is determined by the balance between gravity and surface forces, is easily defined. The surface tension is obtained from the profile of the drop. Recent progress in image analysis and data acquisition systems makes it possible to digitalize drop images directly using a video frame grabber with a digital camera. The digital signals are easily analyzed using different algorithms to determine the surface/interfacial tension from the drop profile. This study concentrates on one of the drop methods, the pendant drop method, which involves the determination of a drop profile of one dense liquid suspended in another liquid at mechanical equilibrium.

Despite theoretical simplicity of using sessile and pendant drops for determining the surface tension of polymer melts, research in this area is limited because of the experimental difficulty associated with maintaining equilibrium of highly viscous melts. This paper examines the surface tension of polystyrene melts using Axisymmetric Drop Shape Analysis (ADSA) at high temperatures. This thesis focuses on attaining a stable pendant drop during experiments and modifying experimental designs.

The method is verified by experiments in the air and nitrogen, where reproducibility tests and statistical analyses are performed. The surface tension of polystyrene (PS) that melts in supercritical carbon dioxide is obtained while the gas solubility is correlated with the surface tension value determined under various conditions. The Sanchez-Lacombe (S-L) equation of state (EOS) is applied to estimate the Pressure-Volume-Temperature (PVT) data

of the PS/supercritical-carbon-dioxide mixtures, which gives density data. The relationship between surface tension and density is described by the empirical Macleod equation. To characterize the stability of pendant drops formed by the polymer melt, the Bond number is found to be useful; in particular, a stable pendant drop is obtained when the Bond number is between 0.4 and 0.8.

This thesis presents experimental results of the surface tension of polystyrene in supercritical carbon dioxide, together with theoretical calculations for a corresponding system. The surface tension is determined by Axisymmetric Drop Shape Analysis-Profile (ADSA-P), where a high pressure and temperature cell is designed and constructed to facilitate the formation of a pendant drop of polystyrene melt. Self-consistent field theory (SCFT) calculations are applied to simulate the surface tension of a corresponding system, and a good agreement with the experiment is obtained. The physical mechanisms for three main experimental trends are explained using SCFT, and none of the explanations depend on the configurational entropy of the polymer constituents. These calculations therefore rationalize the use of simple liquid models for the quantitative prediction of surface tensions of polymers. As pressure and temperature increase, the surface tension of polystyrene decreases. A linear relationship is found between surface tension and temperature, and between surface tension and pressure; the rate of surface tension change with temperature is dependent on pressure.

A linear relationship is found between surface tension and temperature, and between surface tension and pressure within a temperature range of 170-210°C and a pressure range of 500-2,000 psi. Two monodisperse polystyrenes of M_w ~ 100,000 and M_w ~400,000 and a polydisperse polystyrene were investigated to show the temperature and pressure effect on the surface tension in supercritical nitrogen. Regardless of the molecular weight and

polydispersity, the surface tension of polystyrenes decreases as the pressure and temperature increase. Monodisperse polystyrene of a higher molecular weight has a higher surface tension by 6-9 mJ/m^2 at each experimental condition. The surface tension dependence on temperature and on pressure is more significant for the higher molecular weight polystyrene; the surface tension has been varied more in the higher molecular weight polystyrene than in the lower molecular weigh polystyrene. For a polydisperse polystyrene, high surface tension values seem to be determined predominantly by its high molecular weight portion of polystyrene molecules. An empirical equation was generated to relate surface tension to the density difference between the polymer and supercritical nitrogen. This research should have implications in understanding polymer foaming processes and have application in various polymer engineering fields including polymer characterizations, polymer synthesis, and surface modifications.

Acknowledgements

Firstly, I would like to thank my supervisors, Dr. Pu Chen, Dr. Costas Tzoganakis and Dr. Chul B. Park, for their invaluable advice, guidance and encouragement. During my Ph D program, their unfailing support can not be described in any words.

I would also like to thank Dr. K. H Tan in Epson R&D for his helpful suggestions regarding volume measurements. Professor R.B. Thompson in the Department of Physics and Astronomy provided excellent contribution on the theoretical side of this research.

I am really indebted to all of my current and former group members, Dr. Elias Biswas, Dr. Yousung Hong, Nasim Hyder, Dr. Xinguo Xi, Andrew Propich, Shane Fung, Mei Wang and Hong Yang, for their cooperation and help at the University of Waterloo. Their creative ideas and comments helped me focus better on my research. I would also like to thank my friends for their support and enjoyable times during coffee break moments that only good friends can share.

I would also like to greatly acknowledge the Natural Science and Engineering Research Council of Canada (NSERC), Canadian Foundation for Innovation (CFI) and Premier's Research Excellent Award for their financial support. I extend a special appreciation to Mr. John Bolt in the Engineering Machine Shop for his exceptional help making the various equipments over the past 4 years. With respect to donated materials, special thanks go to Dow Chemicals.

Finally, but foremost, I would like to thank my parents and family members in Korea for their unlimited support and understandings. I wish to thank my beloved wife, Soonchul Hwang, and my children Sojung and Sungwoo for their love, patience, encouragement and prayers. I dedicated this thesis to all of them.

Table of Contents

List of Figures

List of Tables

Nomenclature

$\dot{\gamma}$	Applied shear rate, s^{-1}
k_B	Boltzmann's constant, $1.38X10^{-23}$J/K
C_o	Concentration of gas molecules, g/g
N	Degree of polymerization based on that segment volume
χ_{ph}	Flory-Huggins parameters of polymer and hole
χ_{ps}	Flory-Huggins parameters of polymer and solvent
χ_{sh}	Flory-Huggins parameters of solvent and hole
F	Free energy of the system
f_o	Frequency factor of the gas molecules, s^{-1}
ΔG_{homo}	Gibbs free energy for homogeneous nucleation, Cal/mol
γ	Interfacial(surface) tension, mJ/m^2
$N^{\text{o}}_{\text{homo}}$	Number of nuclei generated, cm^{-3} s^{-1}
ΔP	Pressure difference across the curved interface, Pa
$V_{ij}(\lvert\mathbf{r}\rvert)$	Two-body potential between species i and j
R_g	Unperturbed radius of gyration of a polymer, m
ϕ_h	Volume fraction of holes
ϕ_s	Volume fraction of solvent molecules
ϕ_p	Volume fraction of solvent molecules
$\Delta\rho$	Difference in the density of the two bulk phases, Pa
ρ_c	Critical density, cm^{-3}
ΔPo	Pressure difference at a reference datum plane, Pa
$1/\rho_0$	Volume of a single polymer segment cm^3
a	Statistical segment length of a polymer segment
A	Constant
B	Constant

Bo	Bond number
C	Concentration of the gas in the polymer, g/g
C	Constant
Ca	Capillary number
Dh	Horizontal diameter, cm
Dv	Vertical diameter, cm
E_d	Activation energy for diffusion, Cal/mol
Es	Heat of solution, Cal/mol
g	Gravitational acceleration cm/sec^2
H	Henry's law constant, L atm/mol
mh	Slope of the high pressure run
ml	Slope of the low pressure run
n	Macleod's exponent
n	Number of data points.
P	Equilibrium gas pressure, Pa
P	Perimeter, cm
P_c	Critical pressure, Pa
R	Gas constant, 1.987 Cal/(mol K)
R	Radius of ring, cm
R	Radius of the drop, cm
R_1	Radius of curvature in the plane of paper, cm
R_2	Radius of curvature in a plane perpendicular to paper, cm
s	Standard deviation
t cal	Calculated t value
t critical	Tabulated t value at a confidence level of 2 sides
T	Temperature, K
T_1	Temperature, K
T_c	Critical temperature, K
V	Volume, cm^3
V_1	Volume associated with 1 homogeneous system, cm^3

V_2	Volume associated with 2 homogeneous system, cm^3
valueh	Midpoint values of the high pressure runs
valuel	Midpoint values of the high pressure runs
W_{ring}	Weight of the ring, g
W_{tot}	Total weight, b
W	Weight of the drop, g
x	Mean
z	Vertical height measured from the reference plane, cm
Δm	Difference between the slopes of the low and high
η	Viscosity of the polymer, Pa s
ρ_f	Density of the fluid, g/cm^3
ρ_p	Density of the polymer, g/cm^3

Chapter 1
Introduction and Objectives

1.1 Introduction

Surface tension is one of the most important parameters for understanding various processes, such as foaming, suspensions, wetting and blending (Myers, 1991). There are many methods to measure surface tension. Among them, drop shape methods are particularly powerful which rely on the idea that the shape of a sessile or pendant drop is determined by a combination of surface tension and gravity effects. When gravitation and surface tension effects are comparable, the surface tension can be determined from the shape of a drop. The drop shape methods have many advantages: they require only small amounts of the sample in comparison with those of the Wilhemy plate technique (Adamson and Gast, 1997); they easily facilitate the measurement of both liquid-vapor and liquid-liquid interfacial tensions; they can be applied to materials ranging from pure solvents to concentrated solutions, and from organic liquids to molten metals (Andreas *et al.*, 1938). The experimental conditions can be changed to low or high temperatures, and to high pressure or under a vacuum. The pendant drop method is probably one of the most popular methods used to measure the surface and interfacial tension of liquids. It has been used extensively for the evaluation of surface tension of polymers, liquid crystals, and other low-molar-mass liquids (Lahooti *et al.*, 1996). The pendant drop method involves the determination of drop profile of one denser liquid suspended in another liquid at mechanical equilibrium. The balance between gravity and surface forces determines the profile of drop. Recent progress in image analysis and data acquisition has made it possible to obtain direct digitalization of a drop image with a video

frame grabber of a digital camera. The digital signals are further analyzed to determine the surface/interfacial tension from the drop profile (Rotenberg *et al.*, 1983; Anastasiadis *et al.*, 1987; Miller *et al.*, 1994; Song and Springer, 1996; del Rio and Neumann, 1997).

Despite the theoretical simplicity of using sessile and pendant drops for determining surface tensions of various liquids, research in this area has been limited because of experimental difficulty in handling and ensuring equilibrium of highly viscous polymer melts (Roe *et al.*, 1967; Roe 1968; Wu 1969; Wu 1970; Wu 1982; Anastasiadis *et al.*, 1986; Demarquette and Kamal, 1994; Kwok *et al.*, 1998; Wulf *et al.*, 1999a; Funke *et al.*, 2001; Morita *et al.*, 2002; Xue *et al.*, 2004). To overcome this difficulty, new criteria for surface tension measurement of polymer melts have been explored, specifically with respect to equilibration and stability of the experimental pendant drop. The method of Axisymmetric Drop Shape Analysis (ADSA) relies on a numerical integration on Laplace equation of capillarity. This numerical procedure unifies both the method of sessile drop and that of pendant drop. Recent applications include the surface tension measurements of polymer melts in inert gas at high temperature and pressure (Li *et al.*, 2004).

Supercritical fluids have been used as foaming agents in the production of microcellular polymer foams (Cooper, 2000; Tomasko, *et al.*, 2003). Specifically, carbon dioxide and nitrogen have main advantages of being non-toxic and having relatively low critical points. Although small amounts of a supercritical fluid are added to the polymer process, dramatic changes result in physicochemical properties, such as glass transition temperature, viscosity, solubility and surface tension (Lee, *et al.*, 1999). Particularly, the surface tension between polymer and gas phases has been emphasized because it significantly affects the foaming and morphology of the final polymer products.

The research in this thesis is focused on polymer surface tension measurements of polymers in supercritical fluids. First, special attention will be paid to the experimental method that uses Axisymmetric Drop Shape Analysis-Profile (ADSA-P) to measure surface tension of polystyrene in supercritical carbon dioxide. The method is verified by experiments in the air and nitrogen. In the experiments, to characterize the stability of pendant drops formed by the polymer melts, the Bond number is determined to be useful (Park *et al.*, 2006). Second, the effects of temperature and pressure on the surface tension of polystyrene melts in supercritical carbon dioxide have been investigated. The empirical equations to approximate the surface tension of polystyrene in supercritical carbon dioxide as a function of temperature and pressure is developed, which provides predictive power for the surface tension variation. Self-consistent field theory (SCFT) calculations are applied to simulate the surface tension of a corresponding system, and good agreement with experiment is obtained. Then, the molecular weight effects on the surface tension of polystyrenes are studied. The quantitative dependences of temperatures and pressures on the surface tension are examined in mono dispersed polystyrenes and poly dispersed polystyrene.

1.2 Research Objectives

In this thesis, the primary objective of this study is to quantify the surface tension of a typical, commercially available polymer, polystyrene, in supercritical fluids, and to understand its dependence on temperatures, pressure and molecular weight in a systematic way. For this purpose, special attention will be paid to obtain stable pendant drops and to modify the experimental set-up. This study will have diverse impacts on the process optimizations of microcellular foaming process, which includes the understanding of cell nucleation and

growth (Cahn and Hilliard, 1959; Russell, 1980; Colton and Suh, 1987; Goel and Beckman, 1994a).

This thesis consists of eight Chapters: Chapter 1 gives a brief instruction to the thesis and the research objectives. Chapter 2 contains the literature review regarding polymer surface tensions and its applications. Chapter 3 describes the experimental approaches. Chapter 4 focuses on a study of density determination of polystyrene in carbon dioxide and nitrogen. Chapter 5 discusses the effects of temperatures and pressures on surface tension. Chapter 6 summarizes a theoretical study on the effects of temperatures and pressures on the surface tension of polystyrene in supercritical carbon dioxide. Chapter 7 investigates the molecular weight effects on the surface tension in nitrogen. Chapter 8 presents the conclusions and recommendations for future work.

Chapter 2
Literature Review

Interfacial tension is related to polymer miscibility, the performance and durability of the polymer blend systems. There has been great interest in theoretical and experimental studies of interfacial tension. Unfortunately, theoretical models are not sufficiently advanced to predict the interfacial tension between polymers or polymer and gas. Most commercial polymers are modified by their manufacturers and formulated with diverse low molecular additives, e.g., stabilizers, lubricants, metal ion scavengers, etc. These small molecules could act as surface active agents, lowering the interfacial tension. This makes the theoretical prediction of interfacial tension more difficult.

2.1 Surface Tension Measurements

Measurement of the interfacial (surface) tension in polymer melts can be divided into two groups: static and dynamic measurements. Static methods (e.g. pendant drop, sessile drop, and spinning drop) are based on the equilibrium shape of a droplet in a force field (e.g. gravitational or centripetal). These methods require an accurate measurement of the density difference between the polymer and its surrounding phase. Long waiting times are needed before the equilibrium is reached because of the high viscosity of polymers. This may lead to thermal degradation of the polymer. The dynamic methods follow the change in the shape of threads or elongated droplets to an equilibrium shape including thread breakup, retraction of

elongated droplets, and the dynamic shear rheometry on emulsions. The principles of static measurement techniques are briefly reviewed in the following section:

2.1.1 The pendant drop method (PDM)

The pendant drop method is probably the most convenient, versatile, and popular method to measure interfacial tension. It consists of immersing a drop of a molten polymer into the bulk of another molten polymer or vapor environment. The equilibrium drop profile is determined by the balance between gravity and interfacial tension. Interfacial tension can be determined from the drop profile. The interfacial tension can be evaluated by the Laplace equation of capillarity (Lahooti *et al.*, 1996).

The pendant drop method has several advantages: it is useful for both Newtonian and viscoelastic fluids; no assumption about the rheological behavior of the component is made; the interfacial tension is not disturbed during measurements; it can be applied to liquid crystalline polymers; and the experiment setup is simple.

One the other hand, the pendant drop method presents the following potential problems. It requires the knowledge of the density of the materials used, and such information is scarcely reported for polymeric materials. The density differences of two polymers should be larger than 4-5% to reach the equilibrium shape in an acceptable time interval to avoid thermal degradation. Other limitations relate to the requirement that the material with a small density has to be transparent (Kwok *et al.*, 1998). This study involves the pendant drop method to obtain surface tension of polystyrens in supercritical fluids,

2.1.2 The sessile drop method (SDM)

A sessile drop of liquid resting on an ideal substrate will tend to be spherical because surface forces tend to minimize the surface area, which decreases into the square of the linear dimension. The method is very similar to the pendant drop method. The form of the equation is very similar to the one for the pendant drop method, except for a change in the sign of the gravitational term. Specifically, this method is useful for contact angle measurement.

2.1.3 The Drop Weight Method

The procedure, in its simplest form, is to form drops of the liquid at the end of tube, allowing the drop to fall into a container until enough amount has been collected to accurately determine the weight. The method has been devised by Tate in 1864, and a simple expression for weight W of a drop is given by what is known as Tate's law (Adamson and Gast, 1997):

$$W = 2\pi r\Upsilon \tag{2-1}$$

where W is the weight of the drop, r is the radius of the drop and Υ is the surface tension. In practice, the obtained weight (W′) is less than the ideal value (W). The reason for this becomes evident when the process of drop formation is observed closely. It is clear that only a portion of the drop that has reached the point of instability actually falls. The usual procedure is to apply a correction factor to compensate for the errors.

2.1.4 The Ring Method

A method that has been rather widely used involves the determination of the force to detach a ring from the surface of a liquid. It is generally attributed to du Noüy (Adamson and Gast, 1997). Like all detachment methods, one supposes that a first approximation to the detachment force is given by the surface tension multiplied by the periphery of the surface detached. Thus, for a ring,

$$W_{tot} = W_{ring} + 4\pi r\Upsilon \tag{2-2}$$

where W_{tot} is total weight, W_{ring} is the weight of the ring, r is the radius of ring, and Υ is the surface tension.

2.1.5 Wilhemy Slide Method

The basic observation is that a thin plate, such as a microscope cover glass or platinum foil, will support a meniscus whose weight both as measured statically or by detachment is given by an ideal equation.

$$W_{tot} = W_{plate} + p\Upsilon \tag{2-3}$$

where W_{tot} is the total weight, W_{plate} is the weight of the plate, p is the perimeter and Υ is the surface tension.

2.2 Existing Interfacial Tension Data of Polystyrene Melts

Interfacial tensions for various polymer pairs and polymer-gas pairs have been reported using pendant drop method. A brief review of the vast amount of interfacial (or surface) tension data involving polystyrene melts is presented in Table 2.1

Table 2-1 Summary of the literature on the interfacial tension measurement of PS

References	Materials	Temperature(°C)	Interfacial Tension (mJ/m^2)
Wu 1970	PMMA-N_2, PBMA-N_2, PS-N_2	120-200	22-34
Anastasiadis *et al.*, 1988	PS-PMMA	199	0.4-1.4
Kwok *et al.*, 1998	PP,PE,PS-N_2	170-210	19-26
Chen and White, 1993	PS-PE	180	1.1-5.8
Demarquette and Kamal, 1994	PS-PE	186-213	1.4-3.74
Wulf *et al.*, 1999a	PS	170-235	25.8-29.8
Arashiro and Demarquette, 1999	PS-PE	202	5.5-7
Cho *et al.*, 2000	PS-N_2	140	28-32
Morita *et al.*, 2002	PS	240	17-19
Li, *et al.*, 2004	PS-CO_2	200-230	14-28

PS: Polystyrene; PMMA: Polymethyl methacrylate; PBMA: Poly n-butyl methacrylate; PP: Polypropylene; PE: Polyethylene; N_2: Nitrogen; CO_2: Carbon dioxide

2.3 Supercritical Fluids and their Applications

2.3.1 Supercritical Fluids

A supercritical fluid (SCF) is a substance that is compressed beyond its critical pressure and heated above its critical temperature (see Figure 2.1). At these conditions, the vapor and liquid phases become indistinguishable and the fluid behaves as a single phase having some advantageous properties of both a liquid and a gas. For example, SCFs have sufficient density to give appreciable dissolving power, while the diffusivity of solutes in SCFs falls between that in a liquid and in a gas. Because of the high compressibility of fluids near the critical point, their density and dissolving power can be tuned sensitively through small changes in pressure. Other advantages of SCFs include zero surface tension and ease of removal. Typical thermophysical properties of fluid phases are compared in Table 2.2.

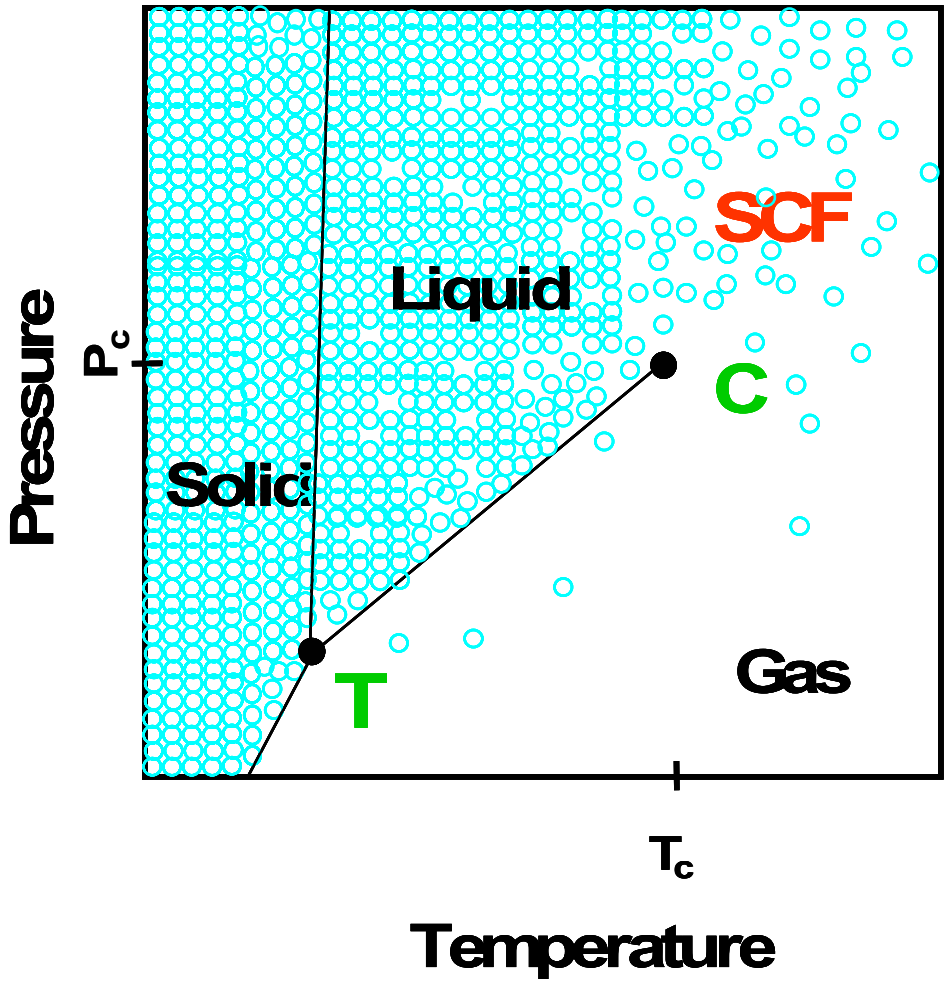

Figure 2-1. Schematic pressure-temperature phase diagram for a pure component showing the supercritical fluid (SCF) region.

(Cansell *et al.*, 1998)

The triple point (T) and the critical point (C) are marked. The circles represent the variation in density of the substance in the different regions of the phase diagram. Note that the density varies continuously between the liquid state and gas state, providing that the liquid-gas equilibrium line (T-C) is not crossed.

Table 2-2 Characteristic magnitudes of thermophysical properties of fluid

(Cansell *et al.*, 1999)

	Liquid	SCF	Gas [a]
Density (g/cm^3)	1	0.1-0.8	10^{-3}
Viscosity (Pa s)	10^{-3}	10^{-4}-10^{-5}	10^{-5}
Diffusion Coefficient [b] (m^2/s)	10^{-9}	10^{-8}	10^{-5}

[a] At ambient conditions

[b] For small molecule solute

Carbon dioxide has been one of the classical and popular substances in supercritical fluid technology, and many studies have been performed about the critical point of CO_2 and its properties in the supercritical state. Michel and Michael (1936) and Michel *et al.* (1937) measured the isotherms of CO_2 between 0 ^oC and 150 ^oC and up to 3000 atm (Michels and Michels, 1936, Michels *et al.*, 1937). The critical conditions for CO_2 are reported as:

T_c = 304.19 K

P_c = 72.87 atm (or 7.38 M Pa or 1071 psi)

ρ_c = 0.468 g/cm^3

Additionally, the critical conditions for N_2 are reported as:

T_c = 126.15 K

P_c = 33.55 atm (or 3.4 M Pa or 493 psi)

ρ_c = 0.314 g/cm^3

2.3.2 Polymer Foams and Microcellular Foams

Incorporation of gases into polymers has been used for producing polymer foams. Foaming processes have been developed in the food industry as well as in the polymer industry. In the food industry, various puffed foods such as cereals, pastas, and confectionery products with improved structures have been produced. However, for this section, only the polymer foaming process is discussed. Polymer foams have been produced in batch or continuous processes, from molten or solid materials, and before or after the shaping process. The first commercial foam appeared between 1910 and 1920 (Madge, 1962). Since then synthetic foams have been found in many areas such as comfort cushioning, packing, insulation and space filling. These conventional foams show relatively poor mechanical properties due to their large cell size and irregular particle size. As reviewed by Kim and Kim, however, rigid foams show better mechanical properties because of the high strength-to-weight ratio (Kim and Kin, 1991). One of the rigid foams is high density microcellular foam, which is characterized by cell density higher than 10^9 cells/cm^3 and a cell size smaller than 10μm. In general, a microcellular foam is produced by using SCFs.

By being exposed to an applied thermodynamic instability, such as depressurization or temperature changes, the SCF precipitates from the solution and a cellular foam structure is finally produced. A microcellular plastic was originally developed by Martini-Vveddensky *et al.* (Martini-Vveddensky *et al.,* 1984). Microcellular plastics were initially developed in batch processes. A polymer saturated with a high pressure gas is subjected to a thermodynamic instability that is induced by rapidly dropping the solubility of gas in the polymer. The rapid solubility drop is attained by a rapid change in pressure or temperature

and as a consequence, the precipitated gases or SCFs generate the cell structures in a polymer. Some applications of microcellular foams are shown in figure 2-2. It has various possible applications due to advantages such as, material cost reduction, insulation, impact resistance, buoyancy and minimum shrinkage,

Figure 2-2 The applications of microcellular foams

2.3.2.1 Microcellular Foams: Batch Process

A batch process for producing microcellular structures was developed by Martini-Vvedensky *et al.* (Martini-Vveddensky *et al.*, 1984). A polymer was saturated with a high pressure gas in a chamber to avoid cell nucleation, the gas saturated-polymer was subjected to a rapid pressure drop and a rapid temperature change resulting in micro cell nucleation and growth. The batch process for microcellular foams has been studied for a solid state of polymer. Wessling *et al*. investigated the saturated polycarbonate sheet in a high pressure CO_2 for 24 hours at room temperature (Wessling *et al*., 1994). The sheet was immediately dipped immersed in a heated glycerol batch at 100^{o}C after the pressure release. Despite being treated below the glass transition temperature of polycarbonate, the sheet was found to foam throughout with the exception of a dense unfoamed skin at the outer surface of the sheet. They showed that the polymer becomes supersaturated with CO_2 during the heating step, and that the rapid mass transfer of CO_2 out of the sheet results in the unfoamed skin structure because the partial pressure of CO_2 at the outside of the sheet is zero. Goel and Beckman showed the temperature and pressure effect on the microcellular foams of poly(methyl methacylate), PMMA, with carbon dioxide in a temperature range from 40^{o}C to 80^{o}C (Goel and Beckman, 1995a, Goel and Beckman, 1995b). A PMMA disc of 2mm thick and 18mm in diameter was pressurized with CO_2 in a closed chamber over 24 hours to ensure equilibrium absorption of gas by the polymer. The pressure was dropped to atmospheric pressure for 1 hr. In those experiments, the effects of temperature and pressure at equilibrium, and saturation time were investigated. The rate of nucleating was increased as the fluid saturation pressure

and saturation time of gas increased. The temperature effect was minimal in altering their conditions.

Kumar and Gebizlioglu and Doroudiani *et al*. investigated the foaming processes of semicrystalline polymers (Kumar and Gebizlioglu 1992, Doroudiani *et al*., 1996). Kumar and Gebizlioglu followed the process used by Martini-Vvedensky *et al*. for poly(ethylene terephthalate) with carbon dioxide. They claimed that the foaming has strong effects from the local carbon dioxide concentrations and fractions of crystallinity of the polymer matrix. Doroudiani *et al*. studied samples having various crystalline levels such as high density polyethylene (HDPE), polybutylene (PB), polypropylene (PP), and poly(ethylene terephthalate) (PET). They found that increasing the crystallinity proportionally decreased the solubility and diffusivity of blowing agent in crystalline polymers. This indicates that sorption only take place in the amorphous region of polymers. Therefore, the cellular structures of resulting foams were found to be increasingly non-uniform as the crystallinity level increased due to the inhomogeneous dissolution and the subsequent nucleation of the CO_2.They revealed that the morphologies of semicrystalline polymer had influence on the solubility and cellular structure.

2.3.2.2 Microcellular Foams: Continuous Process

In order to obtain a microcellular structure in a continuous process, two major processes, continuous formation of a polymer / gas solution and microcell nucleation by thermodynamic instability in the polymer / gas solution, should be considered. Extrusion and injection molding have been studied for the continuous foaming process. Park and Suh utilized an extrusion process to incorporate these two major processes (Park and Suh 1994, Park and Suh

1996a, Park and Suh 1996b). They designed a continuous microcellular process using a single-screw extruder. SCF was injected into the barrel and homogenized to a single-phase solution by dissolution. As shown in figure 2-2, the creation of a single-phase polymer/ SCF solution is governed by the degree of mixing and the diffusivity and striation thickness. They pointed out that the critical parameters in the microcellular extrusion process are the solubility of SCF, degree of mixing, and the processing temperature and pressure. They presented a prototype pf a continuous microcellular process and utilized a rapid pressure drop device to obtain the unique properties of microcellular foams (Park and Suh 1993).

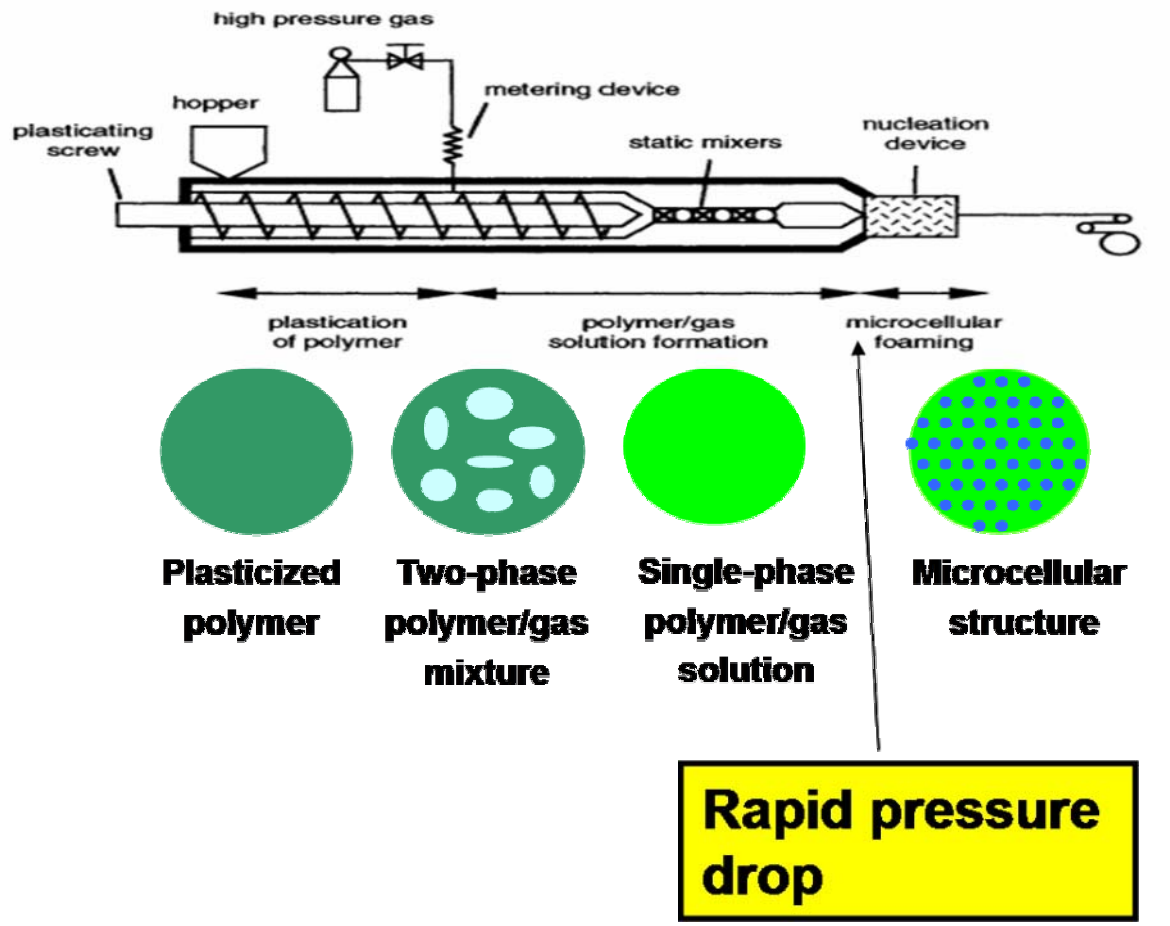

Figure 2-3 Schematic of microcellular foaming processes and morphology changes

Park and Suh also suggested a convective diffusion device to improve the effectiveness of mixing and diffusion for the fast polymer/ gas solution (Park and Suh 1992). They showed the critical parameters of the microcellular continuous process such as the polymer / gas weight ratio, mixing level, processing pressure, process temperature, and processing time.

They presented a metering device consisting of a porous metal for controlling the flow rate of CO_2 and a pump for building up a high pressure of CO_2.

2.3.2.3 Process Parameters in Microcellular Foams

Most of research on microcellular foams has been devoted to the effects of process conditions, and materials properties on the cell structure as shown in figure 2-3. The nucleation and growth mechanism are two main factors of cell formation and its structure; therefore most research has been focused on those mechanisms among the various operating conditions and the cell structures of foams. Park and Suh (Park and Suh 1992) defined the cell nucleation as the transformation of small clusters of gas molecules to energetically stabilized pockets of molecules To obtain the nucleation cell density larger than 10^9cells/cm^3, a very high nucleation rate is critical. Cell nucleation can occur either homogenously or heterogeneously.

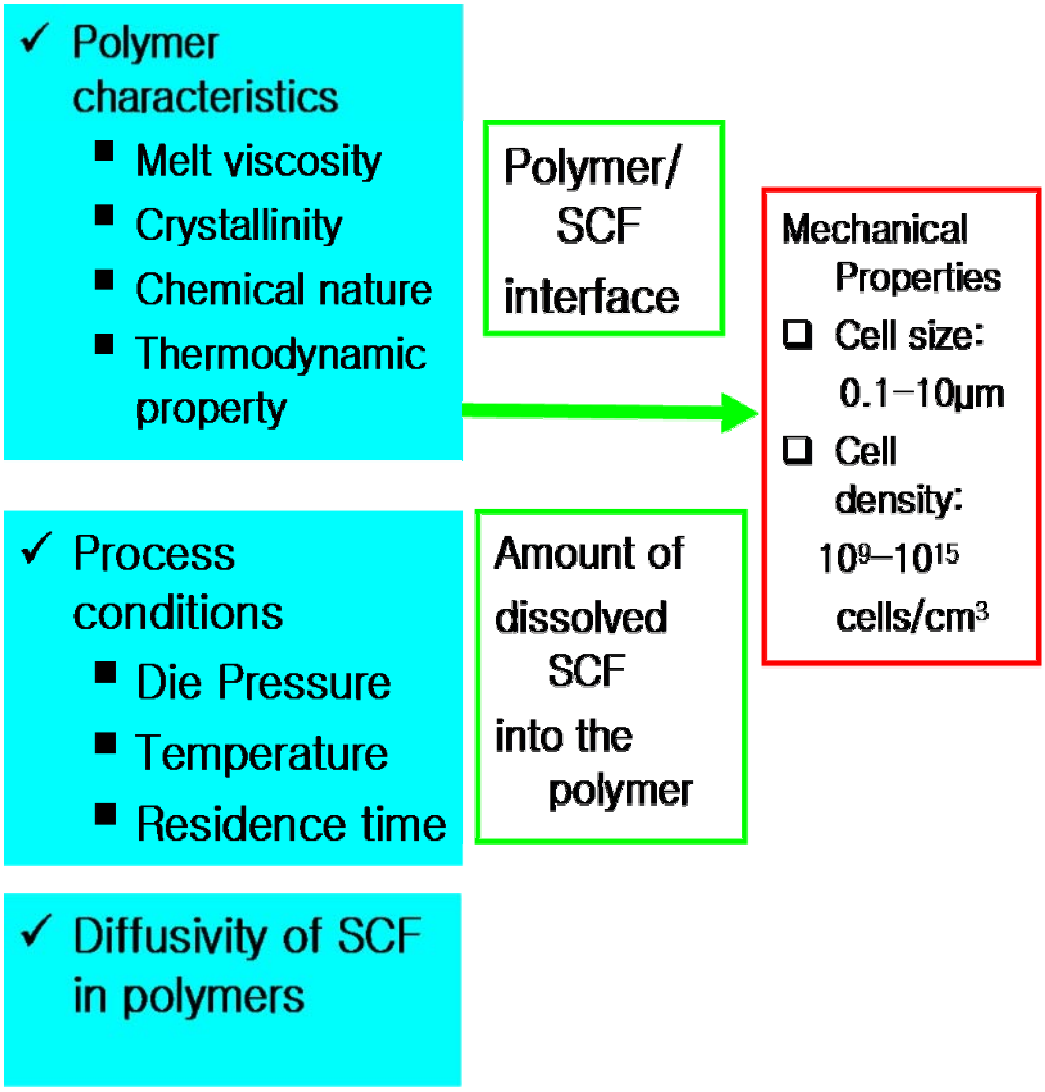

Figure 2-4 Typcial material and process parameters in a continuous microcellular foaming processes

The homogenous nucleation occurs when gas molecules dissolved in a homogeneous polymer come together for a long enough time to obtain a stable bubble nucleus. The homogeneous nucleation rate has been defined by Colton and Suh (Colton and Suh, 1987):

$$N_{\text{homo}}^{\text{o}} = C_o f_o \exp(-\Delta G_{\text{homo}} / k_B T) \tag{2-4a}$$

$$\Delta G_{\text{homo}} = 16\pi\gamma^3 / 3\Delta P^2 \tag{2-4b}$$

where $N_{\text{homo}}^{\text{o}}$ denotes the rate of nucleation, C_o denotes the gas concentration, f_o denotes the frequency factor of molecules joining the nucleating cluster, k_B denotes Boltzmann's constant, ΔG_{homo} denotes the activation energy , γ denotes the surface energy of the polymer and ΔP denotes pressure difference between gas saturation pressure and the environmental pressure, respectively. Heterogeneous nucleation occurs in the presence of an interface between two phases-such as a polymer and an additive. Ramesh *et al.* showed the rubber particles played roles as heterogeneous nucleation sites in polystyrene (Ramesh *et al*., 1994a, Ramesh *et al*., 1994b). Lee argued that blowing agent tends to diffuse into gas phase cavity end to establish equilibrium if it is mixed fully. The blowing agents create small voids due to the incomplete wetting of the polymer melt and voids act as nucleating sites (Lee, 1993). Heterogeneous nucleation has been observed in the foaming process of semi crystalline polymers due to crystalline / amorphous interfaces. Once nucleation has occurred,

by whatever mechanism, cell growth can take place. The nucleation sites receive gas diffusing from the melt and form a cell structure.

From equation (2-5b), a higher saturation pressure and lower environmental pressure lead to a lower activation energy barrier which then leads to a higher nucleation rate. Thus, a higher gas saturation pressure and lower nucleation pressure leads to a higher cell density. Kumar and Suh proved experimentally that cell density increases with the gas saturation pressure (Kumar and Suh, 1990). However, the effect of external pressure on the cell nucleation does not agree with equation (2-5b) in this polystyrene-nitrogen system. They found that the external pressure has no significant effect on the cell nucleation in their experimental conditions. Park *et al*. investigated the effect of pressure drop rate on cell nucleation (Park *et al*., 1995). Various pressure drop rates were obtained by adjusting the die geometry and the residence time. The experimental results showed that both the magnitude and the rate of pressure drop play an important role in microcellular processing of high impact polystyrene (HIPS) / CO_2 system. The higher pressure drop rate has a dominant effect on cell nucleation. It also affected the completion between cell nucleation and cell growth, and resulted in the different cell structures from an identical polymer/gas solution. Shafi *et al.* modeled the effects of processing parameters on cell nucleation and growth. The growth rate increases as the dissolved gas diffusion and gas solubility in the polymer are increasing. Specifically they simulated that lowering the surface tension increases the nucleation rate dramatically and narrows the cell size distribution and produces a much higher bubble density and smaller cell sizes.

The temperature of microcellular foaming process is another major factor affecting the cell structures. Goel and Beckman studied the temperature effect on nucleation with

poly(methyl methacylate), PMMA and carbon dioxide system. They showed that the cell size will increase with increasing temperature. On the other hand, the effect of temperature on cell density is negligible in their experimental conditions. (Goel and Beckman, 1995a, Goel and Beckman, 1995b). They explained the process of the suppression of glass transition of PMMA, which due to the presence of adsorbed carbon dioxide, allows for the cell growth in their process rather than the heating of polymer above its normal glass transition. In addition, lower viscosity leads to higher cell coalescence. Park and Cheung reported coalescence of cells during the foaming process of linear and branched polypropylene (Park and Cheung, 1997). The authors observed fast cell coalescence in the linear polypropylene, which might show a lower viscosity behavior.

In addition, the type of blowing agent and the concentration of blowing agent have been known to be one of the major factors affecting the cell density. Park and Cheung reported that the effect of pressure on cell density was remarkable when carbon dioxide was used, whereas no pressure effect was observed with isopentane in the cell nucleation study of polypropylene (Park and Cheung, 1997). According to the equation of (2-5a), the cell density is expected to increase by increasing gas concentration since the nucleation rate is directly proportional to the amount of dissolved gas. This has been verified experimentally by Park and Suh (Park and Suh 1992, Park and Suh 1993) and other researchers (Goel and Beckman, 1995a, Goel and Beckman, 1995b).

2.4 Polymer / Supercritical Fluid Solution

2.4.1 Solubility of Supercritical Fluids

Supercritical fluids (SCFs) have unique solubility behaviors, a broad range of solubility, and it has been known that a significant amount of SCF can be dissolved in a polymer phase as described in Section 2.3.1. In this section, literature dealing with SCFs solubility in presence of a polymer as the major phase is reviewed.

When the concentration of a dissolved amount of gas is low, the gas solubility in the polymer at a given condition of temperature and pressure can be described by Henry's law:

$$C=HP \tag{2-5}$$

where P is the equilibrium gas pressure (atm), H is Henry's law constant (cm^3(STP)/g- atm), and c is the concentration of the gas in the polymer. Henry's law is valid on the ideal solution state and extreme dilute solution. However, it does not consider the interactions between the polymer and gas. Therefore, the solubility predicted from Henry's law deviates from the actual solubility of gas in real polymer, especially at high pressure. In spite of its deficiencies, Henry's law has been used for polymer systems for many studies. Only limited data for the solubility of gases in polymers were reported and several earlier studies focused on the measurement of Henry's law constants.

A technique to measure simultaneously solubility and diffusivity of gases in molten or thermally softened polymer has been developed by Durrill and Grisky. They studied systems including nitrogen, helium, carbon dioxide, and argon in polyethylene, polyisobutylene, polypropylene, polystyrene and poly(methyl methacrylate) (Durrill and Griskey, 1966). The solubility was determined by weighing the sample before and after saturation. The diffusivity was also obtained by observing the pressure and time relations during the diffusion process. They obtained Henry's law constants and diffusion coefficients

for many systems including polystyrene and carbon dioxide solutions up to 20atm. The temperature dependence of Henry's law constants was derived through an Arrhenius equation form.

$$H_1 = H_o \exp\left(-\frac{E_s}{RT_1}\right) \tag{2-6}$$

In this expression, H_0 and H_1 denote the Henry's law constant (cm^3(STP)/g- atm), Es is the heat of solution (cal/mol),R is gas constant, and T_1 is the temperature (K). In order to predict the heat of the solution, as indicated in equation 2-3, Henry's law constant needs to be established at various temperatures. They published the temperature dependence of both Henry's law constants and diffusivities for the same materials used in their previous study (Durrill and Griskey, 1969). The law constants and diffusivities do not changed according to temperature changes.

Sato *et al*. presented the solubilities of carbon dioxide and nitrogen in polystyrene using a pressure decaying method at temperature from 100 ^oC to 180 ^oC and pressure up to 20MPa (Sato *et al*., 1996). The solubility isotherm of both gases increased almost linearly with pressure and it was observed that the solubility of carbon dioxide decreased with increasing temperature, whereas the solubility of nitrogen increased with temperature. Henry's law constants of polystyrene and carbon dioxide and polystyrene and nitrogen solutions are in good agreement with those of Durrill and Griskey (Durrill and Griskey, 1966). Sato *et al*. observed the solubility of these gases in polyolefins such as polypropylene and high density polyethylene (Sato *et al*., 1996).

Kato *et al*. investigated carbon dioxide sorption behaviour of polystyrene / polycarbonate blend system at 25^{o}C. They claimed that the change of the carbon dioxide sorption amount for the polymer blend was mainly explained by the amount of the crystallite of polycarbonate. The results showed that the effect of the miscible region part of the carbon dioxide behavior is very small (Kato *et al*., 1997).

2.4.2. The Equation of State

Theoretical approaches for explaining the solubility of a gas in a polymer have been performed. These approaches have originated from the prediction of pressure-volume-temperature relationship for a pure component, and expanded to polymer/gas systems. The Flory-Huggins (F-H) theory (Flory 1942, Huggins 1942) is based on the lattice concept and mixing entropy changes that give information about solubility as well as the phase behavior, and it assumes that the volume and enthalpy of mixing are zero. The interaction parameter, χ, was used to correct the energetic effect of mixing.

Sanchez and Lacombe (Sanchez and Lacombe, 1976; Sanchez and Lacombe, 1977; Sanchez and Lacombe, 1978) developed an equation of state (EOS) theory for pure fluids and for mixtures. The lattice-fluid theory describes molecular ensembles in terms of the number of lattice sites occupied by molecular species and the interaction between neighboring molecules. It is based on the lattice-fluid model, with empty sites, which are called holes. Each molecule occupies r-sites (r-mer) and there are unoccupied sites as well. These r-mers are randomly mixed with each other and with vacant sites. The holes are different from the F-H lattice theory because varying the fraction of holes in the lattice can change the density of

the mixture. This S-L EOS needs three pure component parameters to characterize a pure fluid and also one adjustable parameter, δ_{ij}. The adjustable parameter is related to the binary interaction to identify the mixing behaviors. The pure component parameters can be determined by fitting pressure-volume-temperature data to the S-E EOS for the pure component. Some of the characteristic parameters of the solution can also be determined by using mixing rules. However, the other parameters, such as the characteristic pressure and density, should be obtained by comparing the regression of the solubility data and an equation for chemical potentials (Sato *et al*., 1996).

Chapter 3*
Experimental Approaches

3.1 Proposed Approaches

The main objective of this investigation is to measure the surface tension of polymer in supercritical fluids. The first step of this study is to evaluate the reliability and experimental reproducibility of the method with the measurement results. Special attention will be paid to obtain stable pendant drops and to improve experimental set up. The obtained surface tension of the polymer in supercritical fluids will be related with the physical properties, such as molecular weight, molecular weight distribution, viscosity, density and additive of polymer.

Our surface tension measurement method will be applied to measure pressure-volume-temperature (PVT), solubility and diffusivity. The obtained PVT, solubility and diffusivity data will be compared with the equation of state.

All observed properties, such as, surface tension, pressure-volume-temperature, solubility and diffusivity, will be applied to characterize polymer properties and to find optimum process conditions in micro cellular processes.

* This chapter is based on the manuscript of the published studies (Park, *et al*., 2006)

3.2 Proposed Methods

3.2.1 Principle of Pendant Drop Method

The pendant drop method consists of suspending a drop of one liquid from a capillary into the bulk of another fluid (either a gas or another liquid). The shape of the liquid meniscus is governed by the balance of interfacial and gravitational forces. Thus, the interfacial tension can be determined from the equilibrium drop profile and from density difference between the two fluids.

The classical Laplace equation is the basis for all static measurements of interfacial and surface tensions. It states that the pressure difference across a curved interface can be described as:

$$\frac{1}{R_1}+\frac{1}{R_2}=\frac{\Delta P}{\gamma} \tag{3-1}$$

where R_1 is the radius of curvature in the plane of paper, R_2 is the radius of curvature in a plane perpendicular to paper, ΔP is the pressure difference across the curved interface, and γ is the interfacial tension.

Bashforth and Adams transformed the Laplace equation into convenient dimensionless forms and numerical solutions with an accuracy of four and five decimals were tabulated. In earlier studies, the shapes of liquid menisci were measured manually and interfacial tensions were interpreted with different sets of tables. Progress in image analysis and data acquisition systems has made it possible to obtain a direct digitization of the drop image with the aid of a video frame grabber or digital camera. A new technique, called Axisymmetric Drop Shape Analysis-Profile (ADSA-P), has been developed to determine liquid-fluid interfacial tensions from the shape of axisymmetric menisci. In this technique,

images of the drops are digitized with sub-pixel resolution and experimental drop profiles are compared with theoretical ones given by the Laplace equation. A least-square algorithm is used with interfacial tension as one of the adjustable parameter. Other parameters, such as drop volume, surface area, and radius of curvature, can also be obtained. The ADSA-P method was employed in this study and more details are discussed below.

In the absence of external forces, other than gravity, the pressure difference(ΔP) is a linear function of the elevation.

$$\Delta P = \Delta P_o + \Delta \rho g z \tag{3-2}$$

In this expression, ΔPo is the pressure difference at a reference datum plane, Δρ is the difference in the density of the two bulk phases, g is the gravitational acceleration, and z is the vertical height measured from the reference plane.

When the axis x is tangent to the curved interface and normal to the axis of symmetry and the origin is placed at the apex as shown in Fig 3.1, the Laplace equation can be rewritten as:

$$\frac{d\phi}{ds} = \frac{2}{a} - \frac{\Delta \rho g}{\gamma} z - \frac{\sin \phi}{x} \tag{3-3}$$

Mathematically, the interface is described completely as u=u(x, y, z). Due to the symmetry in the system, this may be reduced to the description (see Figure 3.1) of the meridian section alone. A suitable representation of the meridian curve is in a parametric form:

$$x=x(s) \text{ and } z=z(s) \tag{3-4}$$

where s is the arc length measured from the origin,0. In this representation both x and z are single-valued functions of s.

$$\cos\phi = \frac{dx}{ds} \tag{3-5}$$

A geometrical consideration yields the differential identities, and the boundary conditions

$$x(0)=y(0)=z(0)=0 \tag{3-6}$$

from a set of first order differential equations for x, z, and ϕ as functions of the argument s. For given R_o and $\Delta\rho g/\gamma$, the theoretical drop given by the Laplace equation may be obtained by simultaneously integrating three equations.

Once an experimental drop profile is obtained, the ADSA-P program randomly selects 20 coordinates from it and compares them with theoretical drop profiles, using a least square algorithm with interfacial tension as one of the adjustable parameters. The best fit between these two profiles identifies the correct, i.e. operative, interfacial tension. The procedure is repeated 10 times for each experimental drop profile and 95% confidence limits are reported. For this work, typically 95% confidence limits are around $\pm$0.01-0.02mJ/m^2. Besides the drop profile coordinates, the input information required are the acceleration due to gravity and the density difference across the liquid-fluid interface. The details of numerical methods and procedures can be found elsewhere (del Rio and Neumann, 1997).

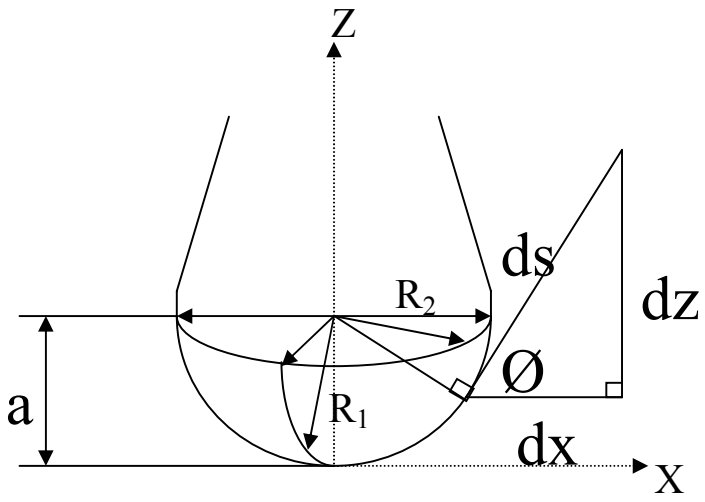

Figure 3-1 Definition of the coordinate system of a pendant drop

3.2.2 Experimental Setup

The apparatus developed for this research consists of a high temperature high pressure optical view cell in which a pendant drop is formed, an optical system to capture the image of the drop, and a data acquisition system with a PC to compute the interfacial tension from the drop profile. Fig.3.2. shows the schematic diagram of the pendant drop apparatus. An IsoStation Vibration Isolated Workstation (1), which provides an ideal working platform for vibration influenced devices, is used to isolate the key instruments from floor motion or vibration. To illuminate the pendant drop, a light source (2) is used. In general, a frosted glass diffuser (3) is used between the light source and the pendant drop. The light diffuser provides a uniformly bright background, which results in images of high contrast. Pendant drops can be obtained by extruding one polymer of higher density with a heated stainless steel syringe (4). With a syringe holder, the syringe can manually dispense precise drops. A high-pressure optical view cell (5) is used to melt the polymer with the lower density. The optical view cell is fixed on a XYZ stage (6) that can finely adjust the position of drops in three directions. A microscope system, including a microscope (7) and CCD camera (8), is used to take drop images and to export image signals to a monochromatic monitor (9) and computer system (10, 11). The microscope and camera are mounted on another XYZ stage (12). The stage is also three-direction adjustable and it has a function to change the angle between the microscope and the horizon as well. The whole optical system is mounted and aligned on an optical rail (13).

The computer (10) has a high-accuracy, programmable frame grabber board for PCI bus, which accepts video signals in many different monochrome formats and digitizes the image.

The board either stores the digitized data to the host computer's memory system or transfers the digitized data to the computer's display images in real time. An ADSA-P program is used to analyze images and implement the numerical procedure that yields results including interfacial tensions, contact angles, and other parameters.

Most cameras and lenses produce slightly distorted images, and this distortion can cause major errors in the final results, particularly in the interfacial tension. A square reticule was used in order to check the distortion of the optical system. By taking the image of a calibration grid and knowing the spacing between the grid lines, ADSA-P can correct the drop image for optical distortion.

The optical view cell, used to hold the pendant drop, has two sapphire windows (see Fig.3.3), mounted perpendicular to the cell axis. Measurements of surface or interfacial tensions involving low molecular weight liquids under atmospheric pressure indicate that the distortion of the sapphire window is not significant. It is believed that the sapphire window's distortion under pressure of less than 30Mpa is negligible as well. Most of the sapphire window's distortion is not significant.

The optical view cell consists of an electrically heated, hollow cylinder stainless steel chamber, in which the pendant drop is formed. A schematic representation of the cell is shown in Fig.3.3. For simplicity the heater is not shown. The inside of cell is cylindrical in shape, with dimension of 30mm (diameter) and 25mm (length). Two flat optical-quality sapphire windows (Meller Optics, Inc.), sandwiched between brass and Teflon gaskets within the chamber, permit illumination and viewing of the drop. The temperature of the cell was maintained with an accuracy of ± 1°F (0.5°C) using a temperature controller (Fuzypro F15) in conjunction with a type-K thermocouple. The thermocouple was located approximately

30mm from the pendant drop and the temperature reading was interpreted as that of the pendant drop environment. A number of threaded ports were drilled to allow for placement and easy removal for cleaning of the sapphire window and for the syringe (to produce pendant drops through the capillary). The pressure tube was attached to the view cell by Swagelok male connections with tapered pipe threads (NPT).

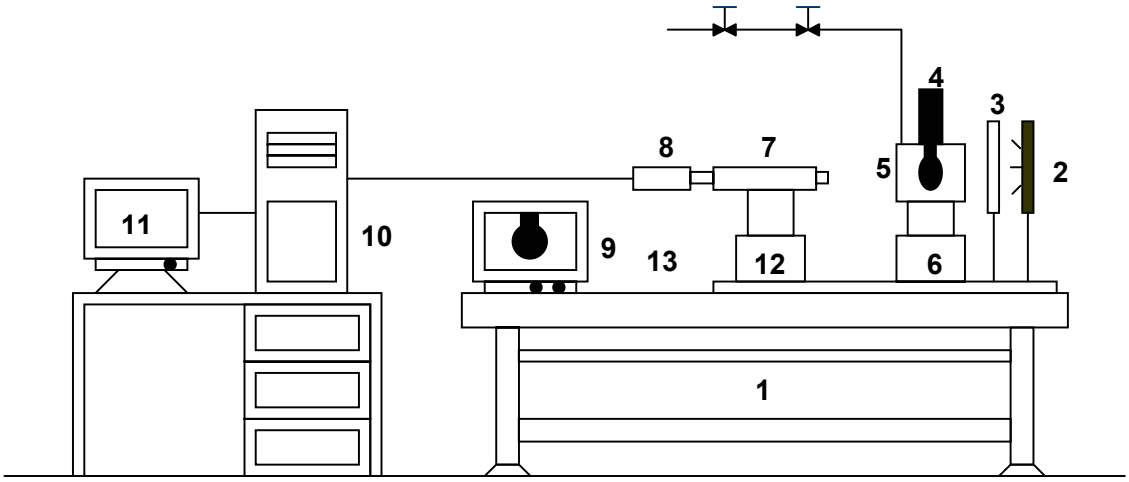

1. Vibration free table 2. Light source 3. Light diffuser 4. Feeding/holding rod for melts
5. View cell with heater 6. XYZ stage 7. Microscope 8. CCD Camera
9. Monitor 10. Computer 11. Monitor 12. XYZ stage
13. Optical Rail

Figure 3-2 Schematic diagram of the pendant drop apparatus

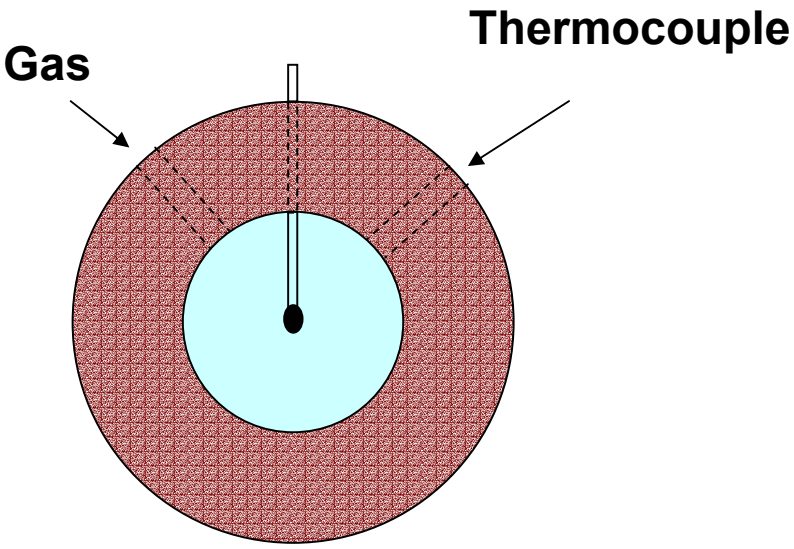

(a). Front View

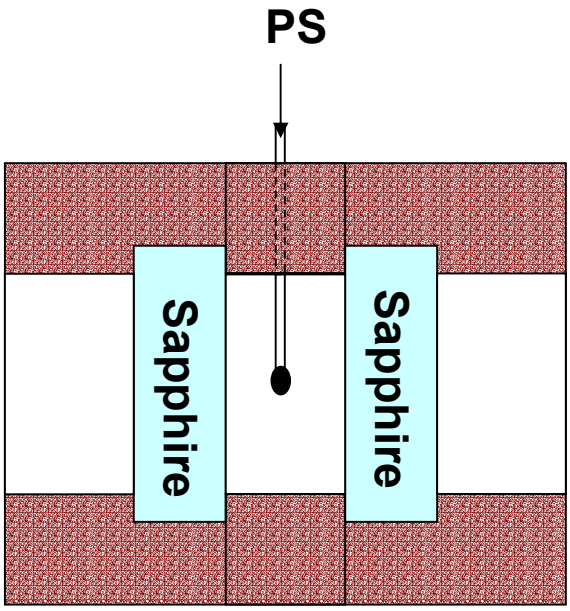

(b). Side View

Figure 3-3 Schematic diagram of the optical view cell

3.3 Materials

3.3.1 Polystyrenes

Polydisperse polystyrene (Styron 685D, weight average molecular weight (Mw) =312,000, polydispersity index =2.6) was obtained from Dow Chemical Company. Two monodisperse polystyrenes were obtained from Polyscience Inc. Table 6-1 shows the molecular weight information of these polystyrenes.

Table 3-1 Physical Properties of the Polymer Polystyrene molecular weights

Polystyrenes (PS)	Supplier	[1]M_w[g/gmol]	[2]M_n [g/gmol]	M_w/M_n
Polydisperse PS	Dow Chemcials	312,000	120,000	2.60
High molecular weight monodisperse PS	Polyscience Inc.	400,000	377,000	1.06
Low molecular weight monodisperse PS	Polyscience Inc.	100,000	96,000	1.04

[1]M_w [g/gmol]: weight averaged molecular weight.

[2]M_n [g/gmol]: number averaged molecular weight.

The data of the molecular weight of the polydisperse PS are from other researchers (Machell, 1990), and those of the monodisperse PSs are from the manufacturers.

3.3.2 Carbon Dioxide

Carbon dioxide of 99.997% purity (SCF/SCE grade with a helium head) was used as received from Air Products and Chemicals

3.3.3 Nitrogen

Nitrogen (critical pressure = 492 psi, critical temperature = -147°C) at 99.99% purity was purchased from PRAXAIR (Danbury, CT, USA).

3.4 Experimental Procedure

A pellet of PS and the holding rod were both cleaned with ethanol. The holding rod and the optical viewing cell were heated up to the desired temperature. A polymer pellet was placed in a position to ensure contact between it and the bottom surface of the rod. The pendant was created upon melting the PS pellet and held at the bottom surface of the rod (of 1.5 mm in diameter). Image acquisition of the pendant drop profile was performed and digitalized each minute. When the observed surface tension variation was small enough (< 5%) for at least 1 hour the surface was considered to have reached equilibrium and the surface tension was adopted as an equilibrium surface tension and used for further analyses.

3.5 Method Verification

The surface tension of water and acetone at room temperature and atmospheric pressure was measured to validate the apparatus. Table 3-2 demonstrates that the measurement data

collected are consistent with the data found in other studies (Raton, 1981). The surface tension of water was measured at different tilt angles; the results are shown in Fig. 3-4. When the pendant drop was tilted, the surface tension values were slightly changed with the angle variation.

Table 3-2 Comparison of measured surface tension with literature values

Substance	density	Surface Tension(mJ/m²)	
		this work(at 24.5°C)	Literature(*)
water	0.998	72.10±0.032	72.14 at 25°C
acetone	0.7899	23.52±0.008	23.70 at 20°C

* Raton, 1981

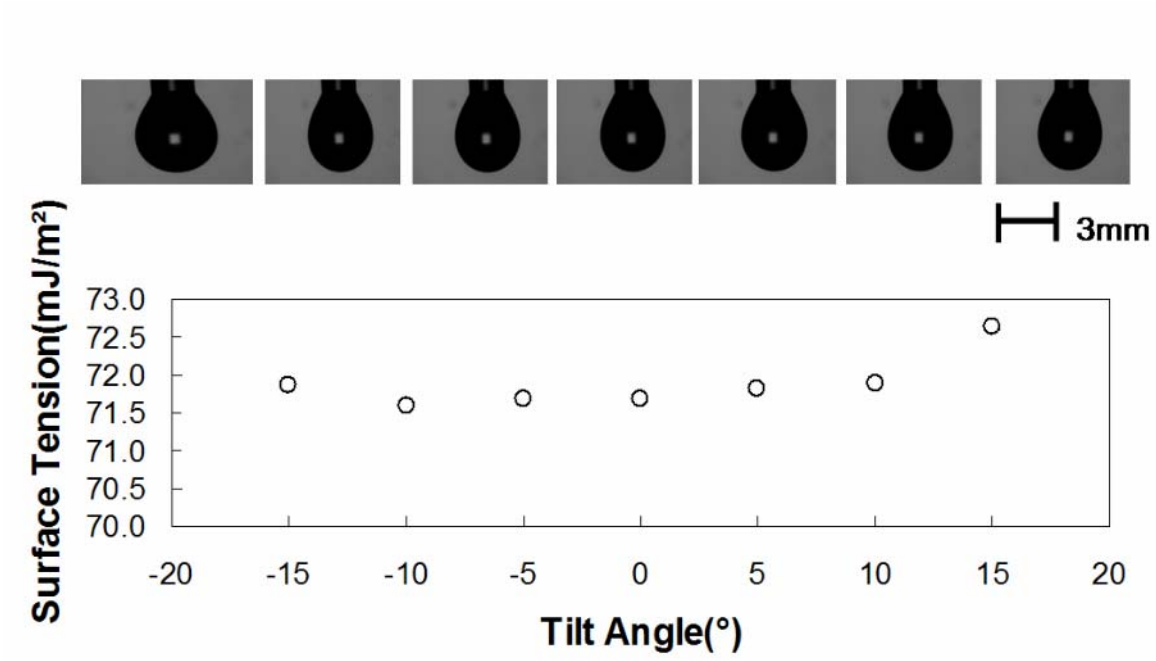

Figure 3-4 Effect of tilt angle on surface tension of water

The tilt angle is defined as the angle between the symmetric line of the drop and vertical lines.

The symmetry of the axis is one of the critical assumptions in Axisymmetric Drop Shape Analysis-Profile (ADSA-P). This assumption is valid for most Newtonian fluids; however, it is not easy to obtain an axisymmetric polymer drop because of the initial shape of polymer melts and its high viscosity. This symmetry was examined from an experimental perspective in order to measure the surface tension of the polymers. The image of the sample drops was grabbed and analyzed using ADSA-P at two different directions, which were perpendicular to one another. If the axis symmetry is not secured, the surface tension may have an error of 5% (see Fig. 3-5). After the axis symmetry is secured, the margin of error can be decreased to about 1%. By measuring the volume of the drop, the axis symmetry was thus reconfirmed: The density was calculated by assuming that no reaction occurs at high temperatures. The density deviation can be decreased from 5% to 1% by using an axisymmetric drop, as is evident in Fig. 3-6.

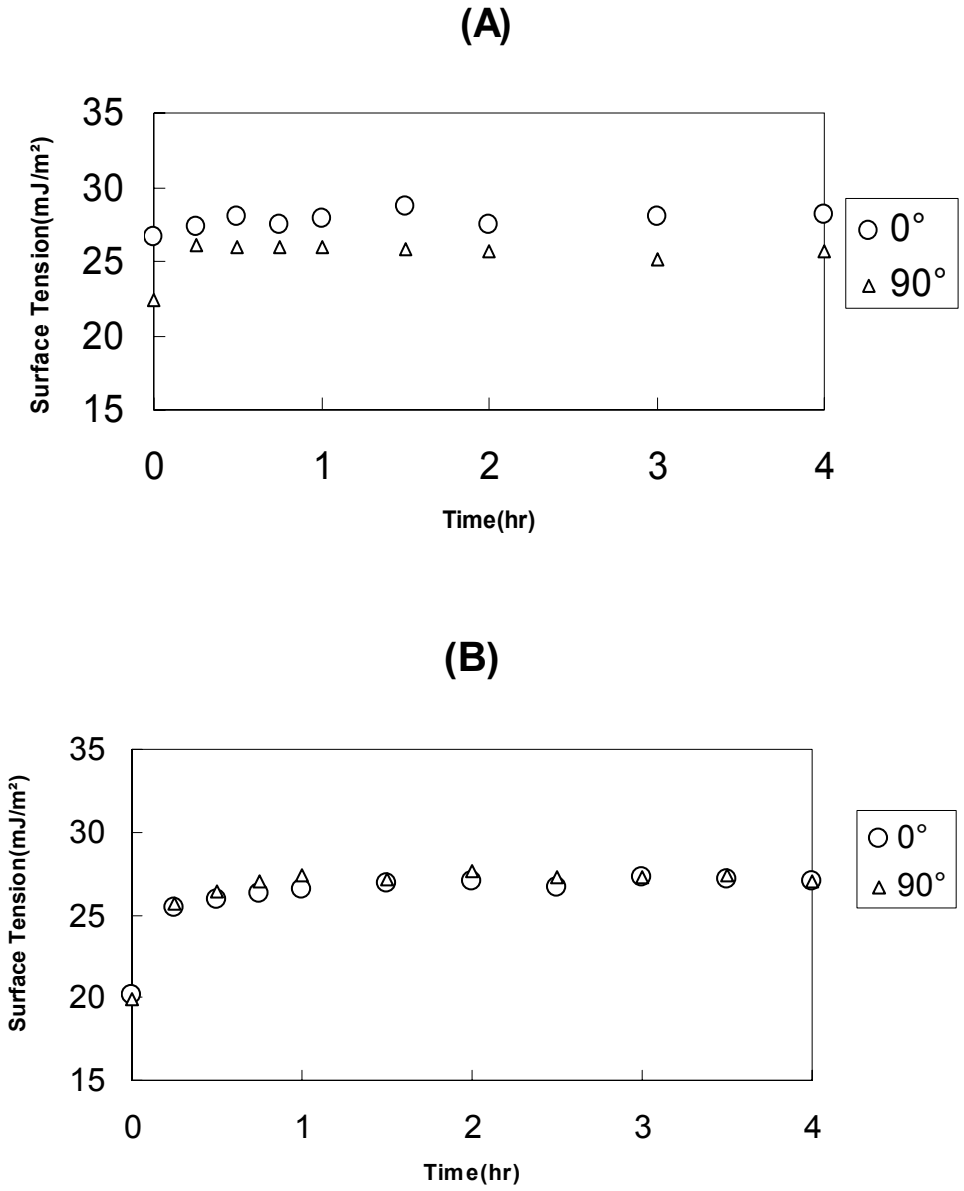

Figure 3-5 Effect of axis symmetry on the surface tension of polymer melts; (a) non axisymmetric drop , (b) axisymmetric drop.

The degree of 0° and 90° represents the respective direction of the microscope from the drop.

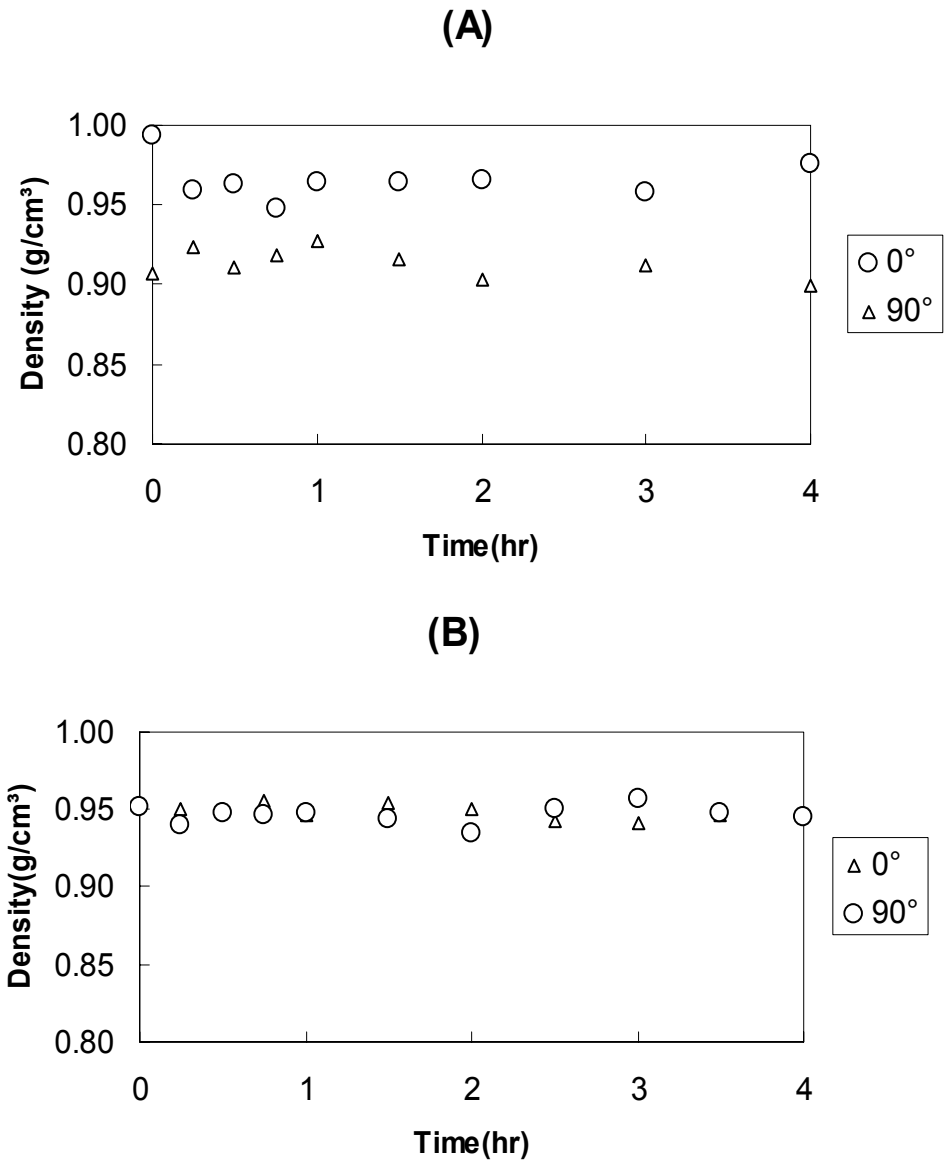

Figure 3-6 Effect of axis symmetry on the density of polymer melts; (a) non axisymmetric drop , (b) axisymmetric drop.

The degree of 0° and 90° represents the respective direction of the microscope from the drop

The reproducibility of the experiment was tested by measuring the surface tension of the PS melts in N_2 at different temperatures. Fig. 3-7 illustrates the surface tension as a function of the following temperatures: 210°C, 200°C, 190°C, and 180°C. For each temperature, two runs were conducted. The surface tension measurements exhibited good consistency from run to run. The polymer surface tension in N_2 was further measured in the order of decreasing temperature. This is illustrated in Fig. 3-8 at four different temperatures: 210°C, 200°C, 190°C, and 180°C. The surface tension values from this experiment proved to be consistent with the data from two other studies (Wu, 1970; Kwok *et al.*, 1998). The question whether the surface tension values of two consecutive temperatures in Fig. 3-8 are actually the same or significantly different can be answered as follows: A t-distribution test was done to ascertain the statistical difference of two consecutive surface tension values (Milton and Arnold, 1995). If the calculated t value was higher than the critical tabulated value, this would suggest that the means are different at the selected significance level. If not, the values would then demonstrate no significant difference. Table 3-3 shows the surface tension values of 10 runs at different temperatures. In this study, the tabulated t values were chosen to achieve a 95% confidence level and a two-sided question (t critical (95%, 2s)) (Milton and Arnold, 1995). The calculated t values are from the following equation:

$$t_{cal} = \frac{\left|x_1 - x_2\right|}{\sqrt{\frac{s_1^2 + s_2^2}{n}}} \qquad (3\text{-}7)$$

where x is the mean; s is the standard deviation; and n is the number of data points.

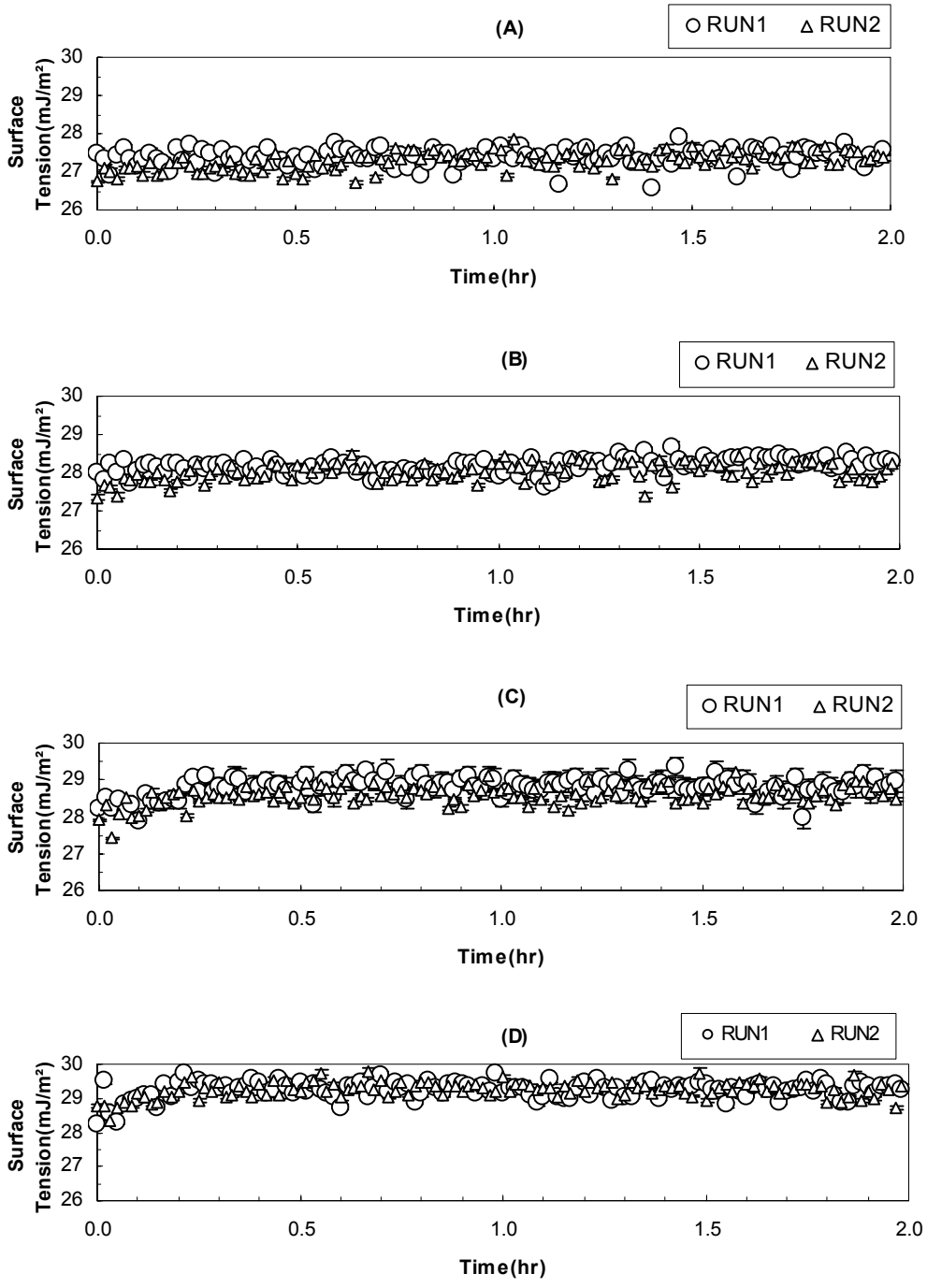

Figure 3-7 Reproducibility test: results of two runs for the surface tension of polystyrene melts in N_2 as a function of temperatures. The temperatures used are (a) 210 ^oC, (b) 200 ^oC, (c) 190 ^oC(d) 180 ^oC. The error bars are the 95% confidence limits calculated from ADSA-P for each image.

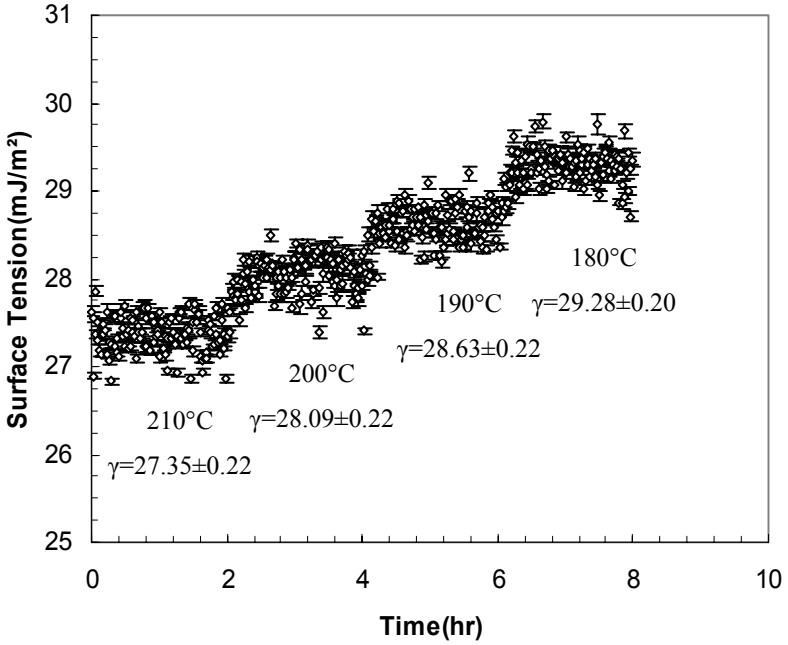

Figure 3-8 Surface tension of polystyrene for different temperatures in atmospheric pressure of N_2

The error bars are the 95% confidence limits calculated from ADSA-P for each image.

Table 3-3 Surface tension of PS melts at different temperatures with ADSA-P

Temperature	180°C		190°C		200°C		210°C	
Run No.	γ(mJ/m²)	95% C.L.	γ(mJ/m²)	95% C.L.	γ(mJ/m²)	95% C.L.	γ(mJ/m²)	95% C.L.
1	29.46	0.31	29.40	0.34	28.79	0.20	28.13	0.28
2	29.37	0.44	28.16	0.30	27.83	0.28	26.77	0.35
3	29.20	0.17	28.73	0.14	28.17	0.18	27.37	0.22
4	29.18	0.17	28.64	0.11	27.95	0.15	27.21	0.15
5	29.32	0.21	28.61	0.25	28.06	0.26	27.36	0.26
6	28.97	0.21	28.47	0.14	27.86	0.21	27.05	0.16
7	29.91	0.34	29.33	0.39	28.31	0.46	27.16	0.50
8	29.28	0.20	28.63	0.21	28.09	0.22	27.35	0.22
9	29.24	0.20	28.82	0.22	28.24	0.20	27.40	0.23
10	29.41	0.14	28.75	0.19	28.27	0.15	27.20	0.17
Mean	29.33	0.25	28.75	0.37	28.16	0.28	27.30	0.35

C.L. : confidence level

The t values were calculated in order to be able to compare the surface tensions of two temperatures. Table 3-4 indicates that the calculated t values were higher than the tabulated ones. This suggests that the surface tension values between two consecutive temperatures have significant differences at a 95% confidence level.

Table 3-4 Statistical comparison of surface tension means at various temperatures

Comparison	n	t cal	t critical(95%,2s)	significant difference
γ (180) / γ (190)	9	4.134	2.262	Yes
γ (190) / γ (200)	9	4.076	2.262	Yes
γ (200) / γ (210)	9	6.092	2.262	Yes

n : degrees of freedom

t cal : calculated t value

t critical(95%,2s) : tabulated t value at a 95% confidence level of 2 sides

ADSA-P was also used to measure the density of polymer melts from the mass and the volume of a polymer drop; the mass could be pre-weighed and the volume was an output of the ADSA-P program. For the determination of density, it was assumed that the mass of polymer drop was maintained constant during the experiment. Table 3-5 shows the density of PS melts at various temperatures. The t-distribution test was done using a similar method to the one described above. However, as shown in Table 3-7, the density values exhibit no significant difference from temperature to temperature. The errors involved in density calculations exceed the minute change in density with increasing temperature. The errors may be attributed to the way the drop volume is calculated with the ADSA-P program. In density calculations, two cut-off points have to be chosen manually near the boundary between the polymer and the metal holder; variations in the cut-off locations can cause the errors in volume calculations and hence affect the density results.

Table 3-5 Density of PS melts at different temperatures using ADSA-P

Temperature	180°C		190°C		200°C		210°C	
Run No.	ρ(g/cm^3)	95% C. L.	ρ(g/cm^3)	95% C. L.	ρ(g/cm^3)	95% C. L.	ρ(g/cm^3)	95% C. L.
1	0.97818	0.00385	0.97230	0.00404	0.96794	0.00270	0.96386	0.00330
2	0.97878	0.00460	0.97230	0.00404	0.96197	0.00385	0.96124	0.00431
3	0.98378	0.00189	0.97218	0.00217	0.96279	0.00247	0.95896	0.00270
4	0.97801	0.00383	0.97268	0.00292	0.96381	0.00353	0.95563	0.00350
5	1.01475	0.00274	1.00816	0.00363	1.01475	0.00377	1.00816	0.00395
6	1.01896	0.00343	1.00148	0.00311	1.01896	0.00501	1.00148	0.00403
7	0.95614	0.00220	0.90880	0.00324	0.95614	0.00474	0.90880	0.00463
8	0.98582	0.00298	0.98763	0.00326	0.96643	0.00338	0.95814	0.00404
9	1.00185	0.00320	0.97994	0.00294	0.97774	0.00279	0.96599	0.00411
10	0.97831	0.00238	0.97516	0.00334	0.96178	0.00320	0.97092	0.00314
Mean	0.98746	0.01908	0.97506	0.02666	0.97523	0.02265	0.96532	0.02703

C.L.: confidence level

Table 3-6 Statistical comparison of surface tension means at various temperatures

Comparison	n	t cal	t critical(95%,2s)	significant difference
ρ(180°C) /ρ(190°C)	9	1.196	2.262	No
ρ(190°C) /ρ(200°C)	9	0.015	2.262	No
ρ(200°C) /ρ(210°C)	9	0.889	2.262	No

n : degrees of freedom

t cal : calculated t value

t critical(95%,2s) : tabulated t value at a 95% confidence level of 2 sides

Although the individual density measurements involve the errors, the overall decreasing trend with temperature is comparable with those of others (Fig. 3-9). It should be noted that the same variations in the cut-off locations may induce uncertainties in surface tension measurement; however, the surface tension change with temperature is sufficiently large, i.e., statistically significant. In this work, only surface tension measurements were used to characterize the surface properties of the polymer melts.

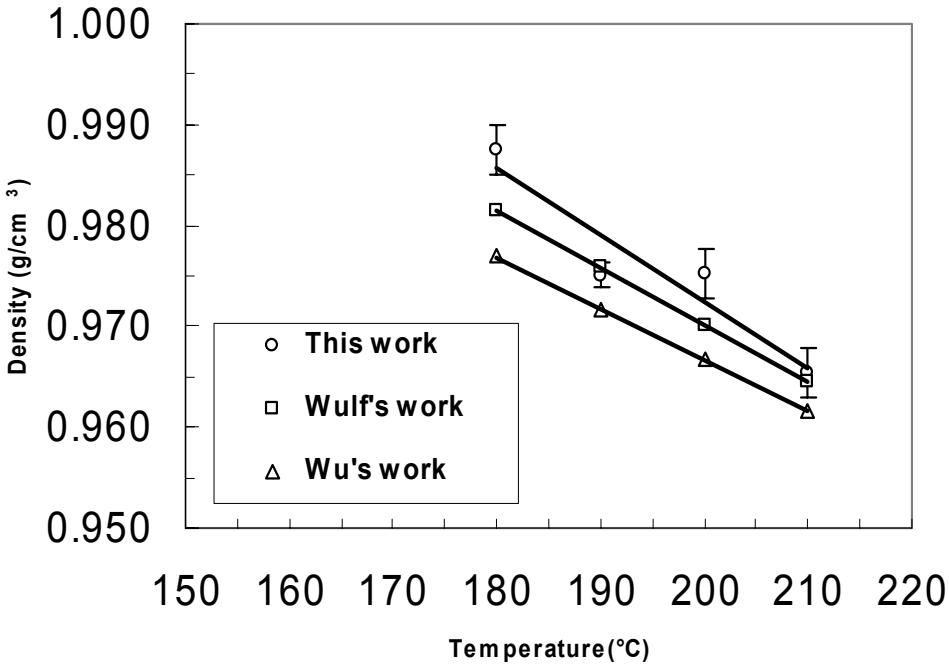

Figure 3-9 Comparison of this result and literature results of density for polystyrene in atmospheric pressure of N_2.The error bars are the 95% confidence level for each of the ten experiments.

Fig. 3-10 shows two different methods for evaluating the equilibrium surface tension of PS melts as a function of temperature. In the extrapolation method, the extrapolation to zero (i.e. $t = \infty$) was taken from the surface tension versus $1/t^{1/2}$ graph (Gonzalez and MacRitchie, 1970; Miller and Kretzschmar, 1991). In the averaging method wherein the final data points were used, the average of the surface tension values was taken as the equilibrium surface tension when the change in surface tension was smaller than 0.0001 mJ m^{-2} s^{-1} for 1 hour. The two types of surface tension agreed well. This agreement indicates that both methods are valid for obtaining the equilibrium value. In this study, however, the "averaging method" was adopted for simplicity.

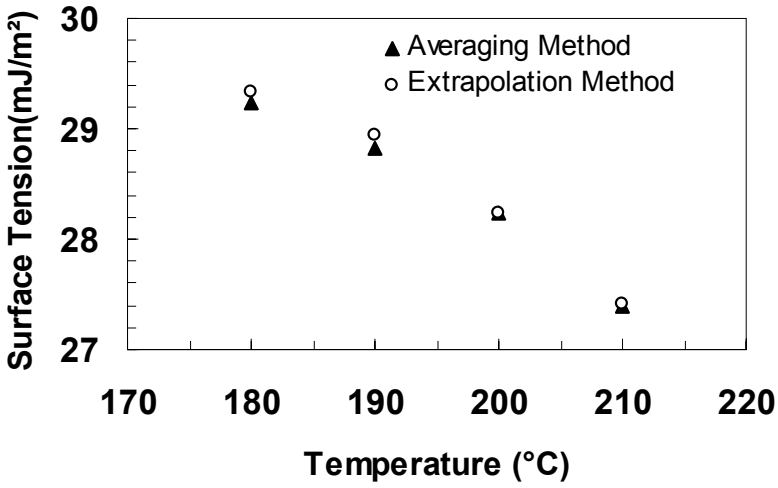

Figure 3-10 Surface tension obtained by the averaging method and extrapolation method at various temperatures

Fig. 3-11 compares the surface tension values of PS in the nitrogen atmosphere obtained in this study with the data found in the literature. We have discovered that the results yielded by this study agree well with those of two other previous experiments within the reasonable margins being considered the different molecular weights and unknown additive effects.

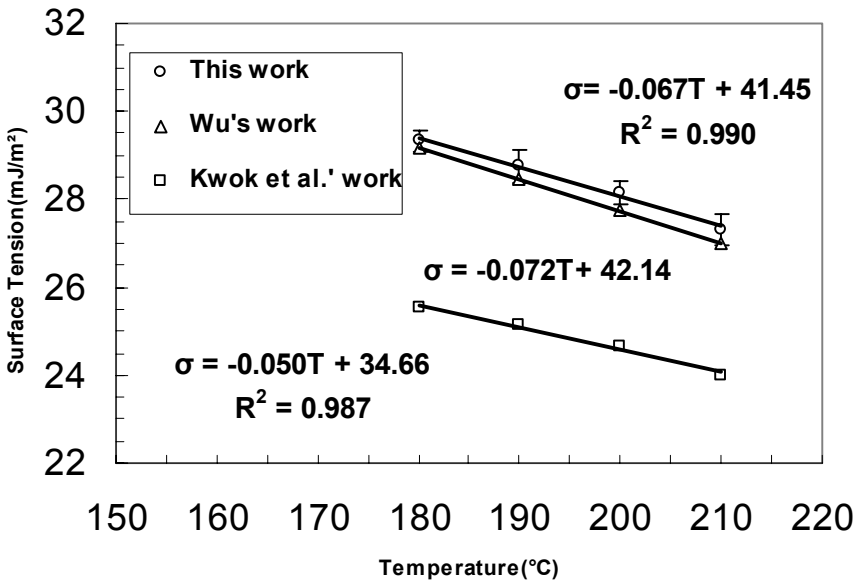

Figure 3-11 Comparison of this result and literature results of surface tension of polystyrene in atmospheric pressure of N_2

3.6 Dimensionless Numbers in Characterizing Drop Stability

To characterize the stability of pendant drops used in the experiment, we look into dimensionless numbers. Many industrial processes involve the dispersion of immiscible fluids. The importance of interfacial tension can be illustrated using the dimensionless capillary number (Ca) (Janssen and Meijer, 1993; Tomasko, *et al.*, 2003):

$$\mathrm{Ca} = \frac{\eta \dot{\gamma} \mathrm{R}}{\gamma} \tag{3-8}$$

where η is the viscosity of the polymer; $\dot{\gamma}$ is the applied shear rate; R is the drop radius; and γ is the interfacial tension or surface tension between the immiscible phases. The ratio of viscous force to surface force governs the situation between drop breakage and coalescence in polymer blending and foaming processes. It determines the domain size of the polymer blends and the cell size of the polymer foams. For a small capillary number, the interfacial force dominates and a steady spherical drop shape exists. If the value is higher than a critical value, the drop is unstable and drop breakage occurs. Within the range of $0.1<\mathrm{Ca}<10$, both coalescence and breakage phenomena take place simultaneously (Tomasko, *et al.*, 2003). The Ca numbers of our pendant drop case had to be very small, while the system was in the interfacial force dominant range because the shear rate was extremely small and the viscous force could have been neglected.

The stability of the polymer pendant drop may be related to the Bond number,

$$Bo = \frac{\Delta \rho g R^2}{\gamma} \tag{3-9}$$

where $\Delta\rho$ is the density difference between two phases; g is the gravitational acceleration; R is the drop radius; and γ is the interfacial or surface tension between the immiscible phases (Adamson and Gast, 1997). The Bond number is the ratio of buoyancy force to surface force. The number is used to indicate whether breakage occurs or the stable pendant drop is maintained. For a small Bond number, the interfacial force is dominant and the drop shape is stable. If the number is higher than a critical value, the drop is unstable and drop breakage will occur. Other researchers have similarly verified these phenomena (Demarquette and Kamal, 1994; Xue *et al.*, 2004).

In their pendant drop study, Ferri *et al.* have demonstrated that the Bond number values can range from 0.1 to 0.22 (Ferri *et al*., 2001). In our study, the drop size was optimized to achieve a stable pendant drop, and the Bond number was useful to determine whether the drop was stable. For large drop sizes, the pendant drops were unstable and breakage occurred because of the dominant gravity force. When the drop was at a critical volume, the Bond number became 1.4, which is greater than 1, and the pendant drop detached from the feeding rod (see Fig. 3-12). However, when the drop was smaller than a certain critical volume, the bond number 0.2, which is close to the lower limit of the critical value of 0.1 (Ferri *et al*., 2001), the drop liquid climbed up along the feeding rod (see Fig. 3-13). In the present study, the Bond number ranging from 0.4-0.8 can avoid the drop breakage and liquid climb-up. The Bond number range is higher than that of Ferri *et al.*, and this may be due to the density difference of the polymer melt. It is noted that the viscosity and melt strength are not considered in this study that deals with the equilibrium state of the interfaces. Fig. 3-14 shows how the vertical radius and the horizontal radius are defined to calculate the Bond number. The vertical diameter (Dv) is defined as the distance between the apex of the drop

and the capillary tip, while the horizontal diameter (Dh) is defined as the horizontal distance at the center of the vertical diameter. The radius of the drop in the Bond number calculations was the average of the vertical radius and the horizontal radius.

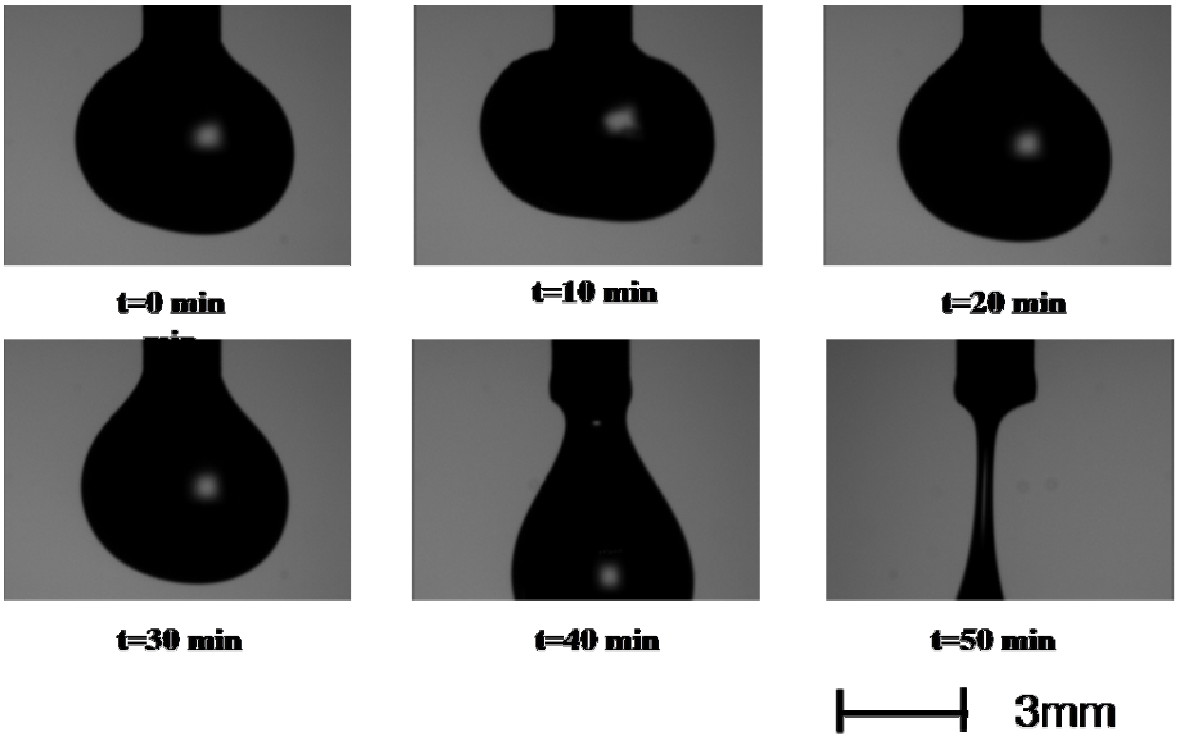

Figure 3-12 Evolution of polymer melts having higher volume than a critical volume

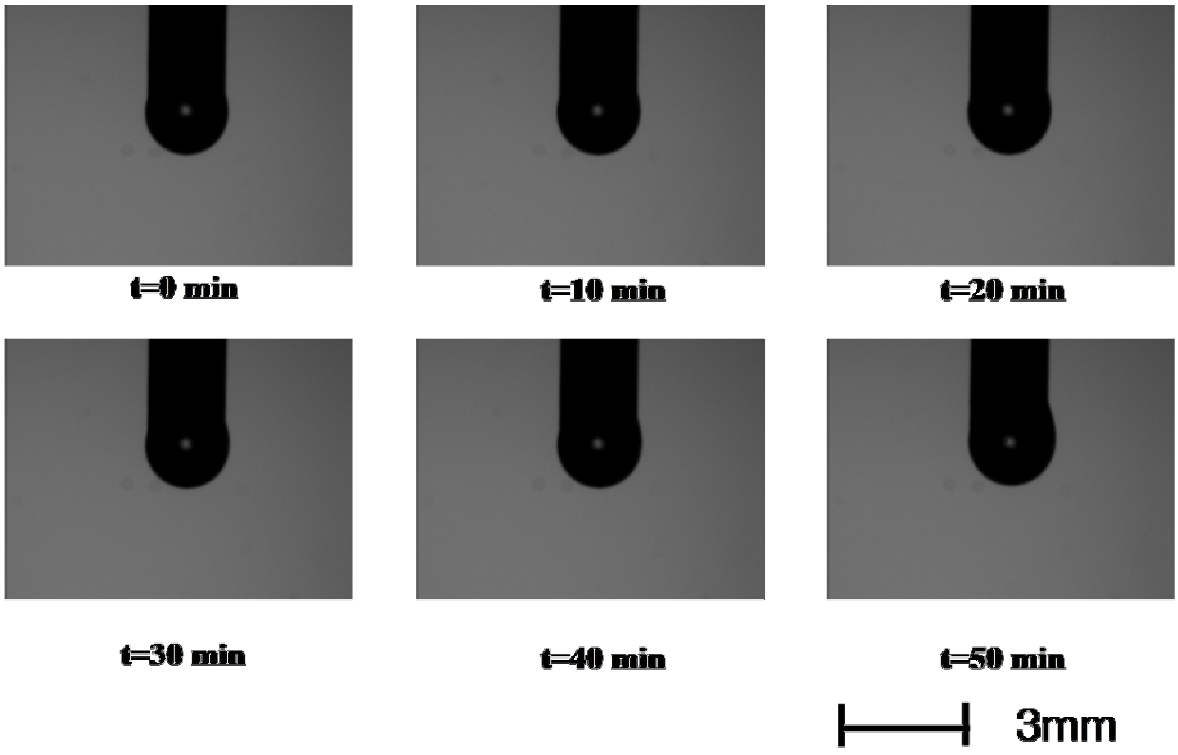

Figure 3-13 Evolution of polymer melts having smaller volume than a critical volume

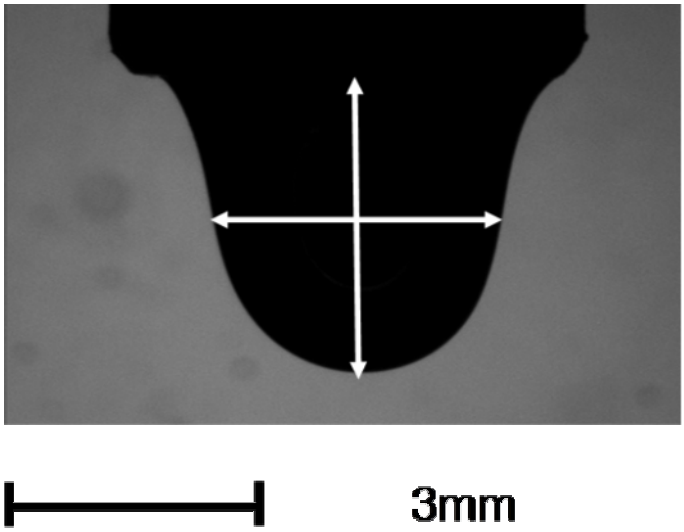

Figure 3-14 Definition of drop radius

*drop radius = (Dv (vertical diameter)/2 +Dh (horizontal diameter)/2)/2

3.7 Surface Tension of Polystyrene in Supercritical Carbon Dioxide

The surface tension of PS was measured in CO_2 under a wide range of pressures at two different temperatures of 210°C and 230°C, and the results are shown in Fig. 3-15. At higher pressures, the surface tension has a lower value. After the critical pressure (1,071psi) was reached, the surface tension continues to decrease.

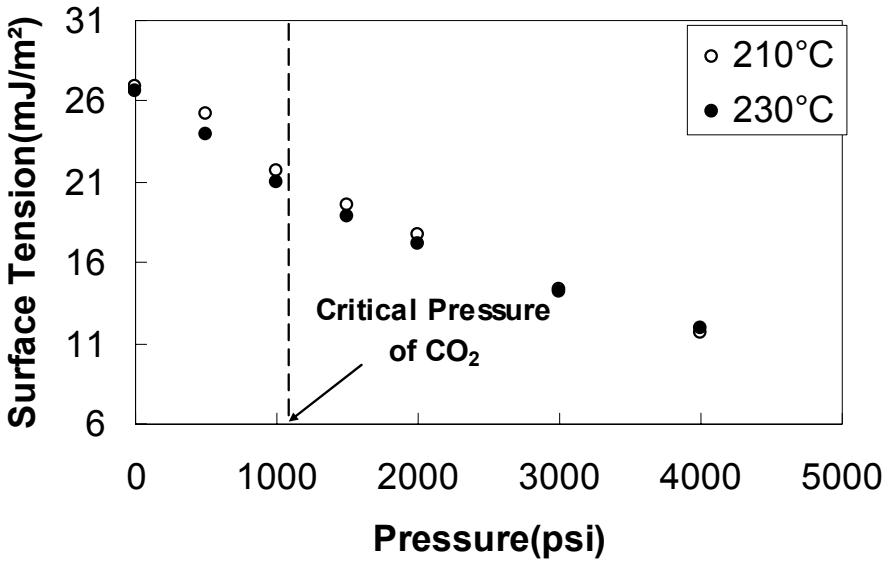

Figure 3-15. Pressure effect on the surface tension of PS in supercritical CO_2

3.7.1 The Relationship Between Surface Tension and Density

The relationship between surface tension and density may be expressed by the generalized Macleod equation (Macleod, 1923)

$$\gamma \text{ (surface tension)} = C\,(\rho_p - \rho_f)^n \qquad (3\text{-}10)$$

where γ is the surface tension; C is constant; ρ_p is the density of the polymer; ρ_f is the density of the fluid; and n is Macleod's exponent. The exponent n is close to 4 for many unassociated liquids of low molecular weight substances (Macleod, 1923; Ferguson and Kennedy, 1936). In this study, the exponent n is 4.5 at atmospheric pressure (see Fig. 3-16), which is very similar to Wu's results (Wu 1970). At atmospheric pressure, the exponent is of a higher value than when a low molecular weight substance is used. This is because the polymer exhibits conformational restriction at the polymer surface. Fig. 3-17 shows the relationship between surface tension and density difference for polystyrene in supercritical CO_2. With an increased pressure in supercritical CO_2, the exponent became approximately 2.5 because the conformational restriction decreased. This correlation can be applied to predict the surface tension at various temperatures and pressures.

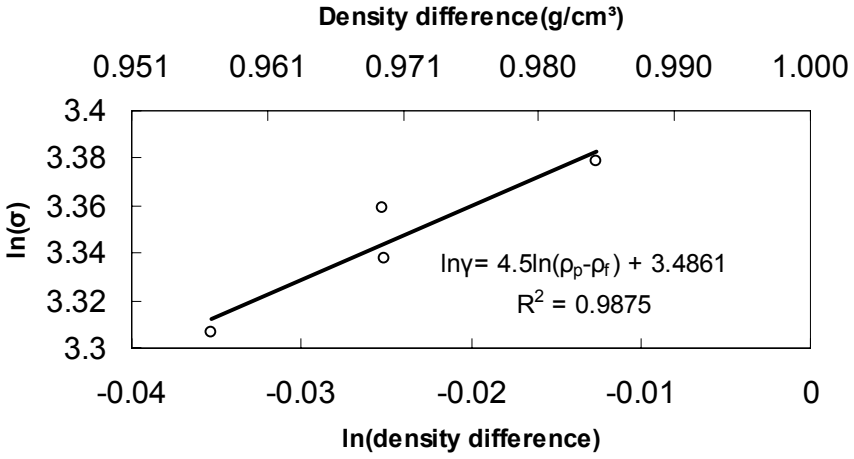

Figure 3-16. Relationship between surface tension and density for polystyrene in atmospheric pressure in N_2. The density difference is defined as the difference of density between polymer and gas.

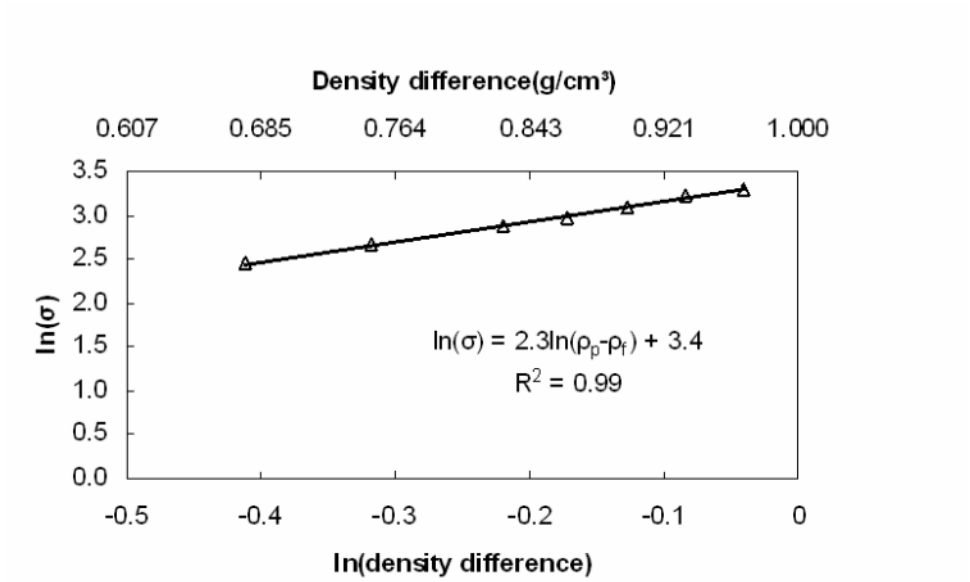

(a) at temperature 210°C

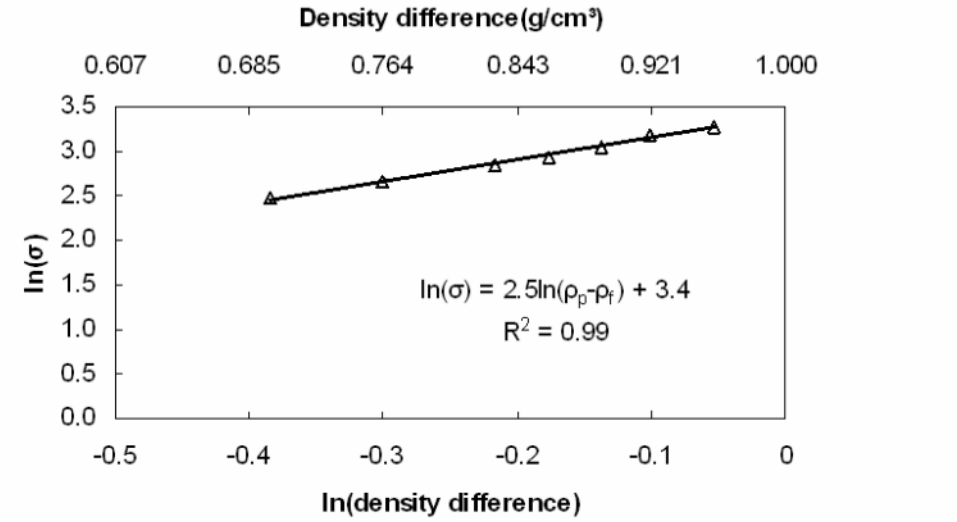

(b) at temperature 230°C

Figure 3-17. Relationship between surface tension and density for polystyrene in supercritical CO_2. The density difference is defined the difference of density between polymer and gas.

3.7.2 The Correlation Between Surface Tension and Solubility

The surface tension and solubility as a function of pressure for PS in supercritical CO_2 at 230^{o}C are shown in Fig. 3-18. As the pressure is increased, the solubility of CO_2 increases and the surface tension decreases (Li *et al.*, 2004).This is reasonable when considering the fact that an increase in gas-phase pressure will likely induce more gas dissolving into the liquid phase. Surface tension can be related to pressure and phase composition in general, and quite often decreases with increasing pressure and gas dissolution into the liquid phase (Li *et al.*, 2004).

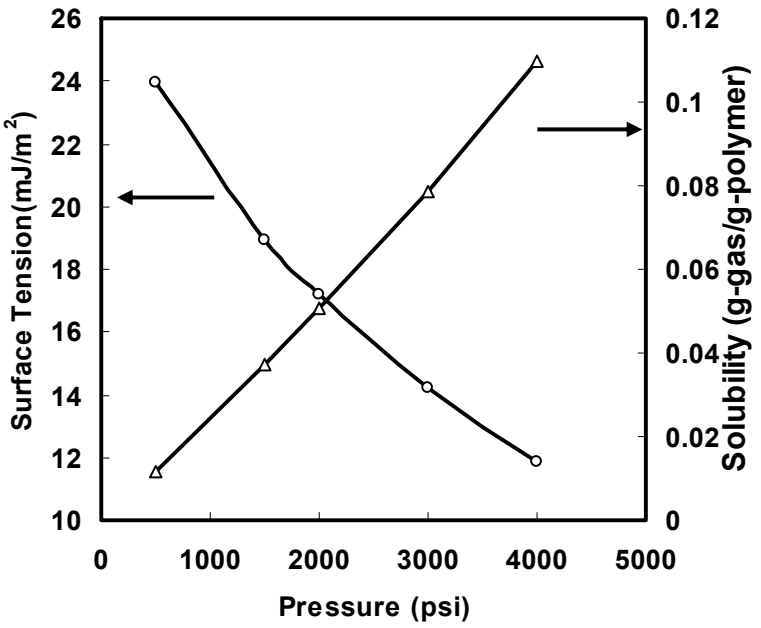

Figure 3-18. Relationship between the surface tension and solubility as a function of pressure for polystyrene in supercritical CO_2 at the temperature of 230^{o}C

Chapter 4
Density Determination of Polystyrene in Carbon dioxide and Nitrogen

4.1 Introduction

Surface tension is one of the most important parameters to understand various polymer processes, such as foaming, suspensions, wetting and blending (Myers, 1991). There are many methods to measure surface tension. Among them, the pendant drop method has many advantages because of the simplicity of apparatus and versatility of applications (Kwok *et al.*, 1998; Mason *et al.*, 2001).

The pendant drop method has a simple experimental setup and has been used extensively from low molar mass liquids and liquid crystals to polymers. This method includes the determination of a dense liquid drop profile in another liquid at the equilibrium interface of two liquids (Jannasch 1998; Cooper, 2000). Although the pendant drop method has the theoretical simplicity, the research to determine surface tension of polymer has been limited because of experimental difficulty in handling and ensuring the equilibrium of high viscous melts (Tomasko, *et al.*, 2003; Lee, *et al.*, 1999; del Rio and Neumann, 1997).The Axisymmetric Drop Shape Analysis (ADSA) method relies on numerical integration of Laplace equation of capillarity. This method has been used for determining polymer surface tensions at high pressure and high temperature (Rotenberg *et al.*, 1983).

For volume measurements of a pendant drop, the drop profile is modeled as its left profile $P_L(y)$ and right profile $P_R(y)$ as shown in Figure 4-1. In this study, the drop volume is

modeled as a series of discs that are perpendicular to the vertical axis of the drop. Midpoint rule is used for volume integration:

$$volume\ of\ drop = \pi \int R(y)^2 \, dy \tag{4-1}$$

where $$R(y) = \frac{P_R(y) - P_L(y)}{2} \tag{4-2}$$

is the radius for each disc centered at $$C(y) = \frac{P_R(y) + P_L(y)}{2} \tag{4-3}$$

It is also possible to use the trapezoid rule. However by integrating at a pixel scale resolution, the difference between the two methods is the same as descretization errors during drop profile extraction.

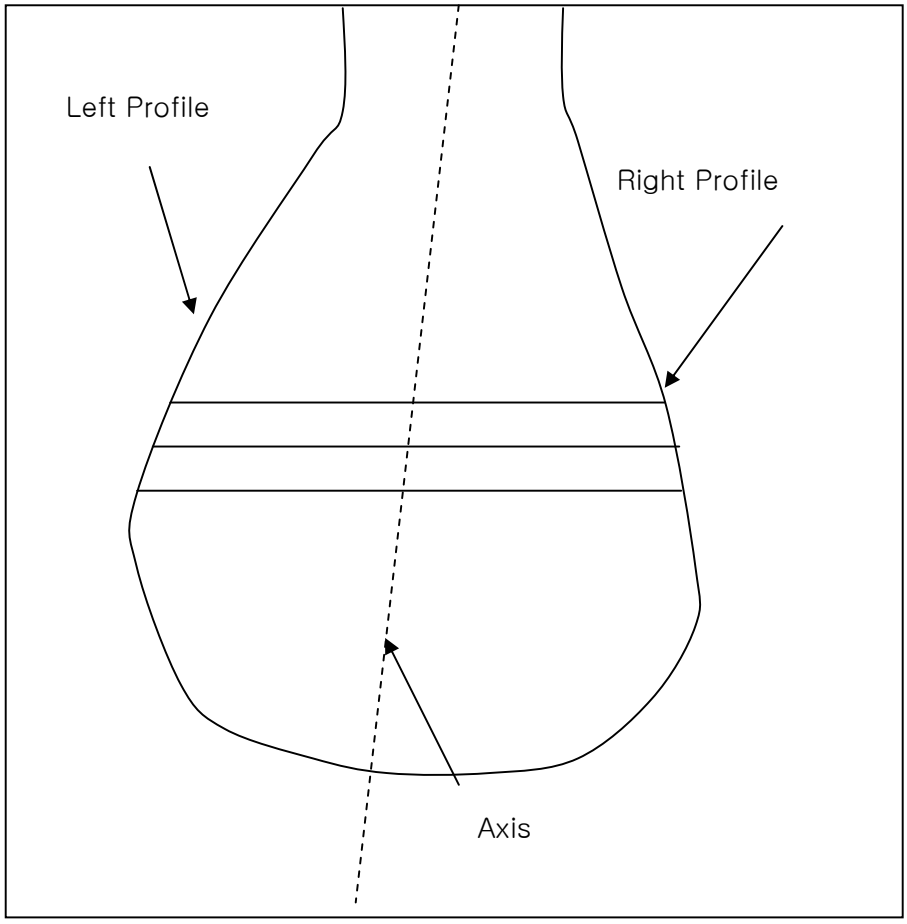

Figure 4-1. Volume integration along Y-axis of a drop image

In the Axisymmetric Drop Shape Analysis (ADSA) method, the density is an input parameter to determine the surface tension. The equilibrium drop profile is determined by the balance between gravity and interfacial tension. Interfacial tension can be determined from the drop profile. The interfacial tension can be evaluated by the Laplace equation of capillarity (Lahooti *et al.*, 1996).

From the algorithm of ADSA-P method, the accurate relation of pressure (P), temperature (T), and volume (V) is essential in improving the accuracy of surface tension. However, density measurements are limited, time consuming and costly (Lau and Burns,

1973; Alexopoulos *et al.*, 1989; Song and Springer, 1996). In previous research work, the sessile drop was employed to measure the surface tension and density simultaneously in high temperature (Anastasiadis *et al.*, 1986; Demarquette and Kamal, 1994; Wu 1970).

The density of polymers is not only as an input parameter for the determination of the surface tension of polymers, but is also used as a function of temperature and pressure, which play as important roles in understanding of many polymer physics and engineering processes. The relation of pressure, temperature, and density in polymers is useful to optimize process parameters, predict polymer-polymer miscibility, and correlate the reducing parameters pf equation of state with molecular structures. Among equations of states, The Tait equation is well known as a successful semi empirical equation for predicting the density of amorphous polymers (Hess, 2004; Quach and Simha, 1971; Zoller *et al*., 1976). As a Tait equation method, the parameters for polystyrene in nitrogen are:

$$v_p = v_o\left[1 - 0.0894\ln\left(1 + \frac{\mathrm{P}}{\mathrm{B(T)}}\right)\right] \tag{4-4}$$

where, v_p is the specific volume (cm^3/g), P is the pressure of samples,

$$v_o = 0.7884\exp(5.790\mathrm{X}10^{-4}\,\mathrm{T}) \tag{4-5}$$

$$\mathrm{B(T)} = 887.2\exp(-4.323\mathrm{X}10^{-3}\,\mathrm{T}) \tag{4-6}$$

Sato et al. employed the Sanchez and Lacombe (S-L) equation of state (EOS) to measure the solubility of gases in high pressure and temperature (Sato *et al*., 1976). The densities of polystyrene saturated with nitrogen were also determined by the Sanchez and Lacombe (S-L) equation of state (EOS) as expressed below:

$$\tilde{\rho}^2 + \tilde{P} + \tilde{T}\left[\ln(1-\tilde{\rho}) + (1-1/r)\tilde{\rho}\right] = 0 \tag{4-7}$$

where $\tilde{\rho}$ is the reduced density, $\tilde{P}$ is the reduced pressure, $\tilde{T}$ is the reduced temperature and r is the number of sites occupied by a molecule; they are defined as

$$\tilde{P}=\frac{P}{P^*},\tilde{\rho}=\frac{\rho}{\rho^*},\tilde{T}=\frac{T}{T^*},r=\frac{MP^*}{RT^*\rho^*} \tag{4-8}$$

where ρ is the density, P is the pressure, T is the temperature, M is the molecular weight and R is the gas constant. In the equation, the characteristic parameters, P^*, ρ^*, and T^*, of the S-L EOS for the mixture were evaluated using the following mixing rules:

$$P^*=\sum_i\sum_j \phi_i\phi_j P^*_{ij},\ P^*_{ij}=(1-k_{ij})(P^*_i P^*_j)^{0.5},\ T^*=P^*\sum_i\frac{\phi_i^0 T_i^*}{P_i^*},$$

$$\frac{1}{r}=\sum_i\frac{\phi^0{}_i}{r^0{}_i},\ \phi_i^o=\frac{\left(\phi_i P^*{}_i/T^*{}_i\right)}{\sum_j\left(\phi_j P_j^*/T^*{}_j\right)},\ \phi_i=\frac{\left(w_i/\rho_i^*\right)}{\sum_j\left(w_i/\rho_i^*\right)} \tag{4-9}$$

where $T^*{}_i$, $P^*{}_i$, ρ_i^*, and $r^0{}_i$ represent the characteristic parameters of the component *i* in its pure state, and in particular, two of the characteristic parameters are defined as

$$T^*=\frac{\varepsilon^*}{k_B},P^*=\frac{\varepsilon^*}{v^*} \tag{4-10}$$

where ε^* is the interaction per mer, and v^* is the close-packed mer volume (Sanchez and Lacombe, 1976; Sanchez and Lacombe,1978).

In this work, the integration method is used to determine the volume of polymers at various conditions. For the calculations, the volume of a drop is taken by intercalating the edge positions of a drop along the drop heights. The weight changes of polymers are considered from solubility values of available literature (Sato *et al*., 1976).

The primary goal of this study is to investigate the possibility of simultaneous measurements of surface tension and density of polystyrenes in supercritical nitrogen using the Axisymmetric Drop Shape Analysis (ADSA) method. For the simultaneous measurements of surface tension and density, a recently designed high-temperature and high-pressure sample cell is employed. At a given pressure (500psi), the temperature effect on surface tension and density is discussed.

4.2 Experimental

4.2.1 Density and Surface Tension Measurements

The volume of polystyrene in nitrogen was measured at different temperatures, from 30 to 210°C, at the pressures of 500 psi. Figure 4-2 shows a 3 dimensional drop which is assumed as a typical pendant drop profile which is shown in Figure 4-3. For density calculations, the volume was measured from the drop images by assuming that the drop is symmetric with the z-axis. The polymer pellets were weighted before the experiment. The solubility of nitrogen was calculated from literature results (Sato *et al*., 1976).

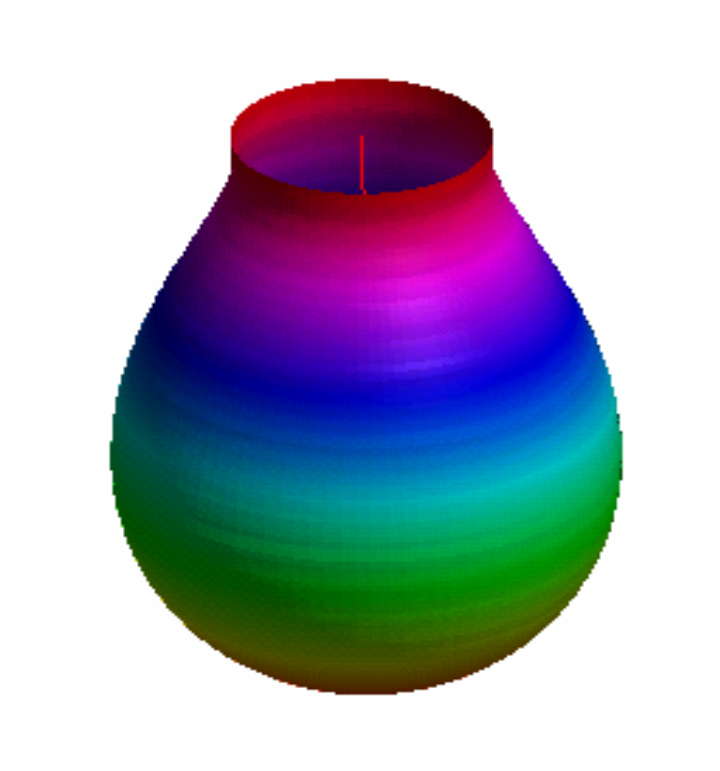

Figure 4-2. Typical pendant drop profile of polystyrene melt in supercritical nitrogen

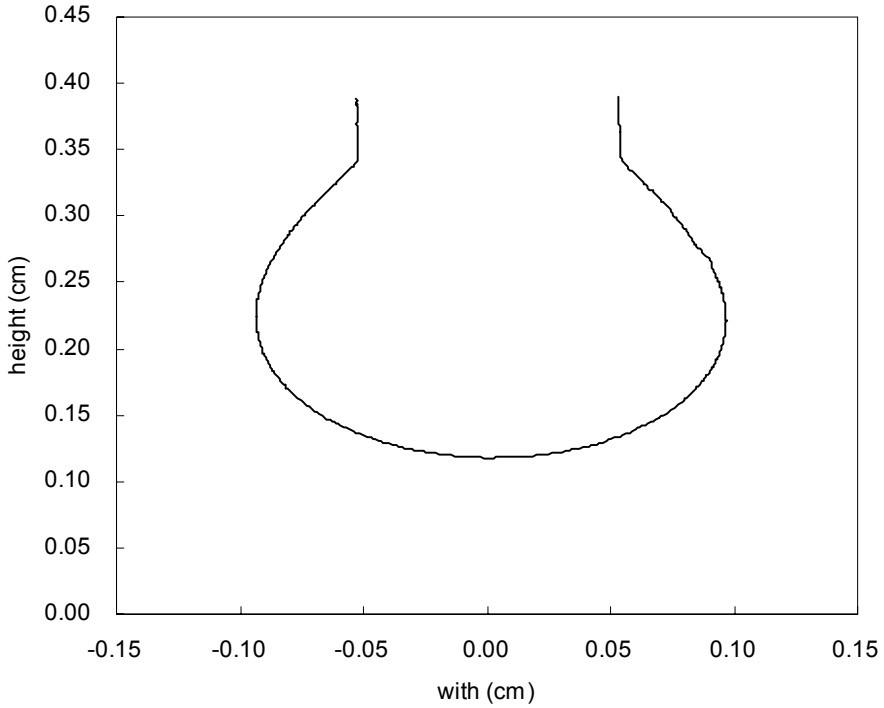

Figure 4-3. Typical pendant drop profile of polystyrene melt in supercritical nitrogen

The characteristic parameters for calculating the density using the S-L EOS are given in Table 4-1. The binary interaction parameter, k_{12}, was determined in order to minimize the relative experimental deviation at each given temperature, and the determined binary interaction parameters at different temperatures are included in Table 4-2.

To achieve these experimental conditions, a high-temperature and high-pressure sample cell was used. This optical viewing cell consisted of a cylinder of stainless steel, which was heated by an electrical band heater. The cylinder was hollow, with an inner diameter of 30 mm and length of 25 mm. Two optical-quality sapphire windows (Meller Optics, Inc.) permitted the illumination and observation of the pendant drop formed by a sample polymer melt. The experimental setup was tested for its accuracy and reproducibility

with a range of polymer-gas combinations, and the details of this setup were described in a recent publication (Park *et al.*, 2006). For the purpose of calibration, the volume was measured by the Axisymmetric Drop Shape Analysis (ADSA) method that was compared with the integration method from the profile as shown in Figure 4-4.

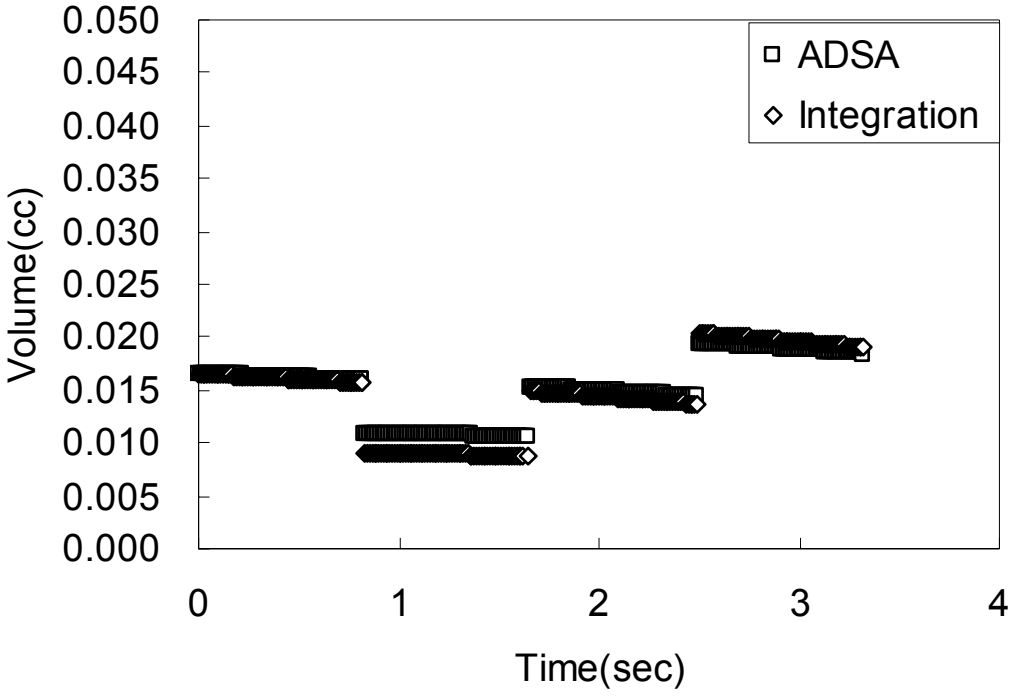

Figure 4-4. Comparison of volume measurements with the Axisymmetric Drop Shape Analysis (ADSA) method and the integration method for various drops

4.3 Results and Discussion

4.3.1 Density Measurements

The density results are shown in Figure 4-5. The agreement of the density measurements is very good over the experimental ranges. Specifically, the results show a successful agreement at higher temperature than the glass transition temperature of the polystyrene. This is rationalized that the Tait equation and the S-L EOS are widely used at the temperatures above the glass transition temperature and the axis symmetric assumption of this work is valid at the conditions. Meanwhile, the discrepancy at the lower temperatures than the glass transition temperature implies that the polymer exists as a glass state so it may have to have extremely high viscosity. This also is due to the difficulties to obtain the axis symmetric drop shapes at the low temperature conditions.

The technique of Axisymmetric Drop Shape Analysis-Profile (ADSA-P) (Cheng *et al.*, 1990; Susnar *et al.*) was used for image analysis and parameter extraction. Surface or interfacial tensions were obtained by fitting the Laplace equation of capillarity to the acquired shape and dimensions of axisymmetric menisci (Andreans *et al.*, 1986). The value of surface tension was generated as a fitting parameter (Cheng and Neumann, 1992) after a least-square algorithm was employed to minimize the difference between experimental and theoretical drop profiles. During this procedure, the density difference between polystyrene and nitrogen was an input parameter (Li, *et al.*, 2004; Xue *et al.*, 2004), which were determined by the Tait equation, Sanchez and Lacombe (S-L) equation of state (EOS), and ADSA-P method (Sato *et al.*, 2001; Wulf *et al.*, 1999a; Wulf *et al.*, 1999b). The result from Tait equation, the density was also used to improve the accuracy of surface tension.

Table 4-1. Characteristic parameters for the Sanchez-Lacombe equation of state (Sato *et al.*, 1996)

Substance	P^* [MPa]	ρ^* [kg/m^3]	T^* [K]
PS	387.0	1108	739.9
Nitrogen	103.6	803.4	159.0

Table 4-2. Binary interaction parameters (k_{12}) of polystyrene and carbon dioxide for different temperatures

Temperature(°C)	Interaction parameter(-)
30	0.245
50	0.239
70	0.233
90	0.227
110	0.221
130	0.215
150	0.209
170	0.203
190	0.197
210	0.191

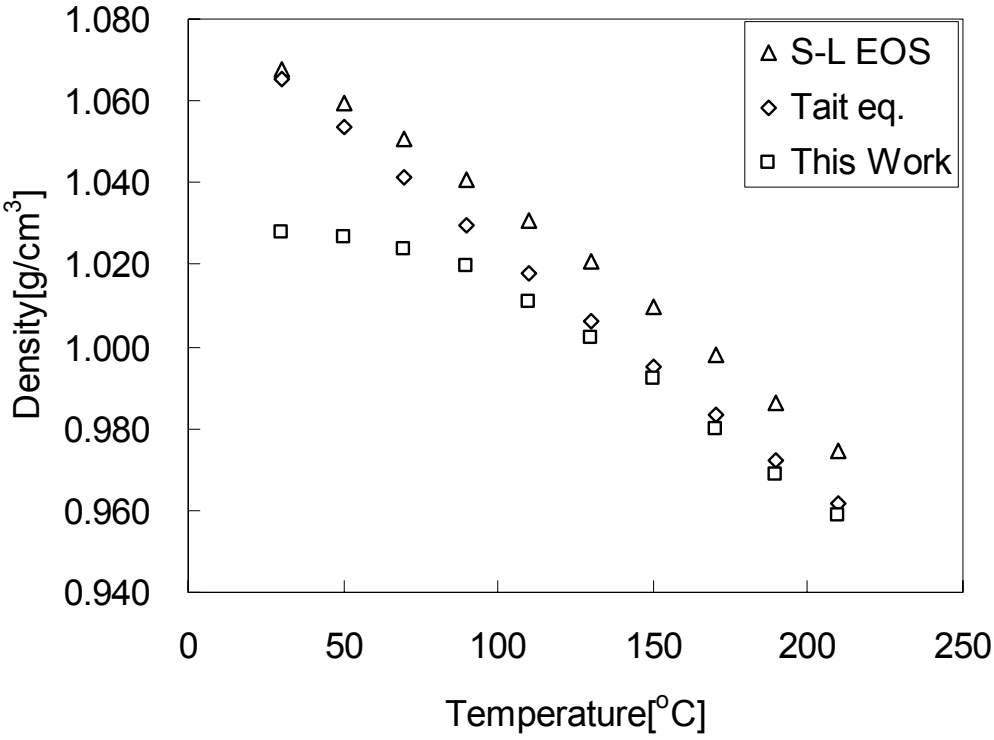

Figure 4-5. Temperature dependence of polystyrene density for three different density calculation methods

4.3.2 Surface Tension Measurements

The density results are shown in Figure 4-6. It is well known that the surface tension is decreased as the temperature increases in many polymer and gas systems that are at the higher temperatures than the glass transition temperature of a polymer. This result is consistent with previous investigations at the higher temperature regions (above 130^{o}C). However, the measurement of the surface tension at temperatures near the glass transition temperature is a difficult task because of the high viscosity of polymers. It this research work, the surface tension up to 130^{o}C showed fluctuations of surface tensions. This is reasonable because the polymer existed in the solid-state at temperatures which are below the glass transition temperature.

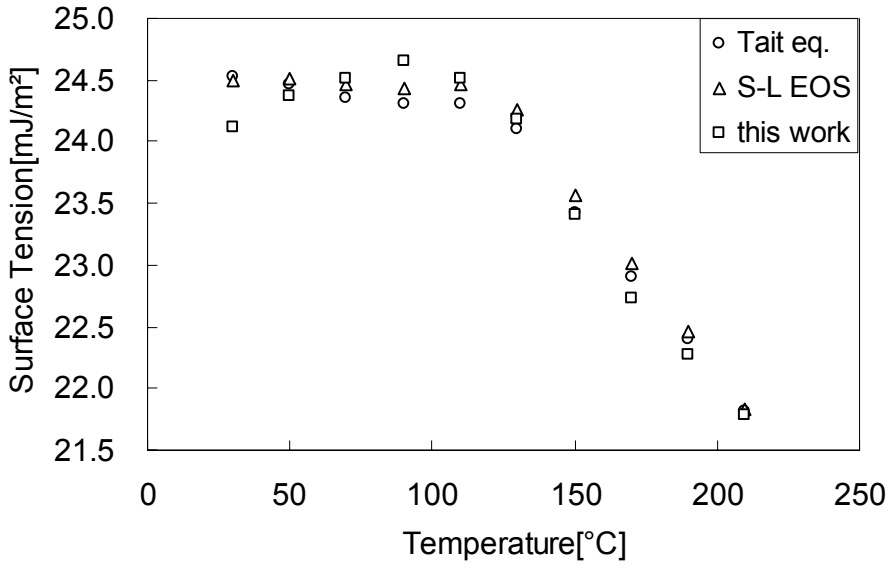

Figure 4-6. Temperature dependence of polystyrene density for three different density calculation methods

4.3.3 Surface Tension Measurements

The glass transition temperatures of polymers at high pressure are measured by differential thermal analysis (Richardson, 1975; Takamiazwa and Toratani, 1992). This work shows that the glass transition temperature is observed by the density measurements and surface tension measurements. In Figure 4-5 and 4-6, sudden changes of density and surface tension are shown as being around 100^{o}C, which is the glass transition temperature of the sample (Royer *at al.*, 2000). Specifically, the significant change of density around 100 ^{o}C in Figure 4-5 is consistent with other results in literature (Utracki, 2007). However, the deviation of surface tension at the temperatures less than 100 ^{o}C shown in Figure 4-6 can be explained

by the fact that polystyrene has behaved like a crystalline state at the temperature ranges. This method can be applied to measure the glass transition temperature of polymers. The relation between molecular weight and surface tension is found in literature (Legrand and Gaines, 1969). This work can be extended to show the relation of molecular weight and surface tension of polymers.

4.4 Summary

A set of the surface tension and density data of a polystyrene in supercritical nitrogen at various temperatures was successfully obtained. Within the experimental temperature ranges, the dependence of surface tension and density on temperature was quantified. It has been found that the polymer has a lower surface tension as the temperatures are increased in the range of above the glass temperature of polymer. However, although it shows the experiential fluctuations, the surface tension of the polymer in nitrogen at temperatures under the glass temperature of polymer has not been changed. This simultaneous characterization of surface tension and density has improved the accuracy of the surface tension measurements of polymer in a gas. This method is applied to measure the glass transition temperature of the polystyrene.

Chapter 5*

Effects of Temperatures and Pressures on Surface Tension of Polystyrene in Supercritical Carbon Dioxide

5.1 Introduction

Surface tension is one of the most important physicochemical properties for polymeric materials in various engineering processes, such as those involving foaming, suspensions, wetting and blending (Myers, 1991). In the foaming of polymer melts, the homogeneous nucleation rate is described by $N_{\text{homo}}^{\text{o}} = C_o f_o \exp(-\Delta G_{\text{homo}} / k_B T)$ according to bubble nucleation theories, where $N_{\text{homo}}^{\text{o}}$ is the number of nuclei generated per cm^3 per second, C_o the concentration of gas molecules (number of molecules per cm^3), f_o the frequency factor of the gas molecules, ΔG_{homo} the Gibbs free energy for homogeneous nucleation, and k_B Boltzmann's constant (Cahn and Hilliard, 1959; Goel and Beckman, 1994a). The Gibbs free energy (ΔG_{homo}) for homogeneous nucleation is given by $\Delta G_{\text{homo}} = 16\pi\gamma^3 / 3\Delta P^2$, where γ is the surface tension between the polymer phase and nucleating bubble phase, and ΔP the pressure difference across the polymer-gas interface. When the polymer in carbon dioxide has a lower surface tension than that of the pure polymer, the Gibbs free energy will be reduced by the cubic power of the surface tension, and the nucleation rate will increase exponentially.

* This chapter is based on the manuscript of the published studies (Park et al, 2007a)

It is evident that changes in surface tension are crucial to polymer foaming processes, and it is necessary to understand and control such a property in order to optimize such polymer-involved industrial operations (Russell, 1980; Colton and Suh, 1987).

There are many methods to measure surface tension. Among them, the pendant drop method has many advantages because of the simplicity and versatility in its setup and its principle (del Rio and Neumann, 1997; Rotenberg *et al.*, 1983). The pendant drop method has been used extensively for low molar mass liquids, liquid crystals and polymers. This method relies on the determination of a drop profile that has dense liquid in another fluid, and when the surface tension of the liquid is obtained from the best fit of the Laplace equation of capillarity which leads to the experimentally determined drop profile (Song and Springer, 1996; Anastasiadis *et al.*, 1986). Although the pendant drop method is theoretically simple, the research to date for determining surface tension of polymers has been limited because of experimental difficulties in handling high viscosity polymer melts under high temperature and high pressure (Demarquette and Kamal, 1994; Kwok *et al.*, 1998). In fact, there has only been limited surface tension data available for a few select polymers, and the range of experimental conditions, to which polymers are subjected during their measurements, has been rather narrow. All of these shortcomings make the understanding and control of the surface tension of polymers difficulty.

Supercritical carbon dioxide has been used as a foaming agent in the production of microcellular polymer foams (Cooper, 2000; Tomasko, *et al.*, 2003). Carbon dioxide has main advantages of being non-toxic and having a relatively low critical point (T_c=31C, P_c=7.376 MPa or 1070 psi). Although small amounts of carbon dioxide are added to the polymer process, dramatic changes result in physicochemical properties, such as glass

transition temperature, viscosity, solubility and surface tension (Lee, *et al.*, 1999). Particularly, the surface tension between polymer and gas phases has been emphasized because it significantly affects the foaming and morphology of final polymer products.

The primary objective of this study is to quantify the surface tension of a typical, commercially available polymer, polystyrene, in supercritical carbon dioxide, and to understand its dependence on temperature and pressure in a systematic way. A recently designed high-temperature and high-pressure sample cell is employed in the surface tension measurement to achieve a wide range of experimental conditions. With the collection of a comprehensive set of surface tension data, an empirical equation to approximate the surface tension of polystyrene in supercritical carbon dioxide as a function of temperature and pressure is developed, which provides predictive power for the surface tension variation. Furthermore, trends of the surface tension change with temperature and pressure are elucidated, and in particular, the effect of temperature on surface tension is shown to depend on the value of pressure.

To understand the surface tension behavior further, theoretical analysis of the experimental trends is given using self-consistent field theory (SCFT). It is difficult to achieve numerical accuracy for realistic values of the present system, so only qualitative agreement is sought. In this context, agreement with experiment is found, and three surface tension trends involving temperature and pressure are explained in terms of components of the surface tension. These components can be related to molecular interactions and configurations of polymers and to some extent, solvents (CO_2 in the present case). The resultant information provides means to change/control the surface tension during polymer processing, through chemical and composition design of polymer materials. Specifically, it is

found that a reduction in surface tension with increasing temperature is due to an expected increased mix of chemical constituents upon reducing the segregation parameters between dissimilar constituents (polystyrene and supercritical carbon dioxide) with increasing temperature. A decrease in surface tension with increasing pressure is, however, due to more similar densities between these dissimilar constituents. Related to this, it is found that the slope of surface tension with temperature itself decreases at higher pressures. SCFT shows this to be due to increased mixing between dissimilar constituents at higher pressure that results from the increased similarity in density. None of these explanations for the experimental trends are found to depend on the configurational entropy contribution to the surface tension of the polymer, so these calculations rationalize the use of simple liquid models (Dee and Sauer, 1998; Jones and Richards 1999) for the quantitative prediction of surface tensions of polymers.

5.2 Experimental

5.2.1 Surface Tension Measurement

The surface tension of polystyrene in carbon dioxide was measured at temperatures from 170 to 210°C, within a wide range of pressures, from 500 to 2500 psi. To achieve these experimental conditions, a high-temperature and high-pressure sample cell was constructed. Briefly, this optical viewing cell consisted of a cylinder of stainless steel, which was heated by an electrical heater. The inside of the cylinder was hollow, with a diameter of 30 mm and length of 25 mm. Two optical-quality sapphire windows (Meller Optics, Inc.) permitted the illumination and observation of the pendant drop formed by a sample polymer melt. The

setup was tested for its accuracy and reproducibility with a range of polymer-gas combinations, and the details of this were described in a recent publication (Park *et al.*, 2006).

The technique of Axisymmetric Drop Shape Analysis-Profile(ADSA-P) (Cheng *et al.*, 1990; Susnar *et al.*) was used for image analysis and parameter extraction. Surface or interfacial tensions were obtained by fitting the Laplace equation of capillarity to the shape and dimensions of axisymmetric menisci acquired (Andreas *et al.*, 1938). The value of surface tension was generated as a fitting parameter (Cheng and Neumann, 1992) after a least square algorithm was employed to minimize the difference between experimental drop profiles and theoretical ones. During this procedure, the density difference between polystyrene and carbon dioxide was an input parameter (Xue *et al.*, 2004; Li, *et al.*, 2004), which was determined by the Sanchez and Lacombe (S-L) equation of state (EOS) (Sanchez and Lacombe, 1976; Sanchez and Lacombe, 1977; Sanchez and Lacombe, 1978).

5.3 Theory

To understand the surface tension and its dependence on temperature and pressure, experimentally determined surface tensions can be compared to surface tensions calculated using self-consistent field theory (SCFT). SCFT is an equilibrium statistical mechanical approach for determining structures in polymeric systems. It is based on a free energy functional, which is to be minimized in order to find the lowest energy morphology. The procedure for deriving such functionals is explained in depth in a number of reviews (Matsen, 2002; Fredrickson and Ganesan, 2002; Schmid, 1998). For the supercritical carbon dioxide-polystyrene system, the appropriate free energy functional can be derived in the canonical ensemble to be

$$\frac{NF}{\rho_0 k_B TV} = -\frac{\phi_s}{\alpha}\ln\left(\frac{Q_s\alpha}{V\phi_s}\right) - \frac{\phi_h}{\alpha}\ln\left(\frac{Q_h\alpha}{V\phi_h}\right) - \phi_p \ln\left(\frac{Q_p}{V\phi_p}\right)$$
$$+\frac{1}{V}\int d\mathbf{r}\{\chi_{ps}N\varphi_p(\mathbf{r})\varphi_s(\mathbf{r}) + \frac{1}{2}\chi_{ss}N\varphi_s(\mathbf{r})\varphi_s(\mathbf{r}) + \frac{1}{2}\chi_{pp}N\varphi_p(\mathbf{r})\varphi_p(\mathbf{r}) \qquad (5\text{-}1)$$
$$-\omega_s(\mathbf{r})\varphi_s(\mathbf{r}) - \omega_h(\mathbf{r})\varphi_h(\mathbf{r}) - \omega_p(\mathbf{r})\varphi_p(\rho)$$
$$-\xi(\mathbf{r})[1-\varphi_s(\mathbf{r})-\varphi_p(\mathbf{r})-\varphi_h(\mathbf{r})]\}$$

where F/V is the free energy of the system per volume V. This free energy is made dimensionless by dividing by k_BT and multiplying by the volume of a single polymer N/ρ_0, where $1/\rho_0$ is the volume of a single polymer segment and N is the degree of polymerization based on that segment volume. It should be noted that since SCFT is a coarse-grained theory, a single segment may include many chemical monomers. On the right hand side of (5-1), ϕ_s, ϕ_p, and ϕ_h are the overall volume fractions of solvent molecules, polymer molecules and "holes", respectively. In order to be consistent with the Sanchez-Lacombe equation of state (Sanchez and Lacombe, 1976) being used experimentally to extract the surface tension, we are also using a Sanchez-Lacombe equation of state to model pressure in the SCFT. This approach was introduced by Hong and Noolandi (Hong and Noolandi, 1981) for SCFT and consists of treating a compressible system as an incompressible system together with vacancies, that is, holes. Higher pressure systems have fewer holes whereas lower pressure systems have more. The Sanchez-Lacombe equation of state thus relates the density to pressure for systems whose variable density is modeled in terms of holes. With this in mind, the volume fractions ϕ_s, ϕ_p, and ϕ_h are not all independent, rather $\phi_s+\phi_p+\phi_h=1$. It should be noted that other approaches for treating compressibility within SCFT are possible, in particular Binder *et al.* have studied solvent-polymer systems thoroughly using a virial expansion to get an equation of state (Binder *et al.*, 2005). The local volume fractions of

solvent, polymer and holes are given by $\varphi_s(\mathbf{r})$, $\varphi_p(\mathbf{r})$, and $\varphi_h(\mathbf{r})$, respectively, in equation (5-1). In conjuntion with them. these are the position dependent chemical potential fields $\omega_s(\mathbf{r})$, $\omega_p(\mathbf{r})$ and $\omega_h(\mathbf{r})$, and a pressure field $\xi(\mathbf{r})$ which enforces incompressibility with respect to *all* the chemical species: solvent, polymer and holes. The physical pressure can then be found, if desired, by calculating the appropriate osmotic pressure within the formalism. The Flory-Huggins parameters are usually defined in terms of dissimilar constituents such as χ_{ps}, χ_{ph} and χ_{sh}. It is felt here however that since the holes are fictitious, it is more meaningful to choose our three independent parameters as χ_{ps}, χ_{pp} and χ_{ss}. They are defined from first principles as

$$\chi_{ij} = \frac{\rho_0}{k_B T} \int d\mathbf{r} V_{ij}(|\mathbf{r}|) \tag{5-2}$$

where $V_{ij}(|\mathbf{r}|)$ is two-body potential between species i and j with $i, j = p, s$ or h (Hong and Noolandi, 1981). Since the potential between holes and anything else should be zero, all χ terms in the free energy involving *h* will vanish. The interpretation of these parameters is then no longer as the dimensionless change in energy upon exchange of segments between pure components, although the use of the term Flory-Huggins parameter will be maintained; they still arise as the first order in a gradient expansion of the potentials. Meanwhile, $\chi_{ps}, \chi_{ph}, \chi_{sh}$ could equally be used instead of $\chi_{ps}, \chi_{pp}, \chi_{ss}$. This would not change any of the results.

Usually, the products (χN) are taken as the segregation parameters instead of just the parameter(χ). The ratio of the volume of a solvent molecule to a polymer molecule is

given by α. Finally, Q_s, Q_p and Q_h are the partition functions for single molecules of solvent, polymer and holes, respectively, subject to the fields $\omega_s(\mathbf{r})$, $\omega_p(\mathbf{r})$ and $\omega_h(\mathbf{r})$. Expressions for these partition functions are given below in equations (5-10), (5-11), and (5-12). The variation of (5-1) with respect to the functions $\varphi_s(\mathbf{r})$, $\varphi_p(\mathbf{r})$, $\varphi_h(\mathbf{r})$, $\omega_s(\mathbf{r})$, $\omega_p(\mathbf{r})$, $\omega_h(\mathbf{r})$ and $\xi(\mathbf{r})$ results in a set of equations for these functions that must be solved self-consistently, and usually, numerically. The equations are

$$\omega_s(\mathbf{r}) = \chi_{ps} N \varphi_p(\mathbf{r}) + \chi_{ss} N \varphi_s(\mathbf{r}) + \xi(\mathbf{r}) \tag{5-3}$$

$$\omega_p(\mathbf{r}) = \chi_{ps} N \varphi_s(\mathbf{r}) + \chi_{pp} N \varphi_p(\mathbf{r}) + \xi(\mathbf{r}) \tag{5-4}$$

$$\omega_h(\mathbf{r}) = \xi(\mathbf{r}) \tag{5-5}$$

$$\varphi_s(\mathbf{r}) + \varphi_p(\mathbf{r}) + \varphi_h(\mathbf{r}) = 1 \tag{5-6}$$

$$\varphi_s(\mathbf{r}) = \frac{\phi_s V}{Q_s} e^{-\alpha \omega_s(\mathbf{r})} \tag{5-7}$$

$$\varphi_h(\mathbf{r}) = \frac{\phi_h V}{Q_h} e^{-\alpha \omega_h(\mathbf{r})} \tag{5-8}$$

$$\varphi_p(\mathbf{r}) = \frac{\phi_p V}{Q_p} \int_0^1 ds q(\mathbf{r}, s) q(\mathbf{r}, 1-s) \tag{5-9}$$

with

$$Q_s = \int d\mathbf{r} e^{-\alpha \omega_s(\mathbf{r})} \tag{5-10}$$

$$Q_h = \int d\mathbf{r} e^{-\alpha \omega_h(\mathbf{r})} \tag{5-11}$$

$$Q_p = \int d\mathbf{r} q(\mathbf{r}, 1) \tag{5-12}$$

and

$$\frac{\partial q(\mathbf{r},\mathrm{s})}{\partial \mathrm{s}} = \frac{\mathrm{Na}^2}{6}\nabla^2 q(\mathbf{r},s) - \omega_p(\mathbf{r})q(\mathbf{r},s) \tag{5-13}$$

In (5-13), a is the "statistical segment length" of a polymer segment; the definition of a and more details about SCFT can be found in references (Matsen, 2002; Fredickson and Ganesan, 2002; Schmid, 1998).

The equations (5-3)-(5-13) are solved numerically in real space, using a Crank-Nicolson algorithm with reflecting boundary conditions (requiring derivatives of spatially dependent functions to be zero at the boundaries) in one dimension in order to find the structure and free energy of the interfacial system. A random initial guess for the fields is taken, the diffusion equations are solved and the local volume fractions found. Also from this guess, the incompressibility constraint is calculated. The local volume fractions together with the incompressibility constraint allow new fields to be computed. This process is iterated until the new fields and the old fields differ by less than one part in 10^{-11} according to the criteria of Thompson *et al.* (Thompson *et al.*, 2004). The independent input parameters for this process are α, $\chi_{ps}N$, $\chi_{pp}N$ and, $\chi_{ss}N$. The volume V (or L in one dimension) is arbitrary, provided it is taken large enough such that the system reaches bulk conditions on either side of the interface. Similarly, ϕ_s and ϕ_p can take a range of values provided there is enough total polymer and solvent present for bulk conditions to be reached. Within reason, by varying the amount of ϕ_s or ϕ_p within reason simply shifts the interface in one direction or the other within the calculated region L. Therefore there are only four important parameters for the model system, although we shall continue specifying the ϕ_s and ϕ_p used in any given calculation for clarity.

Upon obtaining solutions for (5-3)-(5-13), the free energy for the system can be found through (1). The surface tension γ may then be calculated through a generalization of the binary surface tension formula given by Matsen (Matsen, 2002). In dimensionless form, we write this as

$$\frac{R_g \gamma}{a^2 \rho_0 k_B T} = \left(\frac{L}{R_g} \right) \left(\frac{NF}{\rho_0 k_B T V} - \sum_{i=p,s,h} \frac{NF_{si}}{\rho_0 k_B T V} \right) \tag{5-14}$$

where the unperturbed radius of gyration of a polymer $R_g = aN^{1/2}/\sqrt{6}$ is used as the length scale in all our SCFT calculations. In (5-14), we are essentially subtracting off the free energy of the bulk phases on either side of the interface to leave the energy of the interface itself; this is then phrased as a surface tension by dividing by the interfacial area. The free energy of the bulk phases is given by $\sum_{i=p,s,h} \frac{NF_{si}}{\rho_o k_B T V}$, where each of the F_{si} terms is defined as

$$\frac{NF_{si}}{\rho_0 k_B T V} = \frac{NF_{hi}^{(1)}}{\rho_0 k_B T V} \left(\frac{V_{1i}}{V} \right) + \frac{NF_{hi}^{(2)}}{\rho_0 k_B T V} \left(1 - \frac{V_{1i}}{V} \right) \tag{5-15}$$

with $F_{hi}^{(1)}$ and $F_{hi}^{(2)}$ corresponding to the free energies of the homogeneous phases on either side of the interface, according to

$$\frac{NF_{i=polymer}}{\rho_0 k_B T V} = \phi_p \ln \phi_p + \frac{\chi_{ps} N}{2} \phi_s \phi_p + \frac{\chi_{pp} N}{2} \phi_p \phi_p \tag{5-16}$$

$$\frac{NF_{i=solvent}}{\rho_0 k_B T V} = \frac{\phi_s}{\alpha} \ln \left(\frac{\phi_s}{\alpha} \right) + \frac{\chi_{ps} N}{2} \phi_s \phi_p + \frac{\chi_{ss} N}{2} \phi_s \phi_s \tag{5-17}$$

$$\frac{NF_{i=holes}}{\rho_0 k_B T V} = \frac{\phi_h}{\alpha} \ln \left(\frac{\phi_h}{\alpha} \right) \tag{5-18}$$

In (5-16)-(5-18), the volume fractions ϕ_p , ϕ_s and ϕ_h should be taken as the bulk homogeneous volume fractions on either side of the interface according to

$$\phi_i^{(1)} = \varphi_i(z = 0) \tag{5-19}$$

$$\phi_i^{(2)} = \varphi_i(z = L) \tag{5-20}$$

assuming a one-dimensional system with coordinate z, rather than as the overall volume fraction of the system. The construction (5-15) assumes the total system volume V can be split into two according to

$$V = V_1 + V_2 \tag{5-21}$$

where V_1 and V_2 are the volumes associated with two separate homogeneous systems with volume fractions of the various species equal to the bulk values on either side of the interface. Since V is known, V_1 and V_2 are not independent, and it suffices to know V_1, or rather the ratio V_1/V, in order to find the separated free energy F_s in (5-15). The interface calculated using SCFT is actually three superposed contributions due to the three species in the present system. Thus three different volume ratios V_1/V can be found which correspond to the interface of the polymer with the other two species, the interface of the solvent with the other two species, and the interface of the holes with the other two species. These ratios are then written as

$$\frac{V_{1i}}{V} = \frac{\phi_i^{(2)} - \phi_i}{\phi_i^{(2)} - \phi_i^{(1)}} \tag{5-22}$$

where $i = p, s$ or h, for the polymer, solvent or hole interfaces. A derivation of (5-22) is given by Matsen (Matsen, 2002) in case of a binary interface in terms of conservation considerations. The derivation is exactly the same in the present case.

With the expression (5-14) for the surface tension now defined, one can also break this expression up into its component parts in order to facilitate analysis of the results. The free energy (5-1) can be written as $F = U\text{-}TS$ or

$$\frac{NF}{\rho_0 k_B TV} = \frac{NU}{\rho_0 k_B TV} - \frac{NS}{\rho_0 k_B V} \quad . \tag{5-23}$$

Following Matsen and Bates (Matsen and Bates, 1997), the free energy components would then be

$$\frac{NU_{ps}}{\rho_0 k_B TV} = \frac{\chi_{ps} N}{V} \int d\mathbf{r} \varphi_p(\mathbf{r}) \varphi_s(\mathbf{r}) \tag{5-24}$$

$$\frac{NU_{ss}}{\rho_0 k_B TV} = \frac{\chi_{ss} N}{2V} \int d\mathbf{r} \varphi_s(\mathbf{r}) \varphi_s(\mathbf{r}) \tag{5-25}$$

$$\frac{NU_{pp}}{\rho_0 k_B TV} = \frac{\chi_{pp} N}{2V} \int d\mathbf{r} \varphi_p(\mathbf{r}) \varphi_p(\mathbf{r}) \tag{5-26}$$

$$\frac{-S_{Tp}}{\rho_0 k_B V} = \frac{1}{V} \int d\mathbf{r} \rho_p \ln \rho_p \tag{5-27}$$

$$\frac{-S_{Cp}}{\rho_0 k_B V} = \frac{1}{V} \int d\mathbf{r} \rho_p \ln q(\mathbf{r},1) \tag{5-28}$$

$$\frac{-S_{Ts}}{\rho_0 k_B V} = -\frac{\phi_s}{\alpha} \ln\left(\frac{Q_s \alpha}{\phi_s V}\right) - \frac{1}{V} \int d\mathbf{r} \omega_s(\mathbf{r}) \varphi_s(\mathbf{r}) \tag{5-29}$$

$$\frac{-S_{Th}}{\rho_0 k_B V} = -\frac{\phi_h}{\alpha} \ln\left(\frac{Q_h \alpha}{\phi_h V}\right) - \frac{1}{V} \int d\mathbf{r} \omega_h(\mathbf{r}) \varphi_h(\mathbf{r}) \tag{5-30}$$

for the internal energy contribution to the free energy between polymer segment and solvent, solvent and solvent, polymer and polymer, translational entropy contribution to the free energy of the polymer, configurational entropy of the polymer, translational entropy of the solvent and the translational entropy of the holes, respectively. The configurational entropy

accounts for all the different conformations a polymer can take, whereas the translational entropy of the polymer accounts for the remaining positional degrees of freedom of the center of the mass in the molecule. In (5-27) and (5-29), ρ_p is defined as

$$\rho_p \equiv \frac{\phi_p V q(\mathbf{r},1)}{Q_p} \tag{5-31}$$

The components (5-24)-(5-30) can be converted into excess free energy components by subtracting off the corresponding bulk free energy components of the homogeneous phases on either side of the interface in exactly the same way as for the total free energy. Then by dividing by the interfacial area, these can be converted into components of the surface tension, just as the total excess free energy was expressed as a surface tension. These internal energy and entropic contributions to the surface tension will be used to explain the trends observed experimentally and theoretically in the supercritical carbon dioxide-polystyrene system.

5.4 Results and Discussion

5.4.1 Surface tension as a Function of Temperature and Pressure

A typical pendant drop image is shown in Figure 5-1. The surface tension of polystyrene melt in carbon dioxide was measured at five different pressures: 500, 1000, 1500, 2000, and 2500 psi, and five different temperatures: 170, 180, 190, 200, and 210°C. Figure 5-2 shows the surface tension values as a function of time. The average of the surface tension values is taken as the equilibrium surface tension when the change in surface tension is less than 0.0001mJ $m^{-2}s^{-1}$ for 1 hour. Errors are on the order of 0.01 mJ m^{-2}. All measurements show

that the surface tension reaches its equilibrium value quickly, within 15 minutes. The surface tension values from these experiments show trends of being smaller at higher temperatures and higher pressures, consistent with the data from other studies (Li *et al.*, 2004).

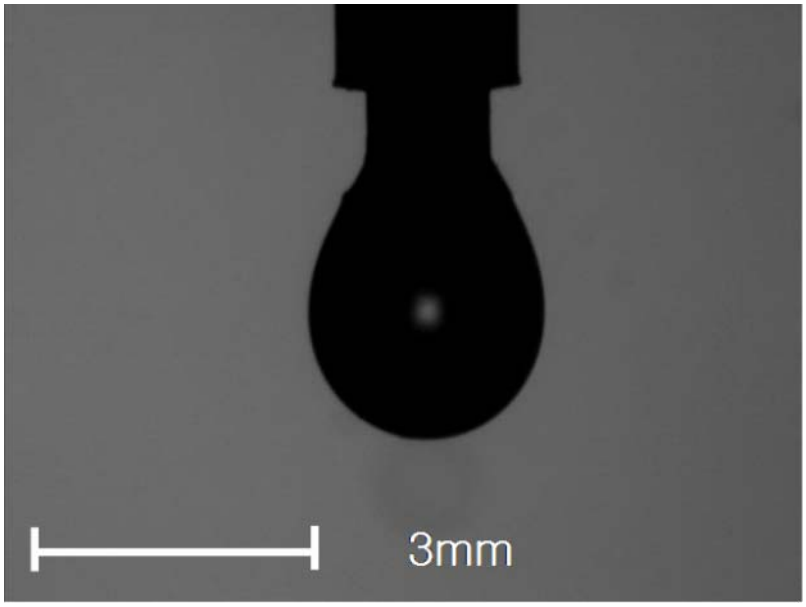

Figure 5-1 A typical pendant drop image of polystyrene in supercritical carbon dioxide

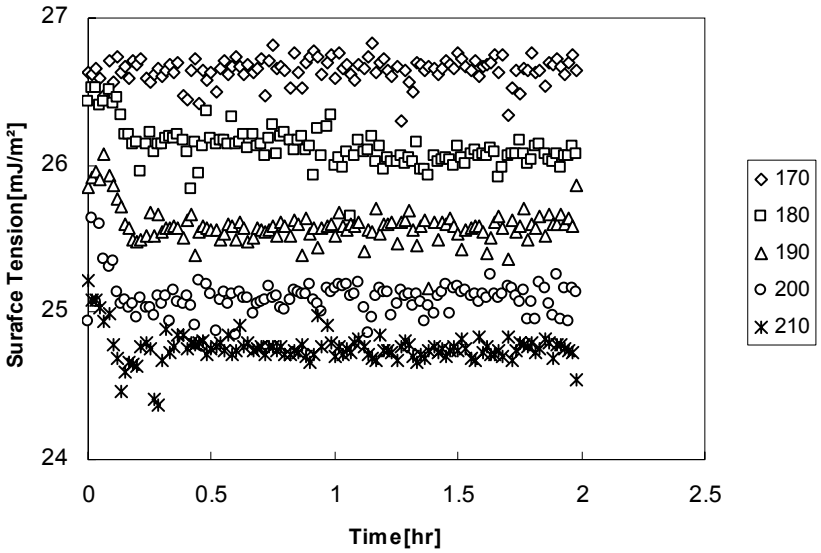

Figure 5-2 Surface tension of polystyrene in supercritical carbon dioxide at a pressure of 500psi..

From Fig. 5-2, equilibrium surface tension values of polystyrene in carbon dioxide under various conditions can be obtained by averaging the plateau data points at each condition; the raw data from ADSA-P were shown in Appendix A. The combined results at various temperature and pressure conditions are shown in Fig. 5-3. It is apparent that the dependence of surface tension on temperature becomes less with increasing pressure. When the pressure value reaches above ~ 2000 psi, such dependence becomes nil. This implies that increasing temperature is effective at reducing surface tension only when moderate pressure is applied during a polymer process.

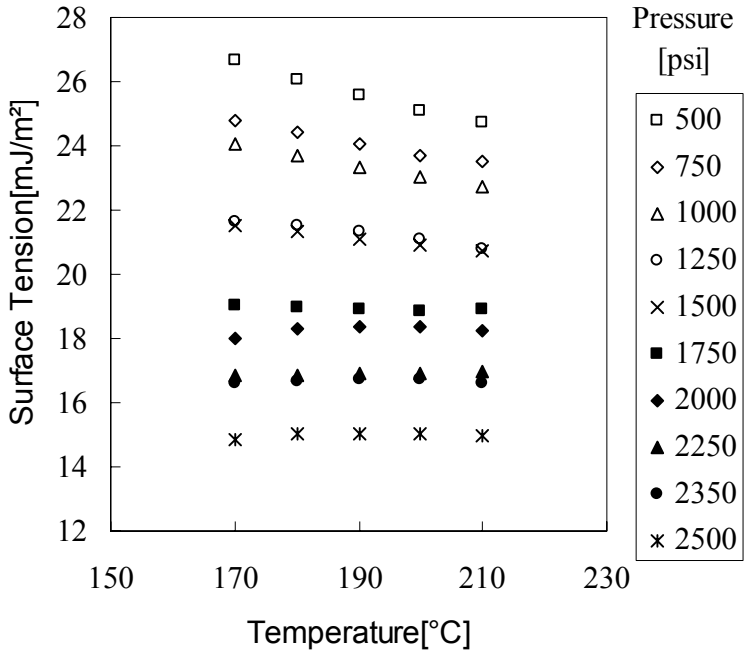

Figure 5-3 The equilibrium surface tension of polystyrene in carbon dioxide at various temperatures and pressures

Statistical investigations for the proposed parameters were studied. The 2nd order linear regression models were carried out for estimating the surface tension from the experimental conditions and t-test was performed to evaluate the validity of the obtained parameters. To find how temperature, pressure and their interaction influence the surface tension, a 2nd order linear regression model is used (Milton and Arnold, 1995). The 2nd order linear regression models were tested for determining the significance of parameters, the second order temperature and pressure were not significant at the 95% confidence level. Table 5-1 shows ANOVA (analysis of variance), indicating the validity of the regression model: the observed F-value is larger than the tabulated F-value at the 95% confidence level. It implies that the suggested model is appropriate with the 95% confidence level, In Table 5-2, the validity of each parameter was also examined using a t-test to show how the parameters have standard deviation in the 95% confidence level: all observed t values as being greater than the tabulated t-value at the 95% confidence level. From these statistical investigations, we can propose the following equation

$$\gamma = 38.7032 - 0.0559\,T - 0.0100\,P + (2.596\text{X}10^{-5})TP \qquad (5\text{-}32)$$

$$(170\ ^{o}\text{C} \le T \le 210^{o}\text{C},\quad 500\ \text{psi} \le P \le 2500\ \text{psi})$$

where the surface tension of polystyrene in supercritical CO_2 γ is in [mJ/m^2], the temperature T in [°C], and the pressure P in [psi]. Note that the second order terms in T and P are absent; statistically, γ is linearly related to T and P. However, there is an interaction term in (TP), indicating γ dependence on T or P is affected by P or T, respectively. This indicates that, for polymer melt processes, one has to adjust both T and P in order to control the value of γ completely.

From (5-32), the following equations can be derived:

$$\frac{\partial \gamma}{\partial T} = -0.0559 + (2.596X10^{-5})P \tag{5-33}$$

$$\frac{\partial \gamma}{\partial P} = -0.0100 + (2.596X10^{-5})T \tag{5-34}$$

$$\frac{\partial^2 \gamma}{\partial P \partial T} = 2.596X10^{-5} \tag{5-35}$$

Table 5-1. ANOVA (analysis of variance) table for a 2nd order linear regression model

	Sum of Square (SS)	Degree of Freedom	Mean Square(MS)
Regression	560.83	3	180.95
Residual	7.62	46	0.165
Total	568.45	49	
F_{obs}=1129.9 $F_{3,46,.0.05}$=2.80, R^2=0.999			

Table 5-2 t-test for evaluating each parameter of the proposed 2nd order linear regression

γ =38.7032 – 0.0559 T – 0.0100 P+(2.596X10^{-5})TP

(170 ^{o}C ≤ T ≤ 210^{o}C, 500 psi ≤ P ≤ 2500 psi)

Parameters	Coefficients	Standard Error	$\|T_{obs}\|$
Intercept	38.7032	2.0083	19.27
Temperature(T)	-0.0559	0.0105	5.30
Pressure(P)	-0.0200	0.0012	8.52
Temperature Pressure (TP)	2.5957E-05	6.13E-08	4.23
$T_{0.025,46}$=2.013			

To evaluate the validity the suggested equation, 5-32, the comparison between experimental values and calculated values form the proposed equation is conducted. Figure 5-4 shows that the experimental values agree well with those of the estimated values from the equation 3-15.

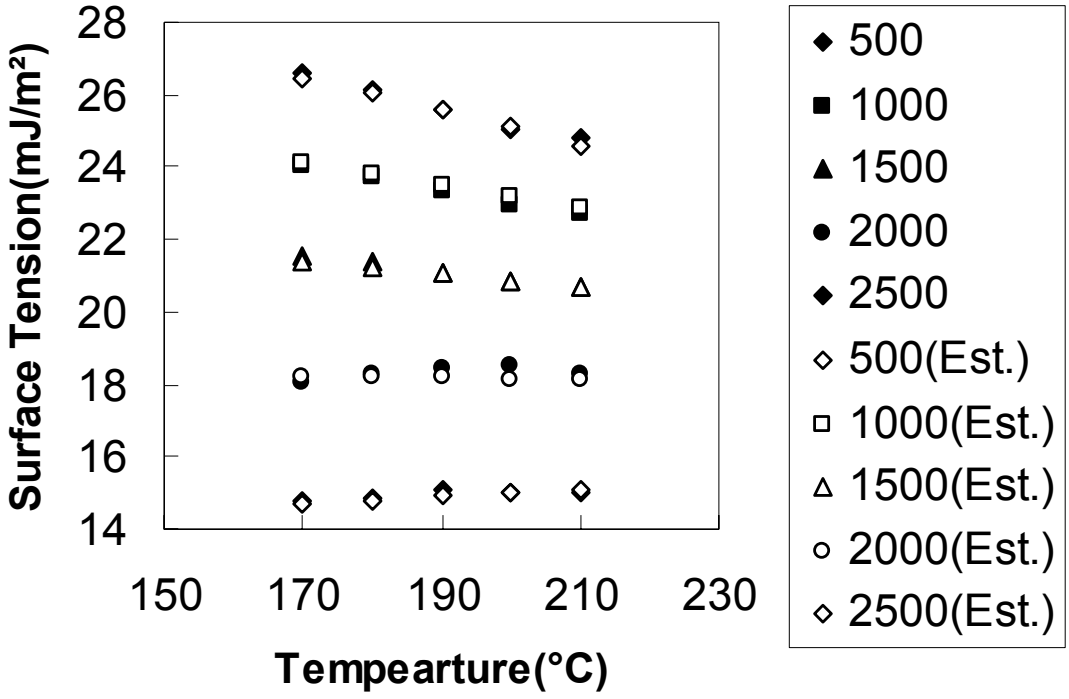

Figure 5-4 Comparison between experimental values and calculated values

There are three main experimental trends presented in Eqs. 5-33 to 5-35. These are the dropping of surface tension as a function of temperature for the pressure being less than ~ 2153 psi, the dropping of surface tension with increasing pressure for the temperature being less than ~ 385°C, and the flattening of the surface tension versus temperature curves with increased pressure (see also Figure 5-3). When the pressure is greater than 2153 psi or the temperature is greater than 385°C, these trends become trivial, which hence defines the validity limits of the above statements and, maybe, the empirical equations.

The self-consistent field theory was used to explain the aforementioned trends. SCFT calculations have been performed to find a dimensionless surface tension ($R_g\gamma / a^2\rho_0 k_{\mathbf{B}}T$) as described in the Theory section, as a function of temperature at two different pressures. The results are shown in Figure 5-5. In this study, the arbitrary temperature unit is employed to minimize the numerical difficulties and to show the trends of temperature dependence of the surface tension. It should be noted that the temperature unit can be assigned from the equation 5-36. For the high pressure run, no holes were included and the overall volume fractions were taken as ϕ_p=0.65 and ϕ_s=0.35 for the polymer and solvent, respectively. This corresponds to an incompressible fluid, and thus is the highest pressure case possible. This was compared against a lower pressure run with ϕ_p =0.60 and ϕ_s=0.30, or in other words, with 10 percent holes by volume. In both cases and at all temperatures, the system size was L=12.0R_g. The ratio α of the volume of a solvent molecule to that of a polymer molecule was taken to be 0.1 for both pressure runs. This is not particularly realistic, as this ratio for the supercritical carbon dioxide-polystyrene system

should be a much smaller number. Too great a size disparity between the different molecular species will however cause numerical difficulties. This results from the extremely high translational entropy that results from having many small solvent molecules. This strongly favours mixing, and makes it difficult to establish an interface unless the Flory-Huggins parameters are turned up extremely high. This in turn makes it difficult to achieve numerical accuracy in the calculations. Rather, we will take a qualitative approach, making sure that trends observed experimentally are nonetheless still observed in the calculations despite a large value for α. The mechanisms found to be responsible for the three aforementioned experimental trends should still be valid for more disparate molecular sizes. For this reason, we have not changed the hole volume fractions into pressure values through osmotic pressure calculations, as was previously mentioned to be possible.

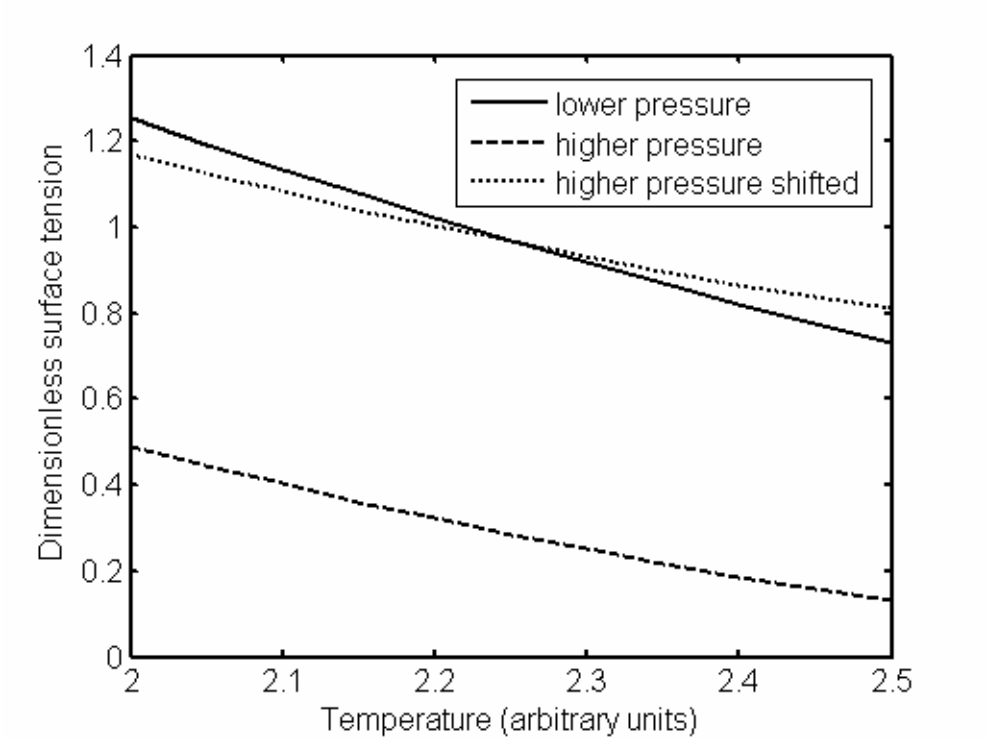

Figure 5-5 Dimensionless surface tension as a function of temperature for two different pressures.

The lower pressure run is the solid curve while the higher pressure run is the dashed curve. The higher pressure run is also plotted a second time by a dotted curve where it is shifted upwards to more easily compare the slopes of the two runs.

The parameters left to specify now are the Flory-Huggins values. Since a qualitative philosophy is being used, our model system does not need to incorporate χ values determined from first principles or from further experimentation. Rather, it suffices to choose values that map our model system qualitatively onto the experimental structure. A relationship between χ (or in this case, χN) and temperature T that is commonly used is (Mai *et al.*, 2004; Mai *et al.*, 2000)

$$\chi N = \frac{A}{T} + B \tag{5-36}$$

where A and B are constants. In the present work, we have three different such parameters, namely $\chi_{ps}N$, $\chi_{ss}N$ and, $\chi_{pp}N$, so we will have three sets of constants, A_{ps}, B_{ps}, A_{ss}, B_{ss} and A_{pp}, B_{pp}. Since we are looking for qualitative trends, we are free to set B_{ps}, B_{ss} and B_{pp} all equal to zero, for simplicity. The most basic model system that we could devise that still produced a structure of the interface that would qualitatively resemble the experimental system involved setting A_{pp}=0. From (5-36), this can only be satisfied for arbitrary T if $\chi_{pp}N$ =0, always. We tried runs with different values of A_{pp} but found no qualitative differences. Lastly, we will choose A_{ps}=100 and A_{ss}=150. This way, we can range T, in arbitrary units, from 2.0 to 2.5 and get

$$2.0 < T < 2.5$$

$$50 > \chi_{ps}N > 40$$

$$75 > \chi_{ss}N > 60.$$

These values produce reasonable interfacial structures, as shown in Figure 5-5 for T=2.0 and T=2.5 at the two different pressures. To assign specific units to the temperature such as

Kelvin or degrees centigrade, the parameters A should be specified in the desired units. The present values were chosen so as to reproduce an appropriate interface while at the same time allowing for numerically accurate calculations.

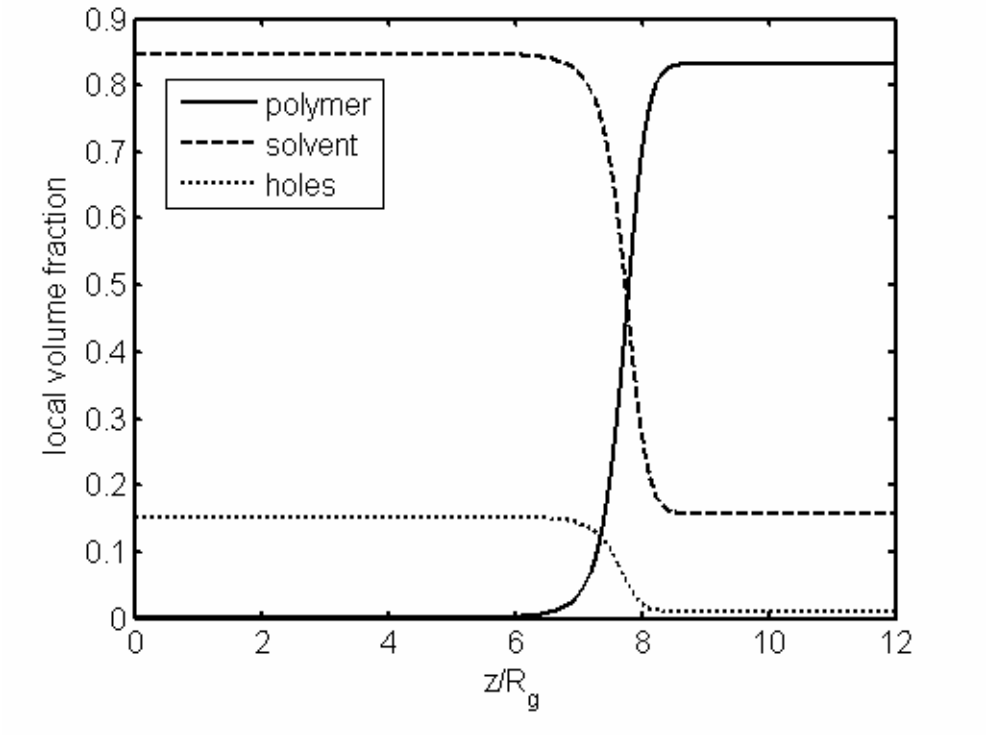
polymer
solvent
holes
local volume fraction
z/R_g
0
0.1
0.2
0.3
0.4
0.5
0.6
0.7
0.8
0.9
0
2
4
6
8
10
12

(a)

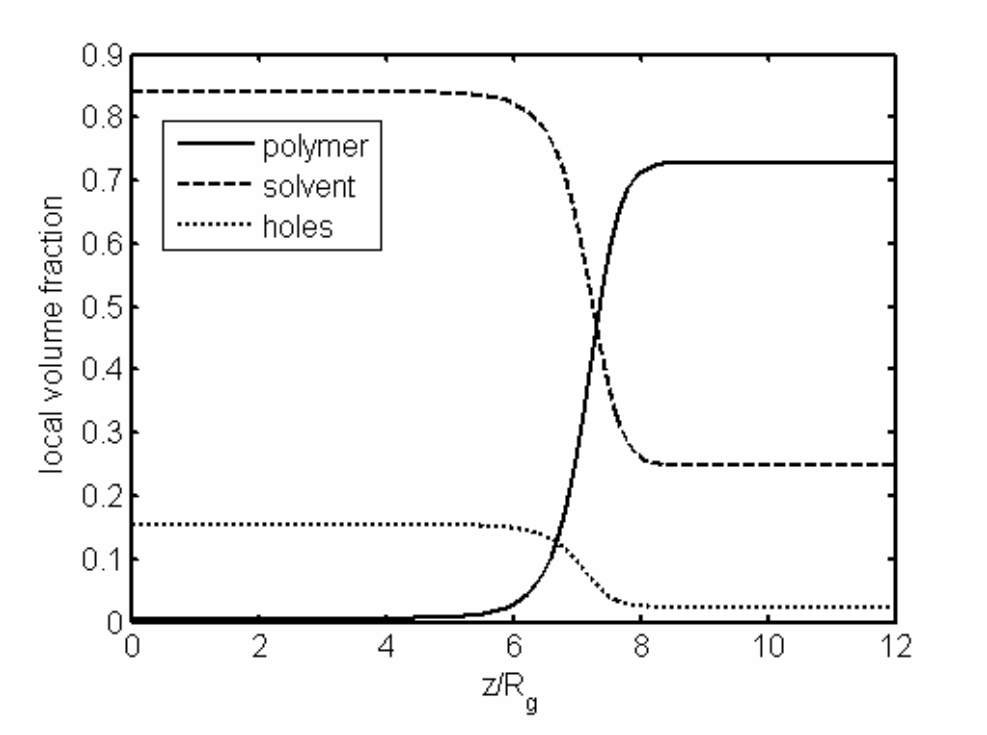
polymer
solvent
holes
local volume fraction
z/R_g
0
0.1
0.2
0.3
0.4
0.5
0.6
0.7
0.8
0.9
0
2
4
6
8
10
12

(b)

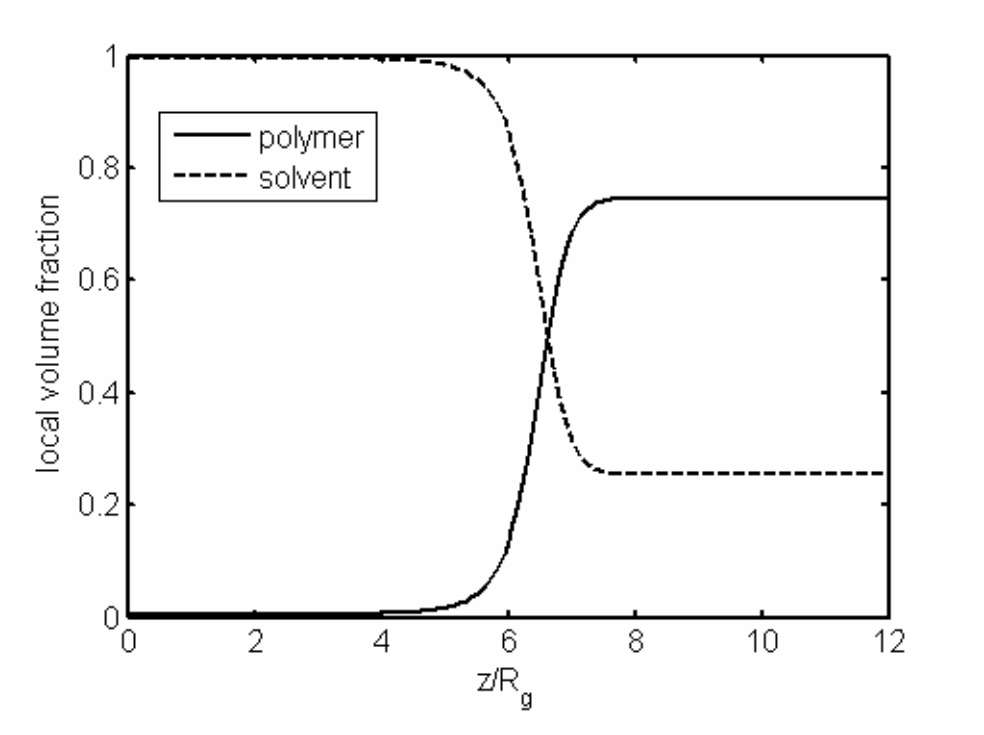
polymer
solvent
local volume fraction
z/R_g
0
0.2
0.4
0.6
0.8
1
0
2
4
6
8
10
12

(c)

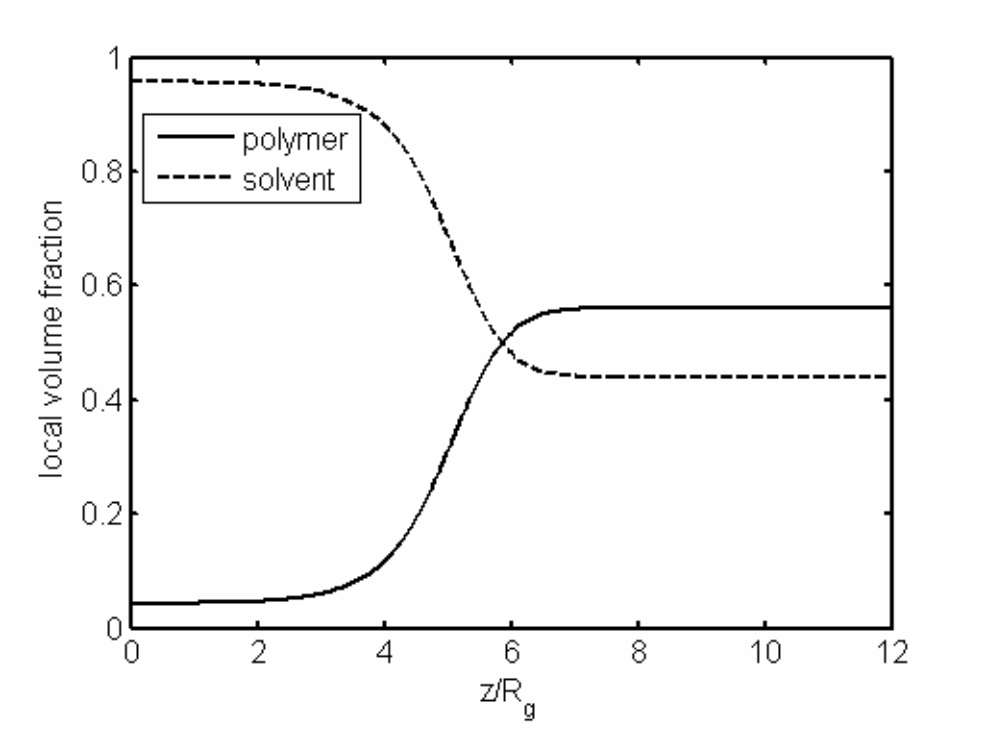

(d)

Figure 5-6 Concentration profiles for SCFT calculations. (a) Lower pressure, T=2.0. (b) Lower pressure, T=2.5. (c) Higher pressure, T=2.0. (d) Higher pressure, T=2.5.

5.4.2 Temperature Dependence

Figure 5-5 can explain the three main trends previously mentioned. It can be seen that the temperature dependence of our model system follows the trends of the experiment and the empirical equation (5-32) at both pressures in that surface tension decreases with increasing temperature. In Figure 5-7 the components of the surface tension which were described in the theory section are plotted. The total surface tension must of course be a positive value, the zero being the absence of any interface. The components however can be either positive or negative. The two main components that can be seen to be contributing to the decrease of surface tension with temperature are the internal energy contribution to the surface tension (open circles on solid curve) and the polymer configurational entropy contribution to the surface tension (crossed dotted curve), see also Table 3, rows m_l and m_h. The translational entropy of the holes contributes negligibly. Of these, the largest contribution is from the internal energy. This contribution can in turn be split into the polymer-solvent, solvent-solvent, and polymer-polymer components of the internal energy contribution to the surface tension, as shown in Figure 5-8. In that figure, the component that is clearly responsible for the overall drop of the total internal energy contribution is the polymer-solvent component; it is the only component with a slope in the correct direction. By translating this conclusion into polymer-solvent processes, one would concentrate on modifying the molecular interaction between the polymer and its solvent when making use of such temperature dependence of surface tension. Under this situation, modifications of polymer or solvent molecular

properties alone could be less effective at reducing surface tension with an elevated temperature.

The fact that the polymer-solvent internal energy contribution is responsible for the drop in surface tension makes perfect sense, in that the free energy of the system can be split according to equation (5-23) into an internal energy part and an entropic part, the two parts having different signs, that is, they oppose each other. The entropic contributions promote mixing whereas the internal energy favours segregation. As the temperature is increased, the $\chi_{ps}N$ parameter decreases, reducing the segregation between polymer and solvent segments. This means the entropy becomes a larger relative portion of the free energy, more mixing takes place and the interface becomes more diffuse; this in turn means there will be a lower surface tension. This is a well-known and well-understood effect that is correctly reproduced here in the model system.

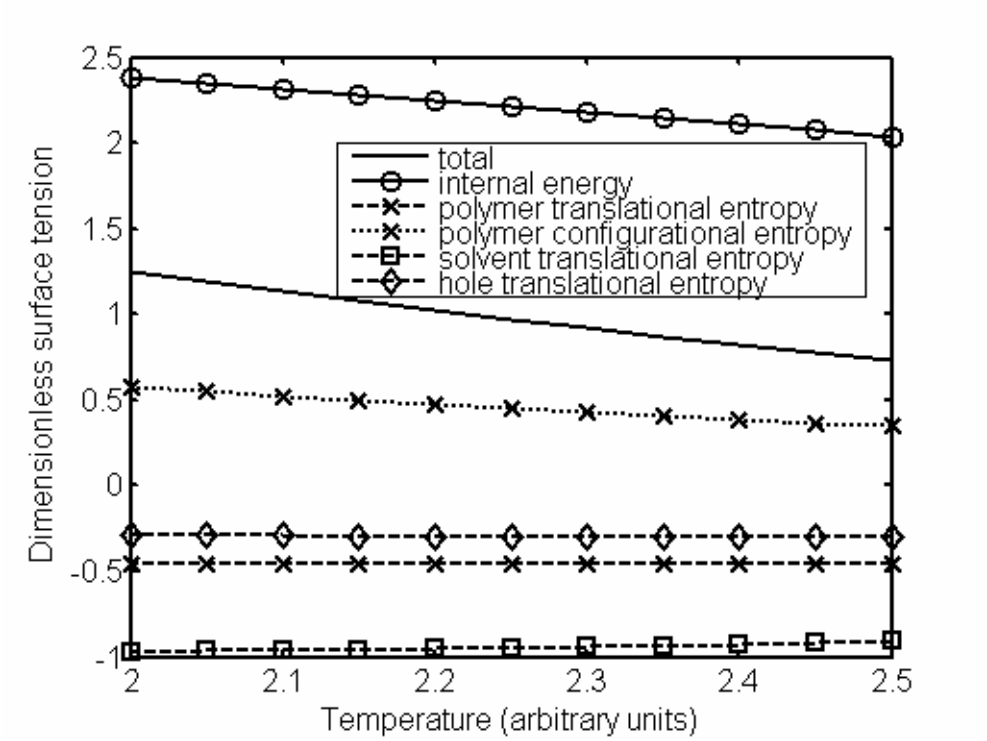
2.5
2
1.5
1
0.5
0
-0.5
-1
2
2.1
2.2
2.3
2.4
2.5
Dimensionless surface tension
Temperature (arbitrary units)
total
internal energy
polymer translational entropy
polymer configurational entropy
solvent translational entropy
hole translational entropy

(a)

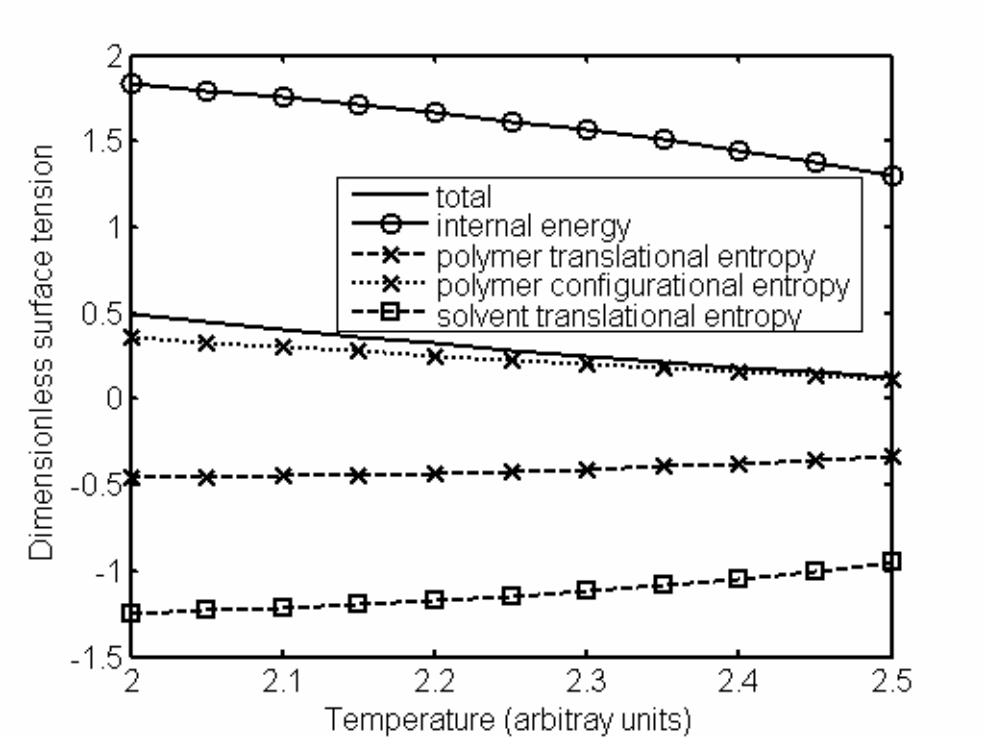

(b)

Figure 5-7 Components of the surface tension for (a) the lower pressure run and (b) the higher pressure run. Different contributions to the surface tension are shown in the legends.

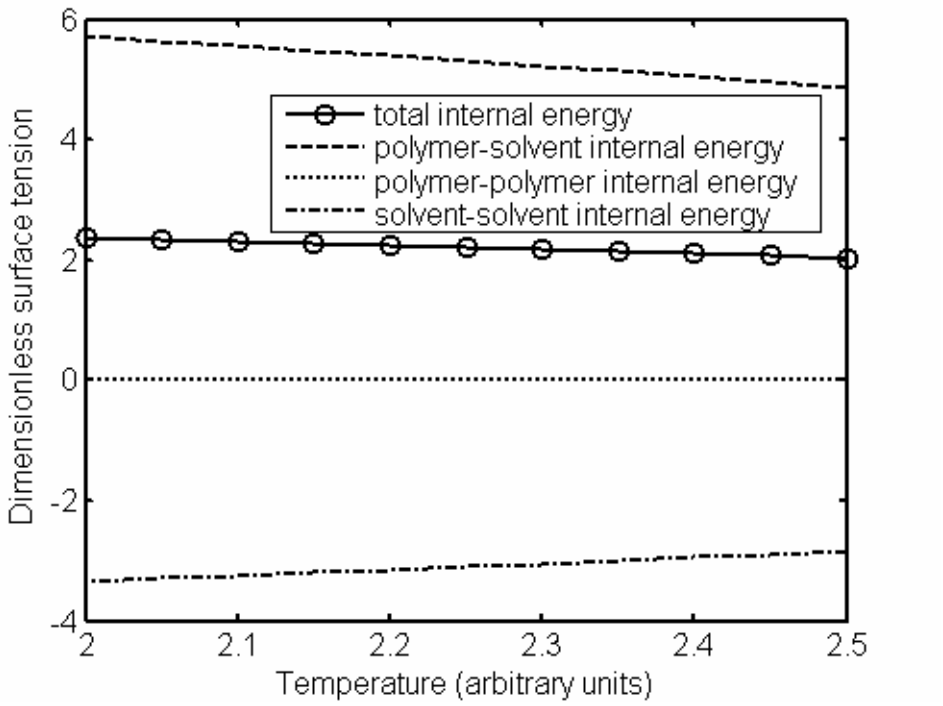
6
4
2
0
-2
-4
2
2.1
2.2
2.3
2.4
2.5
Dimensionless surface tension
Temperature (arbitrary units)
total internal energy
polymer-solvent internal energy
polymer-polymer internal energy
solvent-solvent internal energy

(a)

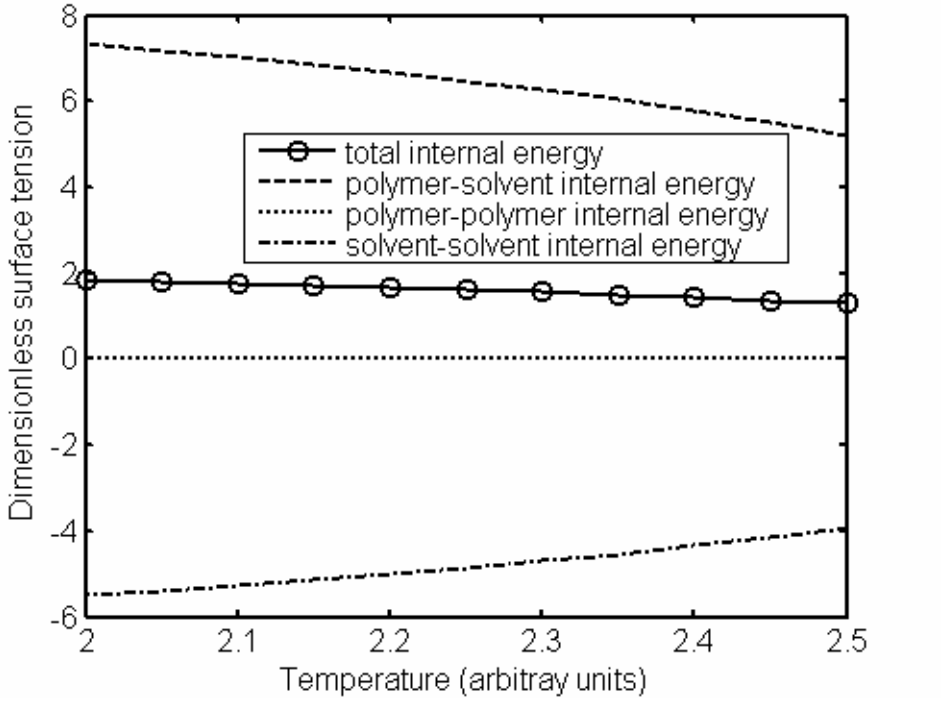
8
6
4
2
0
-2
-4
-6
2
2.1
2.2
2.3
2.4
2.5
Dimensionless surface tension
Temperature (arbitray units)
total internal energy
polymer-solvent internal energy
polymer-polymer internal energy
solvent-solvent internal energy

(b)

Figure 5-8 Sub-components of the internal energy contribution to the surface tension for the (a) lower pressure run and (b) the higher pressure run. Different contributions to the surface tension are shown in the legends.

5.4.3 Pressure Dependence

In Figure 5-5 it can be seen that the surface tension versus temperature curve drops to lower surface tension for a higher pressure. This is again in agreement with the experimental findings and empirical equation (5-32). The components of the surface tension that drop are the internal energy, the configurational entropy of the polymer and the translational entropy of the solvent; this can be seen from Figure 6 by comparing panels **(**a**)** and **(**b**)** or by examining Table 5-5, rows value $_{l}$ and value $_{h}$. Again, the largest single factor causing this drop is the internal energy contribution. In Figure 5-8, however, we see that for the pressure induced tension drop, the responsible sub-component is not the polymer-solvent internal energy as for the temperature case, but rather the solvent-solvent sub-component. Translating this conclusion into industrial polymer-solvent processes, one could simply focus on modifying the molecular self-interaction among solvent molecules when making use of such pressure dependence of surface tension.

The above conclusion can be understood in terms of a reduction of dilution by the holes. At higher pressure, there are fewer holes present. Since $\chi_{ss}N$ has been chosen to be positive, solvent molecules prefer to be in an environment of holes rather than in an environment of other solvent molecules; in the former situation the unfavourable solvent-solvent contact energy is diluted by the holes. With the removal of holes at higher pressure, this dilution is reduced, the solvent-solvent contact energy goes up, and so does the free energy. This effect takes place predominantly in the bulk solvent side of the interface where the majority of solvent molecules can be found. This means the bulk free energy $F_h^{(1)}$ appearing in equation (5-15) and thus in (5-14) is increased. This increased quantity is

subtracted off the total free energy (5-1) to find the surface tension; therefore the surface tension will drop.

This last point may be understood in terms of density. The removal of holes is the same as an increase in density in the region where the holes are being removed. Thus the surface tension drops when the solvent phase increases in density to be more similar to the density on the polymer side of the interface. Thus one can say the drop in surface tension with increasing pressure is due to a reduction of the density difference between the two sides of the interface.

The above analysis of pressure dependence requires a χ_{ss} that is positive, and so it is appropriate here to discuss what might be the case if χ_{ss} were negative. This is important since from the first principles definition of χ_{ss} given in equation (5-2) one would expect that χ_{ss} would normally be less than zero, that is, the solvent molecules would have some slight attraction. For more realistic choices of α, the translational entropy of the solvent would not be negligible. Therefore instead of holes diluting the solvent phase for energetic reasons, the holes would dilute the phase for entropic reasons. The explanation would remain the same for the pressure dependence beyond this, and the density difference interpretation would still hold. As α is increased, the translational entropy of the solvent will become less important, and to maintain the interface structure, χ_{ss} must be made less negative. For a very large α, such as is being used here, χ_{ss} must become positive to draw the hole molecules into the solvent phase to reproduce the experimental configuration. At this point, χ_{ss} must be viewed entirely as a phenomenological parameter.

5.4.4 Pressure Dependence Change in Temperature Dependence with Pressure

In addition to an overall drop in surface tension upon increasing pressure, the temperature dependence of the surface tension is less pronounced at high pressures than at lower pressures. This is seen in Figure 5-5 where the dotted curve is a repetition of the high pressure curve (dashed) shifted upwards to lie on top of the lower pressure curve (solid). One can clearly see the shallower slope with temperatures being of high-pressure results. This is again in agreement with the experimental findings and the empirical equation (5-32).

From Figure 5-7, one can compute linear slopes for all the components of the surface tensions in order to find which components are responsible for this reduction in steepness. Table 5-3, row Δm shows the difference between the component slopes. It is found that the translational entropy components of the polymer, solvent and holes all contribute to the overall reduction in steepness. The hole contribution is negligible compared to the other two and can be safely ignored. Thus it is the polymer and solvent translational entropy contributions to the surface tensions that cause the shallowness of the high pressure results.

This can be explained in terms of the presence or absence of holes. The presence of holes can only affect the system in two ways: through energy dilution as discussed in the pressure dependence subsection, or through adding translational entropy. The latter has already been said to be insignificant, and so we are left with energy dilution alone. At low pressures, the solvent-solvent contacts are diluted by the holes, reducing the system free energy. At high pressures, solvent-solvent contacts cannot be reduced by holes anymore, so the only possibility for reducing these contacts is for the solvent to be near polymer segments.

This induces increased mixing, and thus increased translational entropy of both the solvent and the polymer. This increased mixing partially counteracts the internal energy segregation effect that is a function of temperature. Thus the surface tension profile with temperature is flatter at higher pressures than at lower pressures where this polymer-solvent mixing is unnecessary due to the presence of the holes. In other words, when the solvent is at higher density, there is a greater mixing effect that counteracts the formation of an interface due to a solvent-solvent internal energy reduction upon absorbing solvent into the polymer phase.

For small α values and negative χ_{ss} parameters, the same mechanism is expected to function, except that translational entropy will force the holes into the solvent phase rather than energetic considerations, which is along the lines explained in the pressure dependence section.

Table 5-3 Slopes of the components of the surface tension from figure 5-6 assuming linearity.

Contributions of the various components are labeled without including multiplicative factors. The ml refers to the slope of the low pressure run and the mh refers to the high pressure run. Units are inverse arbitrary temperature. Δm is the difference between the slopes of the low and high pressure runs. Value l and value h are midpoint values of the low and high pressure runs, respectively, taken from figure 5-6.

	γ	U	S_{Tp}	S_{Cp}	S_{Ts}	S_{Th}
m_l	-1.05	-0.69	0	-0.45	0.12	-0.02
m_h	-0.72	-1.07	0.25	-0.49	0.59	0.00
Δm	0.33	-0.38	0.25	-0.04	0.47	0.02
value $_l$	0.97	2.22	-0.46	0.46	-0.95	-0.30
value $_h$	0.29	1.62	-0.42	0.23	-1.14	0.00

5.4.5 Simple Liquid Models

In all three aforementioned trends, theory was able to reproduce and explain the experimental results. The explanations did not require any consideration of the configurational entropy contribution to the surface tension. This then could explain why simple liquid theory models of polymer interfaces such as those discussed by Dee and Sauer (Dee and Sauer, 1998) or Jones and Richards (Jones and Richards, 1999) could be quantitatively reliable. We anticipate that the configurational entropy contributions would become even less significant for lower α values, that is, for more realistic volume ratios between the solvent and polymer. Preliminary

runs with smaller values of α (not included) seem to bear this out. Upon reducing α, the number of solvent molecules must increase in order to preserve the same overall volume fraction of solvent. This increases the translational entropy component of the solvent, and weakens the interface. To have a stable interface for very small α, one must counteract this by greatly increasing the segregations. This will increase the internal energy contribution relative to the configurational entropy of the polymer for a similar width of interface. Thus if the model were to be made more realistic, the configurational entropy would become less important, further justifying the use of simple liquid models. Specifically, if the configurational entropy of the polymer to the surface tension was to be subtracted out of the results, the same qualitative results would be found. This is not true of the other quantitatively significant contributions to the surface tension, see Figure 5-7. Therefore, one can say that the theoretical explanations of the experimental results may not require any consideration of the configuational entropy contribution to the surface tension. In fact, if gradient terms are kept in the SCFT description of the polymer system along the lines of Hong and Noolandi (Hong and Noolandi, 1981), then upon ignoring configurational degrees of freedom of the polymer in the SCFT formalism, one might expect to arrive at a theory very similar to density gradient theory (square density theory, Cahn-Hilliard theory). Theories of this sort have been shown to give very good quantitative agreement (Enders *et al.*, 2005), although being phenomenological, they cannot explain the microscopic origins of the trends they predict. It is precisely this explanatory feature of SCFT that motivates its present use.

5.5 Summary

A comprehensive set of the surface tension data of polystyrene in supercritical carbon dioxide at various temperatures and pressures was obtained successfully. Based on the obtained data, an empirical equation was developed that predicts the surface tension value at a given temperature and pressure. Within the experimental limits on temperature (< ~385°C) and pressure (< ~2153 psi), the trends of surface tension dependence on temperature and pressure can be quantified with partial derivatives of the empirical equation.

Self-consistent field theory calculations were performed on a model system and surface tension trends involving temperature, pressure, and temperature with pressure were explained in the terms of the components of the surface tension. In particular, the reduction of surface tension with increasing temperature was consistent with a reduction of segregation between the molecular constituents; the reduction of surface tension with increasing pressure was due to the increased similarity of density between the polymer (polystyrene) and solvent (supercritical carbon dioxide) constituents; the flattening of the surface tension versus temperature curve with increasing pressure was due to extra mixing between polymer and solvent, which reduces the segregation of the species at high pressures. The extra mixing results from the similar densities of the molecules at high pressures. None of these findings were dependent on the configurational entropy contribution of the polymers to the surface tensions, and so the use of simple liquid models for the prediction of surface tensions is justified. Consideration should be given to the above mechanisms when attempting to engineer surface tension properties.

Chapter 6*
Effects of Molecular Weight on the Surface Tension

6.1 Introduction

The effect of molecular weight on polymer properties and processing has been well documented in literature. Limited studies have been reported on the effect of polymer molecular weight on surface tension (Mason *et al.*, 2001; Jannasch 1998). There has been no report on the molecular weight effect on the surface tension of polymers of high molecular weight in a supercritical fluid. Supercritical fluids, such as carbon dioxide and nitrogen, have been widely used as foaming agents in the production of microcellular polymer foams (Cahn and Hilliard, 1959; Goel and Beckman, 1994a). Although the amount of a supercritical fluid dissolved in the polymer is small, it can result in dramatic changes in physicochemical properties, such as glass transition temperature, viscosity, solubility, and surface tension (Lee, *et al.*, 1999; Anastasiadis *et al.*, 1988; Stafford *et al.*, 1999; Arashiro and Demarquette, 1999).

There are many methods to measure surface tension. Among them, the pendant drop method has many advantages because of its simple setup and versatile applications (del Rio and Neumann, 1997; Rotenberg *et al.*, 1983). The pendant drop method has been used extensively for low molar mass liquids, liquid crystals and polymers (Alexopoulos *et al.*, 1989; Song and Springer, 1996; Anastasiadis *et al.*, 1986). Although the pendant drop method is theoretically simple, research on the surface tension of polymers in a supercritical fluid has

* This chapter is based on the manuscript of the published studies (Park et al, 2007b).

been limited because of experimental difficulties in handling high viscosity polymer melts under high temperature and high pressure (Roe *et al.*, 1967; Wu 1970).

The primary objective of this study is to investigate the effect of the molecular weight on the surface tension of polystyrene melt in supercritical nitrogen. The surface tension is measured as a function of temperature and pressure in monodisperse polystyrenes of two different molecular weights and a polydisperse polystyrene. A recently designed high-temperature and high-pressure sample cell is employed in the surface tension measurement to obtain a wide range of experimental conditions. Using the set of surface tension data obtained, an empirical equation approximating the surface tension of polystyrene in supercritical nitrogen as a function of temperature and pressure is developed.

6.2 Experimental

6.2.1 Surface Tension Measurement

The surface tension of polystyrene in nitrogen was measured at different temperatures, from 170 to 210°C, within a wide range of pressures, from 500 to 2000 psi. To achieve these experimental conditions, a high-temperature and high-pressure sample cell was used. This optical viewing cell consisted of a cylinder of stainless steel, which was heated by an electrical band heater. The cylinder was hollow, with an inner diameter of 30 mm and length of 25 mm. Two optical-quality sapphire windows (Meller Optics, Inc.) permitted the illumination and observation of the pendant drop formed by a sample polymer melt. The experimental setup was tested for its accuracy and reproducibility with a range of polymer-

gas combinations, and the details of this setup and validation for the surface tension measurement were described in a recent publication (Park *et al.*, 2006).

The technique of Axisymmetric Drop Shape Analysis-Profile (ADSA-P) (Cheng *et al.*, 1990; Susnar *et al.*) was used for image analysis and parameter estimation. Surface or interfacial tensions were obtained by fitting the Laplace equation of capillarity to the acquired shape and dimensions of axisymmetric menisci (Andreans *et al.*, 1986). The value of surface tension was generated as a fitting parameter(Cheng and Neumann, 1992) after a least-square algorithm was employed to minimize the difference between experimental and theoretical drop profiles. During this procedure, the density difference between polystyrene and nitrogen was an input parameter (Xue *et al.*, 2004; Li *et al.*, 2004), which was determined by the Sanchez and Lacombe (S-L) equation of state (EOS) (Sanchez and Lacombe, 1976; Sanchez and Lacombe, 1978; Sato *et al*., 1976; Sato *et al*., 2001). The data of density difference between polystyrene and nitrogen at different temperatures and pressures are shown in Table 6-1. The details of the calculations is shown in Appendix-B

Table 6-1. Density difference data between polystyrene and nitrogen at various temperatures and pressures in units of g/cm³.

Temperature (°C)	Pressure(psi)			
	500	1000	1500	2000
170	0.9623	0.9381	0.9147	0.8921
180	0.9564	0.9328	0.9099	0.8878
190	0.9504	0.9272	0.9049	0.8833
200	0.9442	0.9216	0.8997	0.8786
210	0.9380	0.9157	0.8943	0.8736

Note: The density differences of nitrogen and polystyrene saturated with nitrogen are determined by the Sanchez and Lacombe equation of states as expressed below:

$$\tilde{\rho}^2 + \tilde{P} + \tilde{T}\left[\ln(1-\tilde{\rho}) + (1-1/r)\tilde{\rho}\right] = 0 \tag{6-1}$$

where $\tilde{\rho}$ is the reduced density, $\tilde{P}$ is the reduced pressure, $\tilde{T}$ is the reduced temperature and r is the number of sites occupied by a molecule (Sato *et al*., 2001). The reduced parameters are defined as

$$\tilde{P} = \frac{P}{P^*}, \tilde{\rho} = \frac{\rho}{\rho^*}, \tilde{T} = \frac{T}{T^*}, r = \frac{MP^*}{RT^*\rho^*} \tag{6-2}$$

where ρ is the density, *P* is the pressure, *T* is the temperature, *M* is the molecular weight and *R* is the gas constant. It is worth noting that the density differences calculated here do not distinguish the three polystyrenes of different molecular weights within the limited significant digits. As shown in the results of this study, the key parameter influencing the surface tension here is molecular weight.

6.3 Results and Discussion

6.3.1 Effect of Molecular Weight on the Surface Tension

The surface tension of polystyrene melts in supercritical nitrogen was measured at four different pressures: 500, 1000, 1500 and 2000 psi, and five different temperatures: 170, 180, 190, 200 and 210°C. The equilibrium surface tension values of the polystyrenes in nitrogen were obtained from their time-dependent surface tension measurements under each set of conditions. The average of the surface tension values is taken as the equilibrium surface tension when the change in surface tension is less than 0.0001mJ $m^{-2}s^{-1}$ for 1 hour. Errors are in the order of 0.01 mJ m^{-2}. The results are shown in Figure 6-1 for two monodisperse polystyrenes of M_w ~ 100,000 and ~ 400,000, along with a polydisperse polystyrene. The surface tension values are in a range similar to those of other studies (Li *et al.*, 2004).

Monodisperse, rather than polydisperse, polystyrenes are used in investigating the effect of molecular weight on the surface tension because the polydispersity of polystyrene might add an additional influence. Figure 6-1 shows that the higher molecular weight polystyrene has a higher surface tension under all pressure and temperature conditions tested.

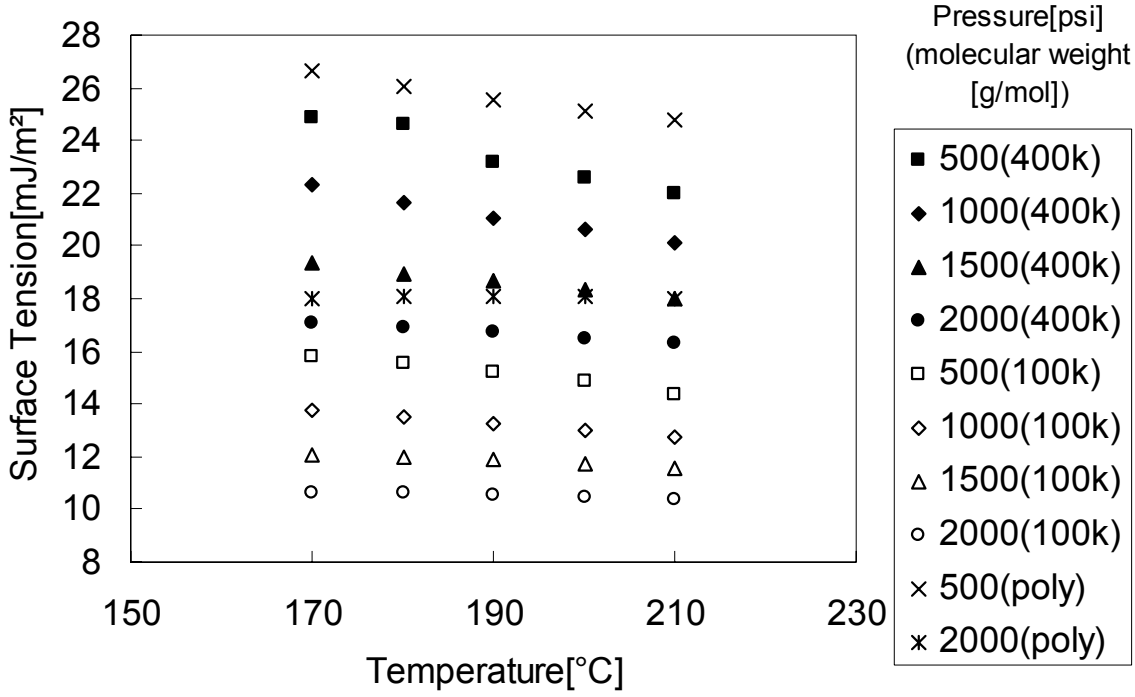

Figure 6-1. Surface tension as a function of temperature for two monodisperse polystyrenes under 4 different pressures and for one polydisperse polystyrene under 2 different pressures. Closed symbols refer to the monodisperse polystyrene of a weight average molecular weight of 400,000 g/mol; open symbols refer to that of a weight average molecular weight of 100,000 g/mol. Crossed and asterisk symbols refer to the polydisperse polystyrene. The lower molecular weight polystyrene shows lower surface tensions. The polydisperse polystyrene has a weight average molecular weight of 312,000 g/mol, and has slightly higher surface tensions than those of the high molecular weight monodisperse polystyrene.

To quantify the temperature and pressure influence on the surface tension, a second-order linear regression model was used (O'Neill *et al.*, 1998). From statistical investigations, we can propose the following equations for the two monodisperse polystyrenes.

$$\gamma\,(M_w\sim 100{,}000,\ \text{Polydispersity}\sim 1) = 25.0362 - 0.0448\,T - 0.0068\,P + (1.97\times 10^{-5})TP \qquad (R^2=0.99) \qquad (6\text{-}3)$$

$$\gamma\,(M_w\sim 400{,}000,\ \text{Polydispersity}\sim 1) = 43.5497 - 0.0942\,T - 0.0120\,P + (3.91\times 10^{-5})TP \qquad (R^2=0.99) \qquad (6\text{-}4)$$

where γ is the surface tension of polystyrene in supercritical N_2, in mJ/m^2, T the temperature in degrees Celsius, and P the pressure in psi. Note that the second order terms in T and P are absent; statistically, γ is linearly related to T and P. There is an interaction term in TP, indicating γ dependence on T or P is affected by P or T, respectively.

Comparison between the above two equations indicates that polystyrene of a higher molecular weight has a stronger temperature and pressure dependence of surface tension than polystyrene of a lower molecular weight. The cross interaction between temperature and pressure effects is also more significant for the higher molecular weight polystyrene.

6.3.2 Effect of Polydispersity on the Surface Tension

Similar to its monodisperse counterparts, the polydisperse polystyrene demonstrates three trends of surface tension variation: The surface tension decreases with increasing temperature and pressure, and the temperature dependence of surface tension is less pronounced at higher pressure (Fig. 6-1). It is noticed that the polydisperse polystyrene has a higher surface tension

than the monodisperse polystyrene of M_W ~ 400,000, even though its molecular weight, both weight-average and number-average, is below 400,000. In a polydisperse polymer, a wide distribution of molecular weight exists; thus, it may not be surprising that a portion of polystyrene molecules possesses a molecular weight greater than 400,000. This large molecular weight portion of polystyrene molecules may contribute more influentially to a high surface tension. In other words, high surface tension values are mainly derived from polystyrene molecules of high molecular weight. This conclusion is also consistent with the fact that the surface tension of monodisperse polystyrene of M_w~ 400,000 is greater than that of M_w ~ 100,000.

6.3.3 Relationship Between Surface Tension and Density

The relation between surface tension and density has been expressed by the generalized Macleod equation:

$$\gamma = C(\Delta\rho)^n \tag{6-5}$$

where γ is the surface tension of the polymer, C an empirical constant, $\Delta\rho$ the density difference between the polymer and its surrounding fluid, and n Macleod's index. Table 6-2 shows the results of the fit of Eq. (6-5) to the experimental data. The values of Macleod's indices obtained for the three polystyrenes range from 4.5 to 4.8, similar to Wu's results (Wu 1982). These values are slightly higher than those of polystyrene in carbon dioxide; the lower molecular weight monodisperse polystyrene has a higher Macleod's index.

Table 6-2. Parameters in the Macleod equation

Polystyrenes(PS)	Macleod's index(n)	constant (C)
Polydisperse PS	4.5±0.3	3.5±0.03
High molecular weight monodisperse PS	4.7±0.1	3.4±0.01
Low molecular weight monodisperse PS	4.8±0.2	3.0±0.01

The parameters were obtained from the generalized Macleod equation, $\gamma = C(\Delta\rho)^n$, where γ is the surface tension, C a constant, $\Delta\rho$ the density difference between polymer and surrounding fluid, and n Macleod's index. The standard errors are obtained at a 95% confidence level.

A detailed mechanistic study of the molecular weight effect on surface tension is currently underway. Dee and Sauer (Dee and Sauer, 1998) showed that density profiles between vapor and liquid phases depend on the molecular weight of polymers. Polymers of a higher molecular weight have a steeper density profile at the interface, indicating that high molecular weight polymers have a narrower interface. The narrower interface causes the stronger barrier to maintain the interface. This may be related to higher surface tensions of polystyrenes with higher molecular weight. Due to the order of nanometer of the interface width, the extensive research should be focused on experimental and theoretical models to gain a better understanding.

6.4 Summary

A set of the surface tension data of two monodisperse polystyrenes of M_w ~ 100,000 and M_w ~ 400,000 and a polydisperse polystyrene in supercritical nitrogen at various temperatures

and pressures was successfully obtained. Within the experimental temperatures of 170^{o}C - 210 ^{o}C and pressures of 500psi - 2000psi, the dependence of surface tension on temperature and pressure was linearly quantified. As the pressure and temperature increase, the surface tension of all polystyrenes decreases. The slope of surface tension changes with temperature is decreased as the pressure is increased. It has been found that the higher molecular weight polystyrene has a higher surface tension by 6-9 mJ/m^2 according to the experimental conditions. The surface tension dependence on temperature, as well as on pressure, is stronger for the monodisperse polystyrene of higher molecular weight. For the polydisperse polystyrene, high surface tension values may be influenced more by high molecular weight portions of polystyrene molecules.

Chapter 7
Original Contributions and Recommendations

7.1 Original Contributions

This thesis presents an experimental method that uses Axisymmetric Drop Shape Analysis – Profile (ADSA-P) to measure the surface tension of polymer melts in supercritical fluids. To characterize the stability of pendant drops formed by the polymer melts, the Bond number is determined to be useful; in particular, a stable pendant drop is obtained when the Bond number is in the range of 0.4-0.8. The method prevents the capillary and necking effect and provides good axisymmetric pendant drops (Demarquette and Kamal, 199). In this method, the surface tension is calculated by a least squares algorithm that fits the shape of an experimental drop to the theoretical drop profile. Other parameters, such as drop volume, surface area, and radius of curvature, can be obtained (Rotenberg *et al.*, 1983; del Rio and Neumann, 1997).

The method is verified by experiments in air and nitrogen, where reproducibility tests and statistical analyses are performed. The surface tension of polystyrene melts in supercritical carbon dioxide, while the gas solubility is correlated with the surface tension value determined under various pressures. At higher pressures, the surface tension becomes lower values. After critical pressure of carbon dioxide is achieved, the surface tension continues to decrease as the pressure increases. The Sanchez-Lacombe (S-L) equation of sates

(EOS) is applied to estimate the pressure-volume-temperature (PVT) date of the polystyrene/supercritical carbon dioxide mixture, which gives density data. The relationship between surface tension and density is described by the empirical Macleod equation.

Self Consistent Field Theory (SCFT) calculations are applied to simulate the surface tension of the corresponding system, and good qualitative agreement with the experiment is obtained. The physical mechanisms for three main experimental trends are explained by using SCFT, and none of the explanations quantitatively depend on the configurational entropy of the polymer constituents. These calculations rationalize the use of simple liquid models for the quantitative prediction of the surface tension of polymer. As pressure and temperature increase, the surface tension of polystyrene decreases. A linear relationship is found between surface tension and temperature, and between surface tension and pressure; the slope of surface tension changes while the temperature is dependent on pressure.

The effect of molecular weight on surface tension is provided by comparing a set of surface tension data of two monodisperse polystyrenes and one polydisperse polystyrene in supercritical nitrogen at various temperatures and pressures. For two monodisperse polystyrenes of Mw ~ 100,000 and 400,000 and one polystyrene, a linear relationship is found between surface tension and temperature and between surface tension and pressure within a temperature range of 170-210^{o}C and a pressure range of 500-2000 psi. With an increase in pressure or temperature, the surface tension of all three polystyrenes decreases. Monodisperse polystyrene of a higher molecular weight has a higher surface tension by 6-9mJ/m^2 under all experimental conditions. The surface tension dependence on temperature and on pressure is more significant for the higher molecular weight polystyrene. For the

polydisperse polystyrene, high surface tension values seem to be related predominately to its high molecular weight portion of polystyrene molecules. An empirical equation, the Macleod relation, was used to relate surface tension with density difference between the polymer and supercritical nitrogen satisfactorily.

7.2 Recommendations

This thesis presents the technique to measure the surface tension of polymers in a supercritical fluid. However, due to the difficulties of dealing with highly viscous polymers under high pressure and temperature, current measurements are limited to a few polystyrenes in carbon dioxide and nitrogen. More experimental measurements on other polymers or polymer pairs of polymer foaming, polymer coating, and polymer blending would be useful in determining the importance of surface phenomena.

In the microcellular foaming process, the free energy for homogeneous nucleation is proportional the cubic power of surface tension between the nucleating bubble phase. Therefore, the study on the relationship between polymer surface tension and process parameters such as pressures and temperatures, and between polymer surface tension and materials parameters such as glass transition temperature, viscosity, crystallity, foaming agents, molecular weights, molecular weight distributions, and copolymers is essential in order to optimize the process. Specifically, the research on the alternatives to prevent the depletion of the ozone layer would focus on the surface tension between the polymers and potentials such as hydrogen-containing chloroflurocarbons, hydrocarbon and inert gases.

Relatively little research has been done on the research involving the control of surface and interfacial properties of polymeric materials to achieve various desired characteristics such as biocompatibility, foaming, wetting, blending, adhesion, friction and wear. The surface properties of these materials can vary from highly hydrophilic to highly hydrophobic. The macroscopic interfacial phenomena that play a role in determining the surface properties include wetting, adhesion and adsorption. These are dependant on the intermolecular and surface forces on a molecular level, as well as the chemical and physical details of the molecular structure of the surfaces, such as the availability of particular functional groups. The structural features of macromolecules contribute substantial changes in interfacial properties. Therefore, it is desirable to be able to control the surface energy of the polymer by modifying its chemical structure.

The surface properties of polymers are affected by surface segregation of low surface energy components. Surface segregation can occur in miscible and immiscible multi component polymer systems, such as polymer blends. In the case of random, block and graft copolymers, the surface tension can be reduced through surface modifications among the copolymer sequences (Jannasch 1998). In the case of high crystallity polymer chains in block and graft copolymers, the structural effects may result in a second polymer component which can be localized at the surface. End functionalized polymers have been used to control polymer surface properties (Mason *et al.*, 2001).

To gain a better understanding of those complicated relationships, the reliable experimental data of surface tension of polymer as well as a quantitative knowledge of the molecular composition of the surfaces is of utmost importance. The Axisymmetric Drop

Shape Analysis Profile (ADSA-P) method has proved to be a powerful technique to distinguish minor changes in surface properties.

In addition to the experimental investigation, a thermodynamic approach will be undertaken to develop the theoretical model to predict the surface properties of polymers in a molecular level design. The detailed characterization of the polymer surface properties of various polymers and the research on end group effects would be carried out using model components. The detailed polymer modification studies with desired applications would perform using both model components and the real systems. The expertise gained from this research could be applied to numerous fields of research such as the pharmaceutical industry, food engineering, specialized copolymer synthesis, coating and foaming.

Chapter 8 References

Adamson, A. W. and Gast, A. P., "Physical Chemistry of Surfaces", John Wiley & Sons, Inc., New York (1997)

Alexopoulos, A. H., Puig, J. E., Franess E. J. " Phase Continuity and Surface Properties of dispersions of AOT/Water Liquid Crystals", J. Colloid Interface Sci., 128, 26-34 (1989)

Anastasiadis, S. H., Chen, J. -K., Koberstein, J. T., Siegel A. F., Sohn, J. E. and Emerson J. A., "The Determination of Interfacial Tension by Video Image Processing of Pendant Fluid Drops", J. Colloid Interface Sci., 119, 55-66 (1987)

Anastasiadis, S. H., Chen, J. K., Koberstein, J.T., Sohn, J. E. And Emerson, J. A., "The determination of polymer interfacial tension by drop image processing: Comparison of theory and experiment for the pair, poly(dimethyl siloxane)/polybutndiene", Polym. Eng. Sci., 26, 1410-1418 (1986)

Anastasiadis, S. H., Gancarz, I. and Koberstein, "Interfacial Tension of Immiscible Polymer Blends: Temperature and Molecular Weight Dependence", Macromolecules, 21, 2980-2987 (1988)

Andreas, J. M., Hauser, E.A., and Trucker W.B., "Boundary Tension By Pendant Drops", J. Phys. Chem. 42, 1001-1019 (1938)

Arashiro, E. Y. and Demarquette, N. R., "Influence of Temperature, Molecular Weight, and Polydispersity of Polystyrene on Interfacial Tension Between Low-Density Polyethylene and Polystyrene", Journal of Applied Polymer Science, 74, 2424-2431 (1999)

Arashiro, E. Y.and Demarquette, N. R. "Use of the Pendant Drop Method to Measure Interfacial Tension between Molten Polymers", Materials Research, 2, 23-32 (1999)

Binder, K., Müller, M.; Virnau, P.; and MacDowell, L.G., "Polymer + Solvent System: Phase Diagram, Interface Free Energies, and Nucleation", Adv. Polym. Sci., 173, 1-110 (2005)

Cahn, J. W. and Hilliard J. E., "Free Enery of a Nonuniform System. III. Nucleation in a Two-Component Incompressible Fluid", J. Chem. Phys. 31, 688-699 (1959)

Cansell, F., Chevalier, B., Demourgues, A., Etourneau, J., Even, C., Garrabos, Y., Pessey, V., Petit, S., Tressaus, A. and Weill F., "Supercritical fluid processing: a new route for materials synthesis", J. Mater. Chem., 9, 67-75 (1999)

Chen, C. C. and White J. L., “Compatibilizing Agents in Polymer blends: Interfacial Tension, Phase Morphology, and Mechanical Properties”, Polym. Eng. Sci., 33, 923-930 (1993)

Cheng, P. and Neumann, A. W., “Computational Evaluation of Axisymmetric Drop Shape Analysis-Profile (ADSA-P)”, Colloids and Surfaces, 62, 297-305 (1992)

Cheng, P., Li, D., Boruvka, L., Rotenberg, Y. and Neumann, A. W., “Automation of Axisymmetric Drop Shape Analysis for Measurements of Interfacial Tensions and Contact Angles”, Colloids and Surfaces, 43, 151-167 (1990)

Cho, D., Hu, W., Koberstein, J. T., Lingelser, J. P. and Gallot Y., “Segregation Dynamics of Block Copolymers to Immiscible Polymer Blend Interfaces”, Macromolecules, 33, 5245-5251 (2000)

Colton, J. S. and Suh, N. P., “Nucleation of Microcellular Foam: Theory and Practice”, Polym. Eng. Sci., 27, 500-503 (1987)

Cooper, A. I., “Polymer synthesis and processing using supercritical carbon dioxide”, J. Mat. Chem. 10, 207-234 (2000)

Dee, G. T. and Sauer, B. B., “The Surface Tension of Polymer Liquids”, Advances in Physics, 47, 161-205 (1998)

del Rio, O. I. and Neumann, A.W., "Axisymmetric Drop Shape Analysis: Computational Methods for the Measurement of Interfacial Properties from the Shape and Dimensions of Pendant and Sessile Drops", J. Colloid Interface Sci., 196, 136-147 (1997).

Demarquette, N. R. and Kamal, M. R., "Interfacial Tension in Polymer Melts. 1: An improved pendant Drop Apparatus", Polym. Eng. Sci., 34, 1823-1833 (1994)

Doroudiani, S, Park, C. B. and Kortschot, M. T., "Effect of the Crystallinity and Morphology on the Microcellular Foam Structure of Semincrystalline Polymers", Polym. Eng. Sci., 36, 2645-2662 (1996)

Durrill, P. L. and Grikey, R. G., "Diffusion and Solution of Gases in thermally Softened or Molten Polymers: Part I. Development of Technique and Determination of Data", AIChE J, 12, 1147-1151 (1966)

Durrill, P. L. and Grikey, R. G., "Diffusion and Solution of Gases in thermally Softened or Molten Polymers: Part II. Relation of Diffusivities and Solubilities with Temperature Pressure and Structural Characterizations", AIChE J, 15, 106-110 (1969)

Ferguson, A., Kennedy S. J., "Free and Total Surface Energies And Related Quantities", Trans. Faraday Soc., 32, 1474-1481 (1936)

Flory, P. J. "Thermodynamics of High Polymer Solutions", J. Chem. Phys. 10, 51-61 (1942)

Fredrickson, G. H., Ganesan, V., and Drolet, F., “Field Theoretic Computer simulation for Polymers and Complex Fluids”, Macromolecules, 35, 16-39 (2002)

Frrri, J. K., Lin,S. Y., and Stebe, K. J., “Curvature Effects in the Analysis of Pendant Bubble Data: Comparison of Numerical Solutions, Asymptotic Arguments and Data”, J. Colloid Interface Sci., 154-168 (2001)

Funke, Z., Schwinger, C., Adhikari, R. and Kressler J., “Surface Tension in Polymer Blends of Isotactic Poly(propylene) and Atactic Polystyrene” Macromol. Mater. Eng.., 286, 744-751 (2001)

Goel, S. K. and Beckman, E. J., “Generation of Microcellular Polymeric Foams Using Supercritical Carbon Dioxide. I: Effect of Pressure and Temperature on Nucleation”, Polym. Eng. Sci., 34, 1137-1147 (1994a)

Goel, S. K. and Beckman, E. J., “Generation of Microcellular Polymeric Foams Using Supercritical Carbon Dioxide. II : Cell Growth and Skin Formation”, Polym. Eng. Sci., 34, 1148-1156 (1994b)

Gonzalez, G. and MacRitchie, F., “Equilibrium Adsorption of Proteins”, J. Colloid Interface Sci., 32, 55-61 (1970)

Hess, M., “The Use of Pressure-Volume-Temperature Measurements in Polymer Science”, Macromol. Symp., 214, 361-379 (2004)

Higgins, M.L. “Thermodynamic properties of solutions of long-chain compounds”, Annals of the New York Academy of Science 43, 1-32 (1942)

Hildebrand, J. H. and Scott, R. L. “Regular Solutions”, Prentice-Hall, New Jersey (1962)

Hong, K. M. and Noolandi, J., “Conformational Entropy Effects in a Compressible Latice Fluid Theory of Polymers”, Macromolecules, 14, 1229-1234 (1981)

Jannasch, P., “Surface Structure and Dynamics of Block and Graft Copolymers Having Fluorinated Poly (ethylene oxide) Chain Ends”, Macromolecules, 31, 1341-1347 (1998)

Janssen, J. M. H. and Meijer, H. E. H., “Droplet breakup mechanisms: Stepwise equilibrium versus transient dispersion”, J. Rheol., 37, 597-608 (1993)

Jones, R. A. L. and Richards, R. W., “Polymers at Surfaces and Interfaces”, Cambridge University Press, New York (1999)

Kato, S., Tsujita, Y., Yoshimizu, H., Kinoshita, T. and Higgins J.S. “Characterization and CO2 sorption behaviour of polystyrene/polycarbonate blend system”, Polymer, 38, 2807-2811 (1997)

Kim, K. U. and Kim, B. C., “Rheological Measurements of Rigid Foam Extrusion” in “Two Phase Polymer system”, Utracki, L.A., Ed., Hanser Publishers, Munich (1991)

Kumar, V. and Gebizlioglu, O. S., “Thermal and microscopy studies of carbon dioxide-induced morphology in crystalline PET foams”, SPE ANTEC, 1536-1540 (1992)

Kwok, D. Y., Cheung, L. K. Cheung, Park, C. B. and Neumann A. W., “Study on the Surface Tensions of Polymer Melts Using Axissymmetric Drop Shape Analysis”, Polym. Eng. Sci.,38, 757-764 (1998)

Lahooti, S., del Rio, O.I., Cheng, P. and Neumann, A. W., “Axisymmetric Drop Shape Analysis(ADSA)” in “Applied Surface Thermodynamics”, Neumann, A. W., Spelt, K.K. , Ed., Marcel Dekker, New York (1996)

Lau, W. W. Y., Burns, C. M., “Kinetics of Spreading. Polystyrene Melts on Plane Glass Surfaces”, J. Colloid Interface Sci., 45, 295-302 (1973)

Lee, M., Park, C. B. and Tzoganakis, C., “Measurements and Modeling of PS/Supercrtical CO2 Solution Viscosities”, Polym. Eng.Sci.,39, 99-109 (1999)

Lee, S. T., “Shear effects on thermoplastic foam nuvcleation”, Polym. Eng. Sci., 33, 418-422 (1993)

Legrand, D. G., Gaines C. L., “The Molecular weight Dependence of Polymer Surface Tension”, J. Colloid Interface Sci., 31, 162-167 (1969)

Machell, J. S., Greener J., Cantestable B. A., “Optical Properties of Solvent-Cast Polymer Films”, Macromolecules, 23, 186-194 (1990)

Macleod, D. B., “On a Relation Between Surface Tension And Density”, Trans. Faraday Soc., 19, 38-41 (1923)

Madge, E. W., “Latex Foam Rubber”, Interscience Pubs, Inc., New York (1962)

Mai , S.-M., Fairclough, J. P. A., Terrill, N. J.,Turner, S. C., Hamley, I. W., Matsen, M. W., Ryan, A. J., and Booth, C., “Microphase Separation in Poly(oxyethylene)-Poly(oxybutylene) Diblock Copolymers” , Macromolecules, 31, 8110-8116 (1998)

Mai, S. -M., Mingvanish, W., Turner S. C., Chaibundit, C., Fairclough, J. P. A., Heatley, F., Matsen, M. W., Ryan, A. J., and Booth C., “Microphase-Separation Behavior of Triblock Melts. Comparison with Diblock Copolymer Melts” , Macromolecules, 33, 5124-5130 (2000)

Martini-Vvendensky, J. E., Suh, N. P. and Waldman, F. A., “Microcellular closed cell foams and Their Method of Manufacture”, USP 4473665 (1984)

Mason, R., Jalbert, C. A., Muisener, P. A. V. O., Koberstein, J. T., Elman, J. F., Long, T.E., and Gunesin, B.Z., “Surface energy and surface composition of end-fluorinated polystyrene”, Advances in Colloids Interface Science, 94, 1-19 (2001)

Matsen, M. W., “The standard Gaussian model for block copolymer melts”, J. Phys.: Condens. Matter, 14, R21-R47 (2002)

Matsen,M. W. and Bates, F. S., “Block copolymer microstructures in the intermediate-segregation regime”, J. Chem. Phys., 106, 2436-2448 (1997)

Michels, A. and Michels C., “Isotherms of CO2 Between 0° and 150° and Pressures from 16 to 250 Atm (Amagat Density 18-206)”, Pro. Roy. Soc. A, 153, 201-214 (1935)

Michels, A., Blaisse, B. and Michels C., “The Isotherms of CO2 in the Neighbourhood of Critical Point and Round the Coexistence Line”, Pro. Roy. Soc. A, 160, 201-214 (1937)

Miller, R. and Kretzschmar G., “Adsorption Kinetics of Surfactants at Fluid interfaces”, Advances in Colloids Interface Science, 37, 97-121 (1991)

Miller, R., Joos, P. and Fainerman V. B., "Dynamic Surface and Interfacial Tensions of Surfactant and Polymer Solutions", Advances in Colloids Interface Science, 49, 249-302 (1994)

Milton, J. S. and Arnold J. C., "Introduction to probability and Statistics: Principles and Applications for Engineering and the Computer Science", McFraw-Hill, Inc., New York (1995)

Morita, A. T., Carastan, D. J. and Demarquette N. R., "Influence of drop volume on surface tension evaluated using the pendant drop method", Colloid Polym. Sci., 280, 857 (2002)

Myers, D, "Surfaces, Interfaces, and Colloids: Principles and Applications", VCH publishers Inc, New York (1991)

O'Neill, M. L., Cao, Q., Fang, M., Johnston, K. P., "Solubility of Homopolymers and Copolymers in Carbon Dioxide", Ind. Eng. Chem. Res. 37, 3067-3079 (1998)

Park, C. B. and Suh, N. P., "Extrusion of Microcellular Filament: A case study of axiomatic design", in "Cellular Polymers", Kumar, V. and Adavami, S.G. Ed., ASME, MD-Vol 38, New York (1992)

Park, C. B. and Suh, N. P., "Extrusion of Microcellular polymers using a rapid pressure drop device", SPE ANTEC, 1813-1822(1993)

Park, C. B. and Suh, N. P., “Filamentary Extrusion of Microcellular Polymers Using a Rapid Decompressive Element”, Polym. Eng. Sci., 36, 34-48 (1996a)

Park, C. B. and Suh, N. P., “Rapid Polymer/Gas solution Formation for Continuous Production of Microcellular Plastics”, J. Manu. Sci. Eng., 118, 639-645 (1996b)

Park, C. B., Baldwin, D. F., Suh, N. P., “Effect of the Pressure Drop Rate on Cell Nucleation in Continuous Processing of Microcellular Polymers”, Polym. Eng. Sci., 35, 432-440 (1995)

Park, H., Park, C. B., Tzoganakis, C. and Chen, P. “Effect of Molecular Weight on the Surface of Polystyrene Melt in Supercritical Nitrogen”, Ind. Eng. Chem. Res. 46, 3849-3851 (2007b)

Park, H., Park, C. B., Tzoganakis, C., Tan, K. H. and Chen, P. “Surface Tension Measurement of Polystyrene Melts in Supercritical Carbon Dioxide”, Ind. Eng. Chem. Res. 45, 1650-1568 (2006)

Park, H., Thompson, R.B., Lanson, C., Tzoganakis, C., Park, C.B. and Chen, P., “Effect of Temperature and Pressure on Surface Tension of Polystyrene in Supercritical Carbon Dioxide”, J. Phys. Chem. B, 111, 3859-3868 (2007a)

Quach, A., Simha, R., “Pressure-Volume-Temperature Properties and Transitions of Amorphous Polymers: Polystyrene and Poly (orthomethylstyrene)”, Journal of Applied Physics, 42, 4592-4606 (1971)

Ramesh, N. S., Rasmussen, D. H. and Campbell G. A., “The heterogeneous nucleation of microcellular foams assisted by the survival of microvoids in polymers containing low glass transition particles. Part II: Experimental results and discussion”, Polym. Eng. Sci., 34, 1698-1706 (1994b)

Ramesh, N. S., Rasmussen, D. H. and Campbell G. A., “The heterogonous nucleation of microcellular foams assisted by the survival of microvoids in polymers containing low glass transition particles. Part I: Mathematical modeling and numerical simulation”, Polym. Eng. Sci., 34, 1685-1697 (1994a)

Raton, B., “CRC Handbook of Chemistry and Physics”, CRC Press: Cleveland, OH, (1981)

Richardson, M. J., Savill N. G., “Derivation of accurate glass transition temperatures by differential scanning calorimetry”, Polymer, 16, 753-757 (1975)

Roe, R-. J., “Surface Tension of Polymer liquids”, J. Phys. Chem. 72, 2013-2017 (1968)

Roe, R-. J., Bacchetta V. L. and Wong P. M. G. “Refinement of Pendant Drop Method for the Measurement of Surface Tension of Viscous Liquid”, J. Phys. Chem. 71, 4190-4193 (1967)

Rotenberg, Y., Boruvka, L. and Neumann, A.W., "Determination of Surface Tension and Contact Angle from the Shapes of Axisymetric Fluid Interfaces", J. Colloid Interface Sci., 93, 169-183 (1983)

Royer, J. R., Gay, Y. J., Desimone, J. M., Khan S. A., "High-Pressure Rheology of Polystyrene Melts Plasticizer with CO_2:Experimental Measurement and Predictive Scaling Relationships", Journal of Polymer Science: Part B: Polymer Physics, 38, 3168-31380 (2000)

Russell, K. C. "Nucleation in Solids: The Induction and Steady state Effects", Advances in Colloids Interface Science, 13, 500-503 (1980)

Sanchez, I. C. and Lacombe, R. H., "An Elementary Equation of State For Polymer Liquids", Polymer Lett. 15, 71-75 (1977)

Sanchez, I. C. and Lacombe, R. H., "An Elementary Molecular Theory of Classical Fluids. Pure Fluids", J. Phy. Chem. 80, 2352-2362 (1976)

Sanchez, I. C. and Lacombe, R. H., "Statistical Thermodynamics of Polymer Solutions", Macromolecules, 11, 1145-1156 (1978)

Sato, Y., Fujiwara, K., Takikawa T., Sumarno, Takishima S. and Masuoka, H., "Solubilities and diffusion coefficients of carbon dioxide and nitrogen in polypropylene, high-density

polyethylene, and polystyrene under high pressure and temperature", Fluid Phase Equil., 162, 216-276 (1996)

Sato, Y., Takikawa, T., Takishima S., Masuoka H., "Solubilities and diffusion coefficients of carbon dioxide in poly(vinyl acetate) and polystyrene", Journal of Supercritical Fluids, 19, 187-198 (2001)

Sato, Y., Yurugi, M, Fujiwara, K., Takishima, S. and Masuoka, H., "Solubilities of carbon dioxide and nitrogen in polystyrene under high temperature and pressure", Fluid Phase Equil., 125, 129-138 (1996)

Schmid, F. J., "Self-consistent-field theories for complex fluids", J. Phys.: Condens. Matter, 10, 8105-8138 (1998)

Shafi, M. A., Lee, J. G. and Flumerfelt, R. W., "Prediction of Cellular Structure in Free Expansion Polymer Foam Processing", Polym. Eng. Sci., 36, 1950-1959 (1996)

Song, B. and Spinger, J., "Determination of Interfacial Tension from the Profile of a Pendant drop Using Computer-Aided Image Processing", J. Colloid Interface Sci., 184, 77-91 (1996)

Stafford, C. M., Russell, T. P., and McCarthy, T. J. "Expansion of Polystyrene Using Supercritical Carbon Dioxide: Effects of Molecular Weight, Polydispersity, and Low Molecular Weight Components", Macromolecules, 32, 7610-7616 (1999)

Susnar, S. S., Hamza H.A., and Neumann, A.W., " Pressure Dependence of Interfacial Tension of Hydrocarbon-water systems using axisymmetric Drop Shape Analysis", Colloids and Surfaces A, 89, 169-180 (1994)

Takamizawa, K., Toratani H., "Application of a high pressure d. t. a. to study the pressure-glassification of polystyrene", Polymer, 33, 1333-1334 (1992)

Thompson, R. B., Rasmussen, K. Ø., Lookman, T., "Improved convergence in block copolymer self-consistent field theory by Anderson mixing", J. Chem. Phys., 120, 31-34 (2004)

Tomasko, D. L., Li, H, Liu, D., Han, X., Wingert, M. J., Lee, L. J. and Koelling, K. W., "A Review of CO2 Applications in the Processing of Polymers", Ind. Eng. Chem. Res. 42, 6431-6456 (2003)

Utracki, L. A., "Pressure-Volume-Temperature of Molten and Glassy Polymers", Journal of Polymer Science: Part B: Polymer Physics, 45, 270-285 (2007)

Wessling, M., Borneman, Z., Bppmgaard, T. V. D. and Smolders, C. A., "Carbon Dioxide Foaming of Glassy Polymers", Journal of Applied Polymer Science, 53, 1497-1512 (1994)

Wu, S. “Surface and Interfacial Tension of Polymer Melts. II. Poly(methyl methacrylate) Poly(n-butyl methacrylate), and Polystyrene”, J. Phy. Chem. 74, 632-638 (1970)

Wu, S., “Polymer Interface and Adhesion”, Marcel Dekker, New York (1982)

Wu, S., “Surface and Interfacial Tension of Polymer Melts I. Polyethylene, Polyisobutylene, and Polyvinyl Acetate”, J. Colloid Interface Sci., 31, 153-161 (1969)

Wulf, M, Michel, S., Grundke, K., del Rio, O. I., Kwok, D. Y. and Neumann, A. W., “Simultaneous Determination of Surface tension and Density of Polymer Melts Using Axisymmetric Drop Shape Analysis”, J. Colloid Interface Sci., 210, 172-181 (1999a)

Wulf, M, Michel, S., Jenschke, W., Uhlmann, P., Grundke, K., “A new method for the simultaneous determination of surface tension and density of polymer melts”, Phy. Chem. Chem. Phys., 1, 3899-3903 (1999b)

Xue, A., Tzoganakis, C. and Chen, P., “Measurement of Interfacial Tension in PS/LDPE Melts Saturated With Supercritical CO2”, Polym. Eng. Sci., 44, 18-27 (2004)

Zoller, P., Bolli, P., Pahud V., Ackermann H., “Apparatus for measuring pressure-volume-temperature relationships of polymers to 350 C and 220 kg/cm2”, Rev. Sci. Instrum., 47, 948-952 (1976)

Appendix-A Typical Raw Data of ADSA-P

The typical raw data is obtained for the surface tesion of polystyrenes in supercritical carbon dioxide at a pressure of 500psi and a temperature of 170^{o}C.

time [sec]	surface tension [mJ/m^2]	stand deviation [mJ/m^2]	surface area [cm^2]	volume [cc]	radius of curvature [cm]
0	26.6364970	0.0821848	0.1149879	0.0043872	0.0931740
60	26.6215940	0.1028915	0.1151578	0.0043922	0.0931600
120	26.6550333	0.0702764	0.1151761	0.0043927	0.0931720
180	26.5961835	0.0663675	0.1151220	0.0043899	0.0931350
240	26.4725843	0.0871483	0.1149564	0.0043819	0.0930550
300	26.7122412	0.0956619	0.1154058	0.0044040	0.0932410
360	26.5574264	0.0704052	0.1151128	0.0043895	0.0931200
420	26.7404612	0.0795262	0.1153175	0.0043995	0.0932310
480	26.6320799	0.0784084	0.1152983	0.0043988	0.0931890
540	26.6657407	0.0947171	0.1148948	0.0043848	0.0931940
600	26.5915981	0.0752695	0.1151193	0.0043899	0.0931350
660	26.7152968	0.0924876	0.1152978	0.0043986	0.0932190
720	26.6874814	0.0978325	0.1152329	0.0043953	0.0931920
780	26.7219228	0.1015433	0.1148830	0.0043846	0.0932180
840	26.5946774	0.0878834	0.1151821	0.0043920	0.0931370
900	26.5614930	0.0872072	0.1151147	0.0043894	0.0931200
960	26.6162014	0.0902290	0.1151110	0.0043902	0.0931520
1020	26.6514580	0.0607708	0.1152270	0.0043942	0.0931670
1080	26.5995128	0.0974954	0.1154715	0.0044099	0.0932480
1140	26.6460427	0.0877957	0.1152143	0.0043947	0.0931770
1200	26.6856622	0.0585740	0.1152127	0.0043937	0.0931800

1260	26.6257029	0.0703773	0.1154367	0.0044044	0.0932000
1320	26.6930748	0.0821223	0.1151913	0.0043934	0.0931880
1380	26.4734082	0.0701198	0.1150315	0.0043849	0.0930630
1440	26.4459984	0.0940909	0.1149151	0.0043803	0.0930430
1500	26.6407634	0.1070042	0.1150306	0.0043853	0.0931310
1560	26.7201174	0.0913205	0.1153621	0.0044006	0.0932180
1620	26.4196143	0.0848919	0.1148958	0.0043789	0.0930230
1680	26.6416848	0.0945022	0.1148324	0.0043813	0.0931670
1740	26.5758594	0.1060286	0.1150836	0.0043891	0.0931340

1800	26.6284366	0.0667022	0.1150394	0.0043863	0.0931360
1860	26.4964739	0.1109797	0.1150796	0.0043916	0.0931390
1920	26.6513290	0.0968120	0.1151667	0.0043922	0.0931670
1980	26.7098432	0.0878669	0.1153590	0.0043995	0.0932020
2040	26.6104111	0.0888306	0.1152550	0.0043949	0.0931490
2100	26.6745925	0.0951951	0.1152578	0.0043967	0.0931950
2160	26.7361249	0.0806722	0.1154005	0.0044027	0.0932350
2220	26.6686378	0.0860253	0.1152167	0.0043952	0.0931910
2280	26.6202779	0.0925520	0.1152563	0.0043987	0.0932030
2340	26.6878033	0.0818553	0.1152965	0.0043978	0.0931970
2400	26.6277938	0.0914314	0.1152435	0.0043955	0.0931680
2460	26.6519581	0.0920479	0.1148976	0.0043839	0.0931750
2520	26.7176505	0.0452049	0.1153128	0.0043986	0.0932130
2580	26.4774098	0.0897535	0.1146804	0.0043755	0.0930950
2640	26.7038186	0.0748326	0.1156283	0.0044151	0.0932860
2700	26.8139944	0.0630914	0.1150668	0.0043910	0.0932560
2760	26.6540450	0.0963084	0.1148467	0.0043813	0.0931650
2820	26.6758171	0.0813567	0.1153054	0.0043990	0.0932060
2880	26.6410262	0.0867987	0.1151950	0.0043936	0.0931700
2940	26.5280300	0.0795288	0.1149972	0.0043829	0.0930720
3000	26.7659652	0.0571026	0.1153962	0.0044030	0.0932520
3060	26.6313052	0.0754979	0.1151712	0.0043925	0.0931620
3120	26.5281747	0.0758783	0.1151077	0.0043897	0.0931140
3180	26.6980923	0.0618679	0.1152279	0.0043941	0.0931830
3240	26.7334916	0.0851025	0.1151850	0.0043932	0.0932030
3300	26.7776009	0.0808191	0.1150876	0.0043906	0.0932270
3360	26.7305777	0.0548904	0.1152743	0.0043973	0.0932170

3420	26.6106691	0.0715156	0.1150101	0.0043863	0.0931420
3480	26.6913343	0.0932833	0.1150174	0.0043880	0.0931920
3540	26.7477527	0.0754716	0.1154070	0.0044037	0.0932500

Appendix-B Density Determination Data

1. Polystyrene in nitrogen

Pressure[psi]	Temperature[°C]				
	170	180	190	200	210
Density Difference					
500	0.9623	0.9564	0.9504	0.9442	0.9380
1000	0.9381	0.9328	0.9272	0.9216	0.9157
1500	0.9147	0.9099	0.9049	0.8997	0.8943
2000	0.8921	0.8878	0.8833	0.8786	0.8736
2500	0.8704	0.8666	0.8625	0.8582	0.8537
3000	0.8496	0.8462	0.8426	0.8387	0.8345
Density of polymer phase					
500	0.9882	0.9817	0.9751	0.9684	0.9616
1000	0.9890	0.9826	0.9759	0.9692	0.9624
1500	0.9899	0.9834	0.9768	0.9700	0.9632
2000	0.9907	0.9842	0.9775	0.9708	0.9639
2500	0.9915	0.9850	0.9783	0.9715	0.9645
3000	0.9923	0.9857	0.9790	0.9721	0.9652
Density of gas phase					

500	0.0259	0.0253	0.0247	0.0242	0.0237
1000	0.0510	0.0498	0.0487	0.0476	0.0466
1500	0.0752	0.0735	0.0719	0.0703	0.0688
2000	0.0986	0.0964	0.0942	0.0922	0.0902
2500	0.1211	0.1184	0.1157	0.1132	0.1108
3000	0.1427	0.1395	0.1364	0.1335	0.1307

2. Polystyrene in carbon dioxide

Pressure[psi]	Temperature[°C]				
	170	180	190	200	210
Density Difference					
500	0.9367	0.9316	0.9277	0.9225	0.9183
1000	0.8843	0.8822	0.8799	0.8775	0.8750
1500	0.8301	0.8307	0.8311	0.8312	0.8311
2000	0.7744	0.7790	0.7821	0.7845	0.7869
2500	0.7185	0.7255	0.7318	0.7384	0.7437
3000	0.6645	0.6750	0.6845	0.6932	0.7012
Density of polymer phase					
500	0.9789	0.9734	0.9678	0.9622	0.9565
1000	0.9706	0.9660	0.9614	0.9568	0.9522
1500	0.9624	0.9587	0.9551	0.9515	0.9480
2000	0.9543	0.9516	0.9489	0.9463	0.9439
2500	0.9464	0.9445	0.9428	0.9412	0.9398
3000	0.9385	0.9375	0.9367	0.9361	0.9357
Density of gas phase					
500	0.0422	0.0417	0.0401	0.0397	0.0382
1000	0.0863	0.0838	0.0815	0.0793	0.0772
1500	0.1323	0.1280	0.1240	0.1203	0.1169
2000	0.1800	0.1725	0.1667	0.1618	0.1570
2500	0.2279	0.2190	0.2110	0.2028	0.1960

3000	0.2740	0.2625	0.2522	0.2429	0.2345